THE ORIGIN AND TECTONIC HISTORY

OF THE

SOUTHWEST PHILIPPINE SEA

by

KEITH EDWARD LOUDEN

B.A., Oberlin College
(1970)

M.Ed., Temple University
(1972)

SUBMITTED IN PARTIAL FULFILLMENT OF THE REQUIREMENTS FOR
THE DEGREE OF DOCTOR OF PHILOSOPHY

at the

MASSACHUSETTS INSTITUTE OF TECHNOLOGY

and the

WOODS HOLE OCEANOGRAPHIC INSTITUTION

September 1976

Signature of Author_____
    Joint Program in Oceanography, Massachusetts Institute of
    Technology - Woods Hole Oceanographic Institution, and the
    Department of Earth and Planetary Sciences, Massachusetts
    Institute of Technology, September, 1976

Certified by_____
    Thesis Supervisor

Accepted by_____
    Chairman, Joint Oceanography Committee in the Earth Sciences,
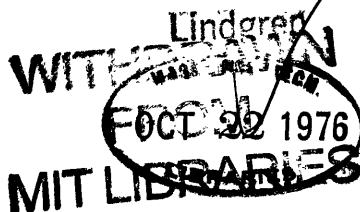   Massachusetts Institute of Technology - Woods Hole Oceanographic
    Institution

TABLE OF CONTENTS

LIST OF FIGURES

LIST OF TABLES

BIOGRAPHICAL SKETCH

I was born in Washington, D.C. on July 11, 1948.
My youth and adolescence was spent in Falls Church, Va.
except for 1964-65 when I lived in Baghdad, Iraq and attended
Al-Hikma University. I attended Oberlin Colege, Oberlin,
Ohio during 1966-70 where I received a B.A. with honors in
physics. From 1970 to 1972 I taught physics and 9th grade
science at Swarthmore High School, Swarthmore, Pa. and
attended Temple University, Philadelphia, Pa. where I
finished an M.Ed. in 1972. In 1972 I entered the Dept. of
Earth and Planetary Sciences at MIT, Cambridge, Ma. and
transfered into their Joint Program in Oceanography with the
Woods Hole Oceanographic Institution, Woods Hole, Ma. in
1973. In Oct. 1976 I shall become a Senior Assistant in
Research in the Dept. of Geodesy and Geophysics, Cambridge
University, Cambridge, England.

My publications include:

(1) Sclater, J.G., D. Karig, L.A. Lawver, and K. Louden,
Heat flow, depth, and crustal thickness of the marginal basins
of the South Philippine Sea, J. Geophys. Res., 81, 309-318,
1976.

(2) Louden, K.E., Magnetic anomalies in the West Philippine Basin, in The Geophysics of the Pacific Ocean Basin and Its Margin, Geophys. Monogr. Ser., vol. 19, AGU, Washington, D.C., in press, 1976.

(3) Louden, K.E., and D.W. Forsyth, Thermal conduction across fracture zones and the gravitational edge effect, J. Geophys. Res., in press, 1976.

(4) Louden, K.E., Paleomagnetism of DSDP sediments and basalt, phase shifting of magnetic anomalies, and rotations of the West Philippine Basin, submitted to J. Geophys. Res., 1976.

ACKNOWLEDGEMENTS

THE ORIGIN AND TECTONIC HISTORY
OF THE
SOUTHWEST PHILIPPINE SEA

by

Keith Edward Louden

Submitted to the Woods Hole Oceanographic Institution -
Massachusetts Institute of Technology Joint Program in
Oceanography on June 2, 1976 in partial fulfillment of
the requirements for the degree of Doctor of Philisophy.

ABSTRACT

This thesis is a collection and analysis of sea-
floor magnetic anomalies, bathymetry, and the paleomagnetism
of DSDP sediments and basalt in the West Philippine Basin,
in an attempt to resolve questions about its origin as a
marginal basin. Our results suggest that this basin was
formed in an Eocene pulse of rapid spreading ($v_{1/2}$ = 41-44 mm/yr)
in a direction (N 21°E) significantly different from later
pulses which opened the more eastern basins of the Philip-
pine Sea. The Central Basin Fault appears to be intimately
associated with this spreading by nature of its structure
and trend, and it may be a remanent of a former ridge system.
Our preliminary calculation of paleopole positions also
suggests that there was a large amount (60°) of clockwise
rotation between this basin and the magnetic pole. This is
consistent with rotations of the Pacific plate with respect
to the magnetic pole and current directions of Philippine-
Pacific relative rotations. Basement depths of 6 km in the
West Philippine Basin imply that its crustal and/or litho-
spheric structure is different from Pacific structure of the
same age.

Thesis Supervisor: John G. Sclater
Title: Associate Professor of Geophysics

SECTION I

INTRODUCTION

Much of the West Pacific margin consists of oceanic basins separating its deep trenches and their associated volcanic island arc chains from the adjacent continents of Australia and Eurasia. The origins and history of these marginal basins have long remained a controversial enigma to both past and present global tectonic theories. Pre-plate tectonic hypotheses considered these regions to be former continental areas that had subsided (e.g. Marshall, 1910; Kuenen, 1935; Glaessner, 1950). Mechanisms for this subsidence included subcrustal erosion (Lawson, 1932), crustal warping due to compression (Umbgrove, 1947) and oceanization (Beloussov and Ruditch, 1961), among many others. It wasn't until seismic refraction techniques became available in the deep oceans during the late 1950's and early 1960's that it was discovered that the crust beneath these basins was similar to that of normal oceans (Gaskell et al., 1959; Shor, 1964; Murauchi et al., 1968). These results have disproven many of the earlier theories, and while some (e.g. Beloussov, 1967) still remain possible, they are currently not widely accepted in the West.

Theories contrasting to those with continental origins include the continental drift theory of Wegener (1929) which treated these basins as extensional gaps left

behind the trailing edge of a moving continent, and the expanding earth theory of Carey (1958) which considered them as extensional 'rhombochasms' between large scale lithospheric units. There were also various compressional theories which explained the arcs within and adjacent to the marginal basins as manifestations of convection currents (Vening Meinesz, 1951; Holmes, 1965; Wright, 1966; Menard, 1964). These were predated by the earlier tectogene folding concepts of Hess (1948).

The advent of global plate tectonic concepts (Wilson, 1965; McKenzie and Parker, 1967; Morgan, 1968; LePichon, 1968), in which trenches were considered to be sites of lithospheric subduction, added more justification to these compressional theories. Problems remained, however, since it was found that high heat flow and shallow water depths, which normally are associated with active intrusion and crustal extension (Sclater and Francheteau, 1970), were reported well to the west of the island arc chains (Yasui and Watanabe, 1965; Vacquier et al., 1966; Yasui et al., 1968a, 1968b, 1970; Sclater and Menard, 1967). This high heat flow has presented major problems to the plate model (McKenzie and Sclater, 1968; Oxburgh and Turcotte, 1970).

It was not until Karig (1970) reported new evidence
suggesting that crustal extension did in fact exist behind
the Tonga-Kermadec island arc, that the earlier extensional
theories (Deitz, 1954; Carey, 1958; Murauchi and Den, 1966;
Tanner, 1968) were revived. This pioneering study was later
supported by additional strong evidence of extension behind
the Mariana island arc (Karig, 1971a), and led to several
attempts at placing this 'inter-arc spreading' hypothesis
within a plate tectonic framework (Karig, 1971b; Pacham and
Falvey, 1971; Sclater, 1972; Moberly, 1972). The primary
result of this work was that there appeared to be significant
differences between values of heat flow and depth vs. age
in the older and now no longer active marginal basins and
typical results for the normal oceans. This seemed to suggest
that either the crust (Karig, 1971b) or the entire lithosphere
(Sclater, 1972) was thinner than normal.

Such attempts at synthesizing and comparing geo-
physical data in marginal basins to pre-existing global
plate tectonic models have been severely hampered by several
problems. Evidence for extension within active marginal
basin troughs is limited and depends primarily on identi-
fication of certain topographic morphologies and sediment
distribution patterns. Geochemical analysis on a few basalts

dredged from the Mariana and Lau basins also shows strong similarities to rocks from major ocean ridge systems. The amount of detailed geophysical data is limited to a few well surveyed regions in these same active troughs, but the recognition of adaquate magnetic anamaly patterns that can be unambiguously identified to world-wide magnetic reversals is confined to other areas such as the Scotia (Barker, 1972) and Tasman (Hayes and Ringis, 1973) seas, which do not conform very well to the type inter-arc spreading model of Karig (1971b). This has meant that unique evolutionary histories of spreading within even the most clearly defined and well studied basins is not yet possible. Controversies exist between possibilities of these basins being either old, trapped oceanic crust or younger crust formed by inter-arc spreading. It is not yet clear whether inter-arc spreading is any different from ridge spreading in normal oceans, whether the older marginal basins have been formed in the same manner as now occurs in the active troughs landward of their island arcs, and whether the many separate marginal basins have a common origin.

Until there exist more unambiguous data, particularly basement ages from both magnetic anomaly identifications and DSDP cores, current geophysical and geological disputes

over the origins of specific marginal basins cannot be
resolved. It is the purpose of this thesis to add new
constraints to the history of one such marginal basin, the
West Philippine Basin, in hopes that this data can help to
resolve present controversies over its history (see the
introduction to section II) and contribute toward the
over-all goal of understanding the basic processes at work
in all such marginal basins. Toward this end we have done
the following:

(1) Collected and plotted most of the existing magnetic
data in the Philippine Sea (Appendix B),

(2) Mapped and identified a set of magnetic lineations
across the Central Basin Fault in the West Philippine Basin
(Section II), and

(3) Performed a detailed paleomagnetic study on basalt
and sediment samples from DSDP sites 292, 290 and 294
(Section III).

Analysis of these additional data leads to the
following results:

(1) The West Philippine Basin was formed south of the
equator by rapid spreading ($v_{1/2}$ = 41-44 mm/yr) during
the mid-to-late Eocene (35-50 mybp).

(2) The Central Basin Fault seems to be intimately associated

with this spreading by nature of the structure and trend
of its topography. In addition, its deep central rift is
also characteristic of the fossil ridges near the Galapagos
spreading center (Anderson et al., 1976). Thus the typical
association in marginal basins of magnetic anomalies with
bathymetric features similar to mid-ocean ridges is continued
by the results of this study.

(3) The direction of this former spreading must have been
distinctly different from that which exists today along the
Mariana and Izu-Bonin arcs. Thus a more complicated tectonic
development than originally suggested by Karig (1971a) is
inevitable.

(4) Phase shifting of the magnetic anomalies and analysis
of the paleomagnetic data for DSDP samples indicates that
a significant rotation of the West Philippine Basin has
occurred since it was formed. This result agrees with the
hypothesis of Uyeda and Ben-Avraham (1972) that this basin
might be a remanent of the former Kula-Pacific ridge system
of Larson and Chase (1972).

(5) The well-defined age determination of the West Philippine
Basin leaves little doubt that there is a significant dis-
crepancy between its depth of over 6 km and normal depths
of 5 km for oceanic crust of a similar age. The reasons for

such an offset are as yet unknown, although as earlier
suggested by Karig (1971b) and Sclater (1972), the crust
and lithosphere might be significantly different than normal
(Appendix A; Sclater et al., 1976; Seekins and Teng, 1976).
(6) There is no need in our analysis to require either
non-rigid plate interactions between the Philippine and
Pacific plates nor significant rotation due to inter-arc
spreading. Paleomagnetic pole positions for the West
Philippine Basin are consistent with present day plate
motions as determined by earthquakes on the margins of the
Philippine Sea (Katsumata and Sykes, 1969; Fitch, 1972;
Karig, 1975). Furthermore, the paleopole positions for
Guam (Larson et al., 1975) which lies on this boundary is
also consistent with such a polar wandering curve. This
implies that rotations along the island arc chain need not
be of separate origin to the rotation between the major
plates.

What remains clear from this study is the necessity
for further measurements in the Philippine Sea of the basic
physical properties of its crust, upon which all other
analyses rely. These include the seismic structure of the
deep water basins and the magnetic properties beneath sea-
floor spreading anomalies. When these measurements are

made we can begin to form additional concrete constraints on the geophysical processes which have formed this one example of a marginal basin. The uniqueness or generality of this one example among many will remain uncertain for the immediate future.

REFERENCES

Anderson, R.N., G.F. Moore, S.S. Schilt, R.C. Cardwell, A. Trehu and V. Vacquier, Heat flow near a fossil ridge on the north flank of the Galapagos spreading center, J. Geophys. Res., 81, 1828-1838, 1976.

Barker, P.F., A spreading center in the East Scotia Sea, Earth Planet. Sci. Letters, 15, 123-132, 1972.

Beloussov,V.V., Some problems concerning the oceanic earth's crust and upper mantle evolution, Geotectonics, 1, 1-6, 1967.

Beloussov, V.V. and E.M. Ruditch, Island arcs in the development of the earth's structure, J. Geol., 69, 647-658, 1961.

Carey, S.W., The tectonic approach to continental drift, in Continental Drift: A Symposium, Univ. Tasmania Press, Hobert, p. 177, 1958.

Dietz, R.S., Marine geology of northwestern Pacific: Description of Japanese bathymetric chart 6901, Bull. Geol. Soc. Amer., 65, 1199-1224, 1954.

Fitch, T.J., Plate convergence, transcurrent faults and internal deformation adjacent to southeast Asia and the western Pacific, J. Geophys. Res., 77, 4432-4460, 1972.

Gaskell, T.F., M.N. Hill, and J.C. Swallow, Seismic measure-
ments made by H.M.S. Challenger in the Atlantic, Pacific,
and Indian Oceans and in the Mediterranean Sea, 1950-53,
Phil. Trans., Roy. Soc. London, A, 251, 23-85, 1959.

Glaessner, M.F., Geotectonic position of New Guinea, Bull.
Am. Assoc. Petrol. Geologists, 34, 856-881, 1950.

Hayes, D.E. and J. Ringis, Sea-floor spreading in the Tasman
Sea, Nature, 243, 454-458, 1973.

Hess, H.H., Major structural features of the western north
Pacific, an interpretation of H.O. 5485, Bathymetric
chart, Korea to New Guinea, Geol. Soc. Amer. Bull., 59,
417-446, 1948.

Holmes, A., Principles of Physical Geology, Thomas Nelson,
London, 1288 pp., 1965.

Karig, D.E., Ridges and basins of the Tonga-Kermadec island
arc system, J. Geophys. Res., 75, 239-255, 1970.

Karig, D.E., Structural history of the Mariana island arc
system, Bull. Geol. Soc. Amer., 82, 323-344, 1971a.

Karig, D.E., Origin and development of marginal basins in
the western Pacific, J. Geophys. Res., 76, 2542-2561,
1971b.

Karig, D.E., Basin genesis in the Philippine Sea, in Initial
Reports of the Deep-Sea Drilling Project, ed. J.C. Ingle,

D.E. Karig, et al., v. 31, U.S. Government Printing
Office, Washington, D.C., 857-879, 1975.

Katsumata, M. and L.R. Sykes, Seismicity and tectonics of
the western Pacific: Izu-Mariana, Caroline and Ryukyu-
Taiwan regions, J. Geophys. Res., 74, 5923-5948, 1969.

Kuenen, P.H., The Snellius Expedition, Geological Results,
5, part 1, Kemink en zoon N.V., Utrecht, 124 pp., 1935.

Larson, E.E., R.L. Reynolds, M. Ozima, Y. Aoki, H. Kinoshita,
S. Zasshu, N. Kawai, T. Nakajima, K. Hirooka, R. Merrill,
and S. Levi, Paleomagnetism of Miocene volcanic rocks
of Guam and the curvature of the southern Mariana island
arc, Geol. Soc. Amer. Bull., 86, 346-350, 1975.

Larson, R.L. and C.G. Chase, Late Mesozoic evolution of the
western Pacific Ocean, Geol. Soc. Amer. Bull., 83,
3627-3644, 1972.

Lawson, A.C., Insular arcs, foredeeps, and geosynclinal seas
of the Asiatic coast, Bull. Geol. Soc. Amer., 43,
353-382, 1932.

Le Pichon, X., Sea-floor spreading and continental drift,
J. Geophys. Res., 73, 3661-3697, 1968.

Marshall, P., Ocean contours and earth movement in the
Southwest Pacific, Rept. Australian Assoc. Adv. Sci.,
12, 432-450, 1910.

McKenzie, D.P. and R.L. Parker, The North Pacific, an
example of tectonics on a sphere, Nature, 216, 1276-
1280, 1967.

McKenzie, D.P. and J.G. Sclater, Heat flow inside the island
arcs of the northwestern Pacific, J. Geophys. Res.,
73, 3173-3179, 1968.

Menard, H.W., Marine Geology of the Pacific, McGraw-Hill,
New York, 271 pp., 1964

Moberly, R., Origin of lithosphere behind island arcs, with
reference to the western Pacific, Geol. Soc. Amer. Mem.
v. 132, 35-55, 1972.

Morgan, W.J., Rises, trenches, great faults, and crustal
blocks, J. Geophys. Res., 73, 1959-1982, 1968.

Murauchi, S. and N. Den, Origin of the Japan Sea, (in
Japanese) paper presented at monthly colloquium of the
Earthquake Res. Inst., University of Tokyo, 1966.

Murauchi, S., N. Den, S. Asano, H. Hotta, T. Yoshii, T.
Asanuma, K. Hagiwara, K. Ichikawa, T. Sato, W.J. Ludwig,
J.I. Ewing, N.T. Edgar and R.E. Houtz, Crustal structure
of the Philippine Sea, J. Geophys. Res., 73, 3143-3171,
1968.

Oxburgh, E.R. and D.L. Turcotte, Thermal structure of island
arcs, Bull. Geol. Soc. Amer., 81, 1665-1688, 1970.

Packham, G.H. and D.A. Falvey, An hypothesis for the formation of marginal seas in the western Pacific, Tectonophysics, 11, 79-109, 1971.

Sclater, J.G., Heat flow and elevation of the marginal basins of the western Pacific, J. Geophys. Res., 77, 5705-5719, 1972.

Sclater, J.G. and J. Francheteau, The implications of terrestrial heat flow, observations on current tectonic and geochemical models of the crust and upper mantle of the earth, Geophys. J. Roy. Astron. Soc., 20, 509-542, 1970.

Sclater, J.G., D. Karig, L.A. Lawver and K. Louden, Heat flow, depth, and crustal thickness of the marginal basins of the South Philippine Sea, J. Geophys. Res., 81, 309-318, 1976.

Sclater, J.G. and H.W. Menard, Topography and heat flow of the Fiji plateau, Nature, 216, 991-993, 1967.

Seekins, L.C. and T. Teng, Lateral variations in the structure of the Philippine Sea, in preparation, 1976.

Shor, G.G., Structure of the Bering Sea and the Gulf of Alaska, Marine Geology, 1, 213-219, 1964.

Tanner, W.F., Tensional basins on the eastern edge of Asia, J. Geol. Soc. Japan, 74, 583-588, 1968.

Umbgrove, J.H.F., The Pulse of the Earth, Martinus Nijhoff, The Hague, 358 pp., 1947.

Uyeda, S. and Z. Ben-Avraham, Origin and development of the Philippine Sea, Nature Phys. Sci., 240, 176-178, 1972.

Vacquier, V., S. Uyeda, M. Yasui, J. Sclater, C. Corry, and T. Watanabe, Studies of the thermal state of the earth, 19 heat flow measurements in the northwest Pacific, Bull. Earthquake Res. Inst. Tokyo Univ., 44, 1519-1535, 1966.

Vening Meinesz, F.A., A third arc in many island arc areas, Koninkl. Ned. Akad. Wetenschap. Proc., B, 54, 432-442, 1951.

Wehener, A., Die Entstehung der Kontinente und Ozeane, 4th ed., Methuen, London, 212 pp., 1929.

Wilson, J.T., A new class of faults and their bearing on continental drift, Nature, 207, 343-347, 1965.

Wright, J.B., Convection and continental drift in the southwest Pacific, Tectonophysics, 3, 69-81, 1966.

Yasui, M. and T. Watanabe, Terrestrial heat flow in the Japan Sea (1), Bull. Earthquake Res. Inst. Tokyo Univ., 43, 549-563, 1965.

Yasui, M., T. Kishii, T. Watanabe, and S. Uyeda, Heat flow
     in the Sea of Japan, in The Crust and Upper Mantle of
     the Pacific Area, Geophys. Monogr. Ser., vol. 12,
     ed. L. Knopoff et al., AGU, Washington, D.C., 3-16,
     1968a.

Yasui, M., K. Nagasaka, and T. Kishii, Terrestrial heat
     flow in the Okhotsk Sea (2), Oceanogr. Mag., 20, 73-
     86, 1968b.

Yasui, M., D. Epp, K. Nagasaka, and T. Kishii, Terrestrial
     heat flow in the seas around the Nansei Shoto (Ryukyu
     Islands), Tectonophysics, 10, 225-234, 1970.

SECTION II

MAGNETIC ANOMALIES IN THE WEST

PHILIPPINE BASIN

ABSTRACT

We present a comprehensive collection of magnetic anomalies in the West Philippine Basin together with several bathymetric profiles and nannofossil age dates for JOIDES sites 290 and 291. From this data we locate symmetric magnetic anomalies that have strikes roughly parallel to the Central Basin Fault. They can be identified as numbers 17-21 if the basin originated south of the equator and opened at a rate of 41-44 mm/yr. This adds justification but not total proof for the theory that the Central Basin Fault may be an extinct spreading center which slowed and then ceased spreading 40 m.y. ago. It is still possible that island arc spreading created these anomalies, but if so, the origin and evolution of such an arc cannot be simply connected to the later development of the Parece Vela and Shikoku Basins to the east. Other results show that the elevation of this region is 1 km lower than would be observed for similar aged crust in the North Pacific. If the JOIDES dates and our anomaly interpretations are correct, then the lack of a correspondingly large negative gravity anomaly suggests major differences between this extinct ridge and those known to be currently spreading.

INTRODUCTION

One of the most significant difficulties in the original
formulation of plate tectonics was its failure to account
for tensional features on the concave side of island arcs.
Karig's later analysis of these features (Karig, 1970,
1971a) which he synthesized into his theory of inter-arc
spreading (Karig, 1971b, 1974) has therefore been a major
contribution to our understanding of these marginal basins.
Unfortunately, there is as yet little geophysical proof that
older, and now no longer active, sections of marginal basins
were formed by the same processes that we observe in active
troughs. This is important since only a small fraction of
these basins are presently active.

The study of magnetic anomalies which could presumably
yield new insights into the origins of inactive marginal basins
have so far had mixed success. Results fall into two general
categories:

   (1) Characteristic anomalies are not apparent, but
       there are low amplitude lineations parallel to the
       trench.

   (2) Characteristic anomalies that can be correlated to
       world-wide events are observed together with a
       well-defined bathymetric ridge.

The Japan Sea typifies the first case (Isezaki and Uyeda,
1973) and is similar to what is observed in the actively
spreading basins of the Tonga (Lawver, personal communication)
and Mariana (Karig, 1971a) island arcs. The apparent lack of
characteristic magnetic signatures is explained by the diffuse

nature of inter-arc as opposed to mid-ocean ridge spreading,
and is one of the differences that distinguish these two
spreading modes (Karig, 1970; Matsuda and Uyeda, 1971).
The second type is observed in the Tasman (Hayes and Ringis,
1973) and Scotia (Barker, 1972) seas and is typical of
mid-ocean ridges.

The possibility of ridge spreading in marginal basins
raises several questions. If ridge spreading exists, is it
related to inter-arc spreading or are there two separate
processes that together determine the history of these basins?
Can such ridge spreading be related to mid-ocean ridge systems
of the past or does it have a separate origin?

A good place to seek the answer to these questions lies
in the Western Philippine Sea. This region (Figure 1) is
separated from the eastern sections of the Philippine Sea by the
Oki-Daito and Palau-Kyushu Ridges. Its main bathymetric
feature is the Central Basin Fault (Hess, 1948) which runs
NW-SE and splits the area into nearly equal halves. This
trend is quite different in direction to that observed in the
ridges to the east, which run north-south and parallel to
the Mariana and Bonin trenches. What makes the West Philippine
Basin of interest is that it is the only region where ideas
favoring alternative modes of spreading have been in direct
dispute. Karig proposed that this region was formed in an
Eocene pulse of inter-arc spreading - an older manifestation
of what is presently occurring in the Mariana Trough (Karig,

FIGURE 1

Ship tracks superimposed on a 2000 m, 3000 m,
and 4000 m contour map of the Philippine Sea
(Chase and Menard, 1969). Major bathymetric
features are identified.
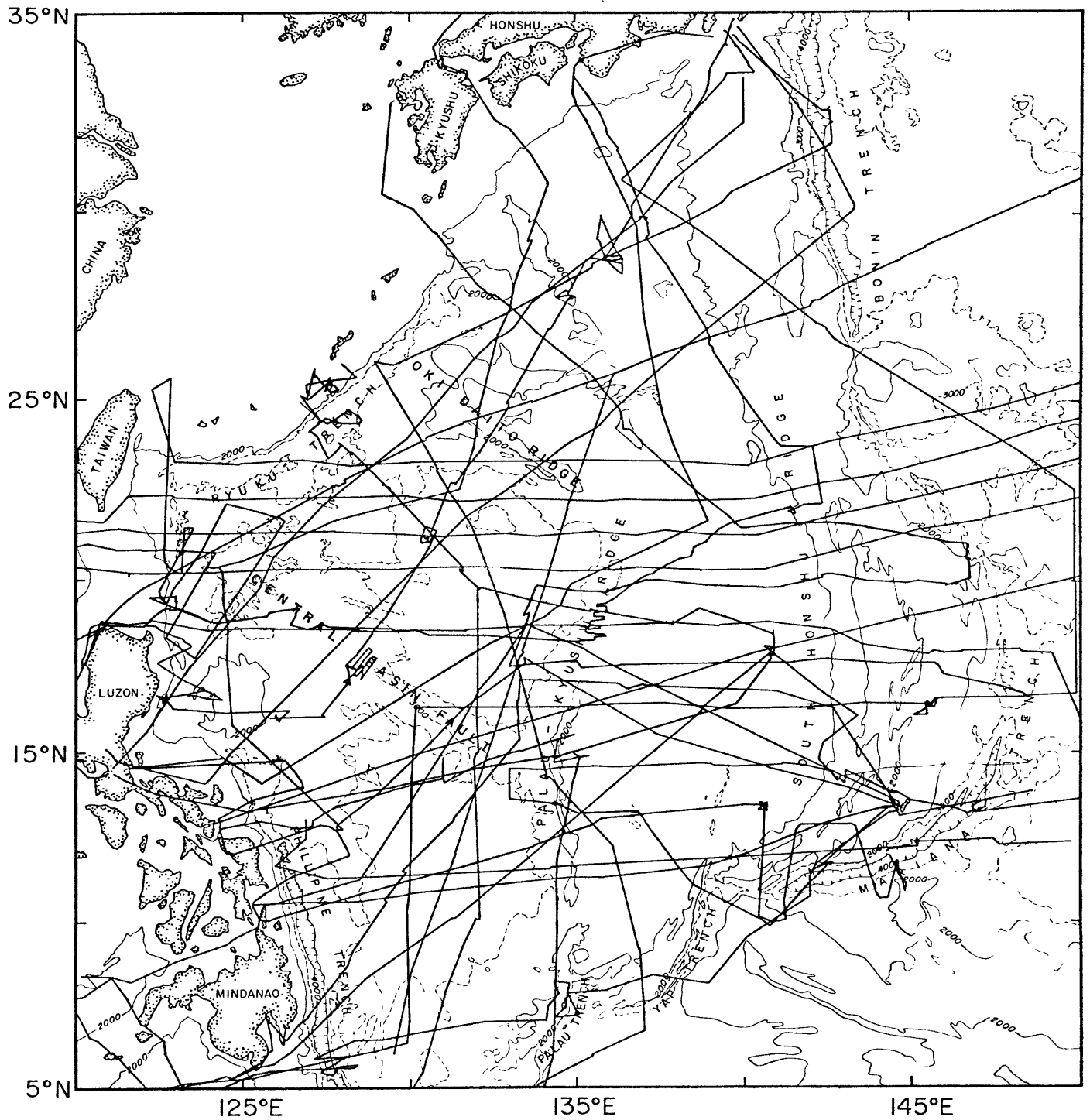
1971a). He treated the Central Basin Fault as a strike-slip
fault with several hundred kilometers of left-lateral offset
(Karig et al., 1973). Counter to this was evidence presented
by Ben-Avraham et al. (1972) of NW-SE trending magnetic
anomalies symmetric about the Central Basin Fault. Uyeda and
Ben-Avraham (1972) therefore proposed that the Central Basin
Fault was an extinct spreading center which is related to
the Kula-Pacific ridge system of Larson and Chase (1972).

This paper is a study of this region as a particularly
interesting example of an inactive marginal basin. By such
a study we hope to clarify the processes that have shaped
its history. Specifically, we synthesize magnetic, bathymetric
and Deep Sea Drilling data in an attempt to:

(1) locate any magnetic lineations and confirm or reject
those published by Ben-Avraham et al. (1972),

(2) correlate specific anomalies with world-wide reversals,

(3) determine the nature of the Central Basin Fault, and

(4) relate our findings to possible theories of this
basin's origin.

ANALYSIS OF THE MAGNETICS

Lineations

Our first step was to collect all the known magnetic
data in the Philippine Sea. Those lines which are utilized
for this work are shown in Figure 1. While processing this
data we were able to run our own line during leg 7 of the

Tasaday Expedition of Scripps Institute of Oceanography
(Nov.-Dec., 1973). We ran this line at right angles to the
Central Basin Fault and close to the lines which Ben-Avraham
et al., (1972) had earlier published. We hoped that if
lineations existed, they would at least be traceable in this
limited area of denser coverage.

Figure 2 shows the magnetic anomalies in the Western
Basin plotted at right angles to each ship's track. The
scale is smaller than normal because of the low amplitudes
of the anomalies. There are two difficulties that such low
amplitude anomalies pose. One is the considerable effect
that diurnal and semi-diurnal variations in the Earth's present
field has upon the amplitude. This might be on the order of
10-30 gammas for each component, so that the total effect
could be as large as 50 gammas (Chapman and Bartels, 1940).
The other factor that affects the zero level of the anomalies
but which leaves the shape unchanged is the secular variation,
which in this region is as great as tens of gammas per year
(Vestine, 1967). Both of these effects can be seen in the
large offsets in certain profiles in Figure 2, but can be
neglected in this study since our anomalies have a wavelength
of 50 n.m. or less and we are only matching shapes and not
contouring equal values.

We have concentrated our study on the anomalies located
between lines A-A' and B-B' in Figure 2. This is where our

FIGURE 2

Magnetic anomalies in the West Basin of the

Philippine Sea plotted at right angles to

track together with an identification of each

ship track, 2000 m and 3000 m contours, and

the location of JOIDES sites 290 through 295

(JOIDES, 1973).
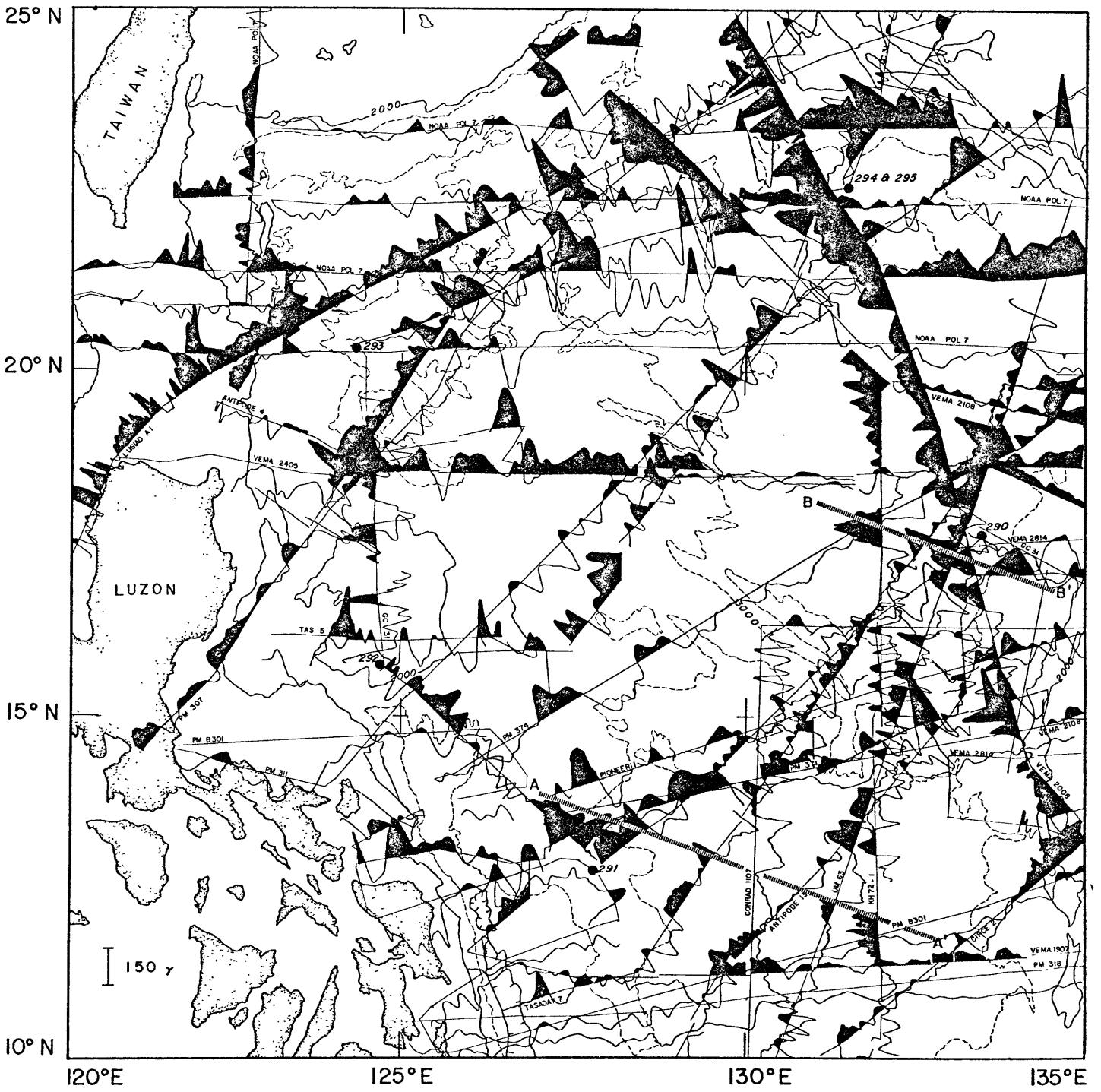
coverage is greatest and where we can use JOIDES data taken

in the West Philippine Basin during leg 31 of the Glomar

Challenger (JOIDES, 1973) most effectively. The long wave-

length anomalies close to lines A-A' and B-B' are particularly

noticeable and distinctive. It is possible that there are more

lineations to the north of this area; however, if so, they are

certainly more confused than those in the south and we feel

that the orientation and density of our tracks is not sufficient

to unravel the confusion into an indisputable pattern. In

Figure 3 we project the anomalies between lines A-A' and B-B'

along a direction of N21°E. This direction is determined

primarily by the strike of the large wavelength anomaly near

line A-A'. Notice also that in Figure 2 the anomalies for

tracks in a direction perpendicular to the projection show

low amplitudes and long wavelengths, as expected when running

parallel to a mid-ocean ridge. But caution must still be taken

at accepting this result since offsets between tracks can

produce a spurious trend. At the present we have no evidence

from either magnetics or topography that such offsets occur

in this restricted area, and have therefore positioned our

projected tracks only by the crossings between them in

Figure 2.

Even with consideration for these precautionary words,

we feel that these lineations are real, and that our measured

trend of N69°W (at right angles to the direction of projection)

FIGURE 3

Stacked magnetic anomalies which occur between

lines A-A' and B-B' of figure 2 projected along

a direction N 21°E. The relative position of

each profile is indicated by the location of

points A, A', B, B' as well as by relative num-

bers to the right and left of each profile.

These numbers increase in an eastward direction.

JOIDES sites 290 and 291 are located on the

GC 31 profile.
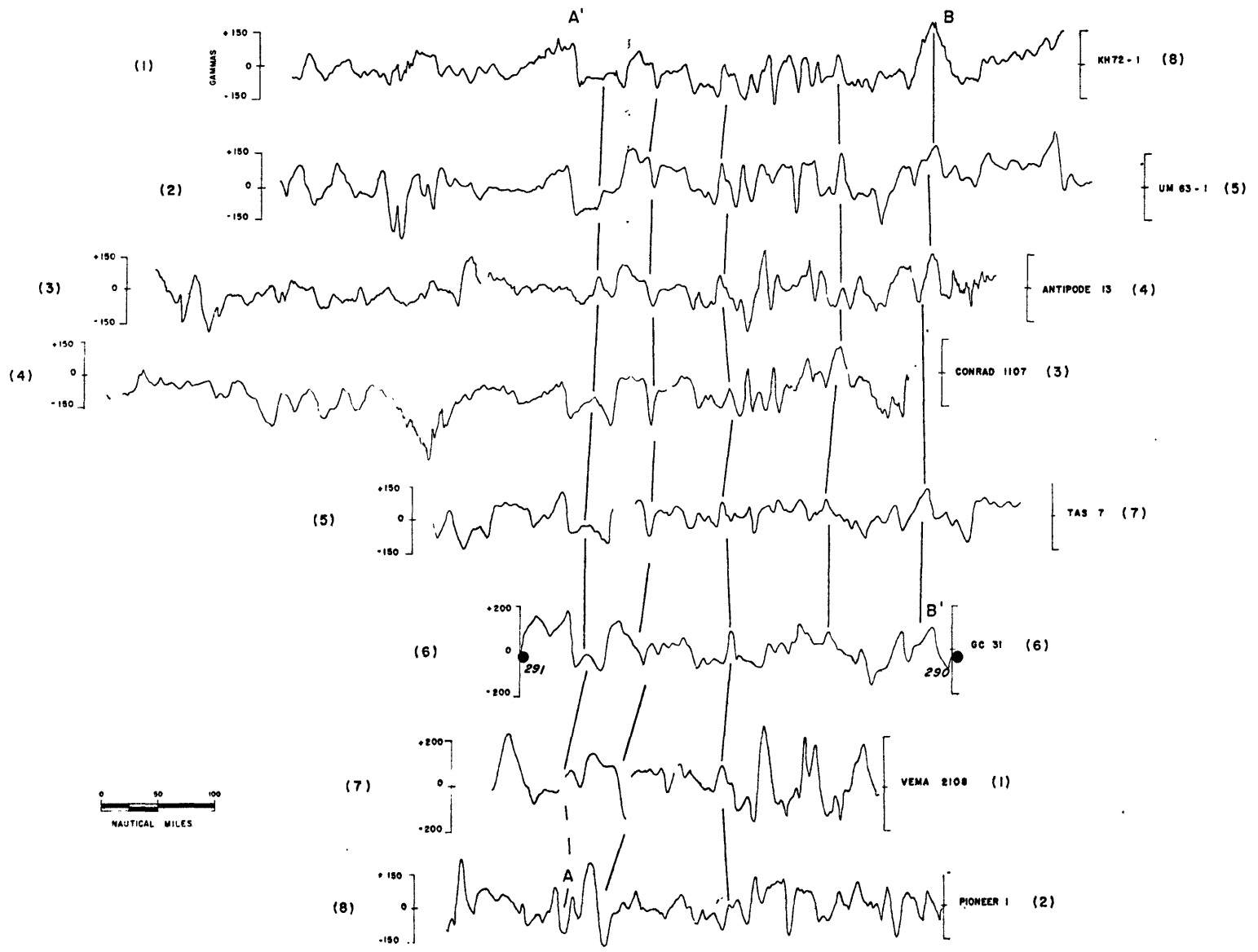
is valid. This confirms that those anomalies of Ben-Avraham et al. (1972) form traceable lineations (but in a direction 20° counterclockwise to their original prediction of N50°W). The extent of these lineations is rather limited, but one may still conclude from this evidence that at least the southern part of the West Philippine Sea opened in a nearly north-south direction. This is contradictory to the early inter-arc spreading hypotheses, which would predict a west to east direction of opening - the same as occurred in the Parece Vela Basin to the east (Karig, 1971a). Another objection is the lack of a uniform progression in the dates for JOIDES sites 290 through 295 that were drilled during leg 31 of the Deep Sea Drilling Project (Karig et al., 1973). We agree with the more recent statement of Karig et al. (1973) that this basin must have had a more complex history than was originally thought. If inter-arc spreading occurred at all, it must have been in a direction significantly different than is observed to the east.

The absence of recorded seismic events within the West Philippine Basin (Barazangi and Dorman, 1969; Fitch, 1972; Shimamura et al., 1975) probably indicates that there is no current generation of crust. It is most likely older than the Parece Vela Basin to the east (Karig, 1971a) as indicated by its thicker sediment cover (Ingle et al., in press). We conclude that the West Basin opened before the start of inter-arc spreading

in the Parece Vela Basin by one of the following two

processes:

(1) symmetric spreading by the Central Basin Fault, or

(2) spreading from a ridge that no longer exists, such
    as in a piece of trapped oceanic crust.

In the first case we would see symmetry about the Central

Basin Fault in our magnetic anomalies. This is the contention

of Ben-Avraham et al. (1972) which we will refer to as the

symmetric model. In the second case there would be no symmetry

and our anomalies would be matched by a model of spreading

from only one side of a ridge. This we will refer to as the

non-symmetric model. Notice that each model could have originated

either in a mid-ocean ridge system or as spreading behind an

island arc.

Phase Shifting

Relative poles of rotation for the Pacific-Philippine

plate system have been determined by fault plane solutions

(Fitch, 1972), but they are poorly constrained and still a

matter of debate (Karig, personal communication). Otherwise

very little is known about the plate motions of the Philippine

Sea. Such knowledge is important if we wish to compare our

magnetic anomalies to those representative of other oceans or

to a theoretical model based on a standard time scale. Changes

in paleolatitude and paleostrike produce changes in the

inclination of the remanent magnetization which can cause
large changes in the amplitude and shape of the anomalies,
making valid correlations difficult or impossible. This is
especially true when close to the equator as we are in this
case.

A very useful approach to the problem of matching
anomalies when little is known about their original orientation
is a method developed by Schouten and others (Cande and
Schouten, 1971; Cande et al., 1973; Cande and Schouten, in
prep.). In this method the anomaly is formulated in terms
of an angle θ called the skewness parameter:

$$\theta = I'_r + I' - 180° \qquad \text{(Cande and Schouten, in prep.)} \quad (1)$$

where I'_r = effective inclination of the remanent field

I' = effective inclination of the ambient field

The influence of both the magnetic inclination and the strike
of the anomaly structure are combined in the angle θ since
the effective inclinations are defined by,

$$\tan I' = \tan I_o / \sin \alpha \qquad \text{(Gay, 1963)} \qquad (2)$$

where I_o = inclination of the magnetic field

α = strike of the lineations.

The Fourier transform of an anomaly formulated in this manner can be represented as,

$$M(k) = C.J(k).E(k).e^{j\theta}. \qquad \text{(Schouten, 1971)} \qquad (3)$$

$$\text{where } C = (\sin I \sin I_r)/(\sin I' \sin I'_r) \qquad (4)$$

is a real constant. $J(k)$ is the Fourier transform of the function that represents the distribution of magnetization in the anomaly producing layer.

$$E(k) = 2\pi(e^{-ak} - e^{-bk}) \qquad (5)$$

where a and b are the depths to the top and bottom of the magnetized layer. If two sets of anomalies have the same origin but are now separated from each other, $E(k)$ and $J(k)$ would be identical. Changes in amplitude and shape from one set to the other would be determined solely by the term $C.e^{j\theta}$. Multiplication of this term by $e^{-j\theta}$ would make $M(k)$ real and independent of θ. That would leave us with deskewed (symmetric) anomalies which have different amplitudes but identical shapes.

What is done is to input a profile of magnetic anomalies and then change the value of θ until no skewness is observed in the output profile. It is therefore the actual shape of the anomalies that determines a value for θ. Using eq. (1) and eq. (2) one can then calculate possible sets of values for the paleolatitude and strike of the anomalies. In the most general case one can determine two possible values for θ.

These would be 180° apart and represent two deskewed solutions, one of which is the inverse of the other and occurs when inverted positive anomalies become negative anomalies. Recognition of the possibility that anomalies can be inverted was the key to the Larson and Pitman (1972) correlation of the Keithley lineations to three other sets of anomalies in the Pacific. This established a worldwide correlation of Mesozoic anomalies and led to the first attempt at a Mesozoic time scale. In their case the Pacific anomalies were inverted with respect to the Keithley lineations, and was the main reason why they had been invalidly correlated in an earlier attempt by Vogt et al. (1971). We believe that a similar situation led to earlier unsuccessful attempts by Ben-Avraham and the author to correlate the Philippine anomalies of Ben-Avraham et al. (1972).

Results of our application of Schouten's method to the anomalies of Figure 3 are shown in Figure 4. These anomalies represent the deskewed inverse of the original anomalies. The other, non-inverted solution has been eliminated because it would lead to values of I'_r greater than 90° and therefore is not a physically real solution. This leaves us with only one possible θ value, resulting from the inversion of our original anomalies and ranging from -160° to -180°. In our case $I_o = 28°$ and $\alpha = 110°$ which means that $I' = 30°$ from eq. (2).

FIGURE 4

Phase shifted magnetic profiles compared with

a symmetric spreading model at top and a non-

symmetric model (spreading from only one side

of a ridge) at the bottom. The degree of phase

shifting is indicated in parentheses next to the

identification of each profile. The dotted

line locates the central valley of the Central

Basin Fault. Anomaly numbers are based on the

system of Heirtzler et al. (1968)

AGE (M.Y.)   AXIS   AGE (M.Y)

50   45   40 40   45   50   SCLATER ET AL.(1974)

55   50   45   45   50   HEIRTZLER ET AL.(1968)

SOUTH   22   21   20   19   18   17 17   18   19   20   NORTH

GAMMAS

500
0
-500   SYNTHETIC

75
-75   KH 72-1 (200°)

75
-75   UM 63-1 (160°)

75
-75   ANTIPODE 13 (160°)

75
-75   CONRAD 1107 (160°)

75
-75   TAS 7 (160°)

75
-75 _291_   290 GC 31 (180°)

150
-150   N PAC 41° N

0   50   100

NAUTICAL MILES

21   20   19   17   14   13
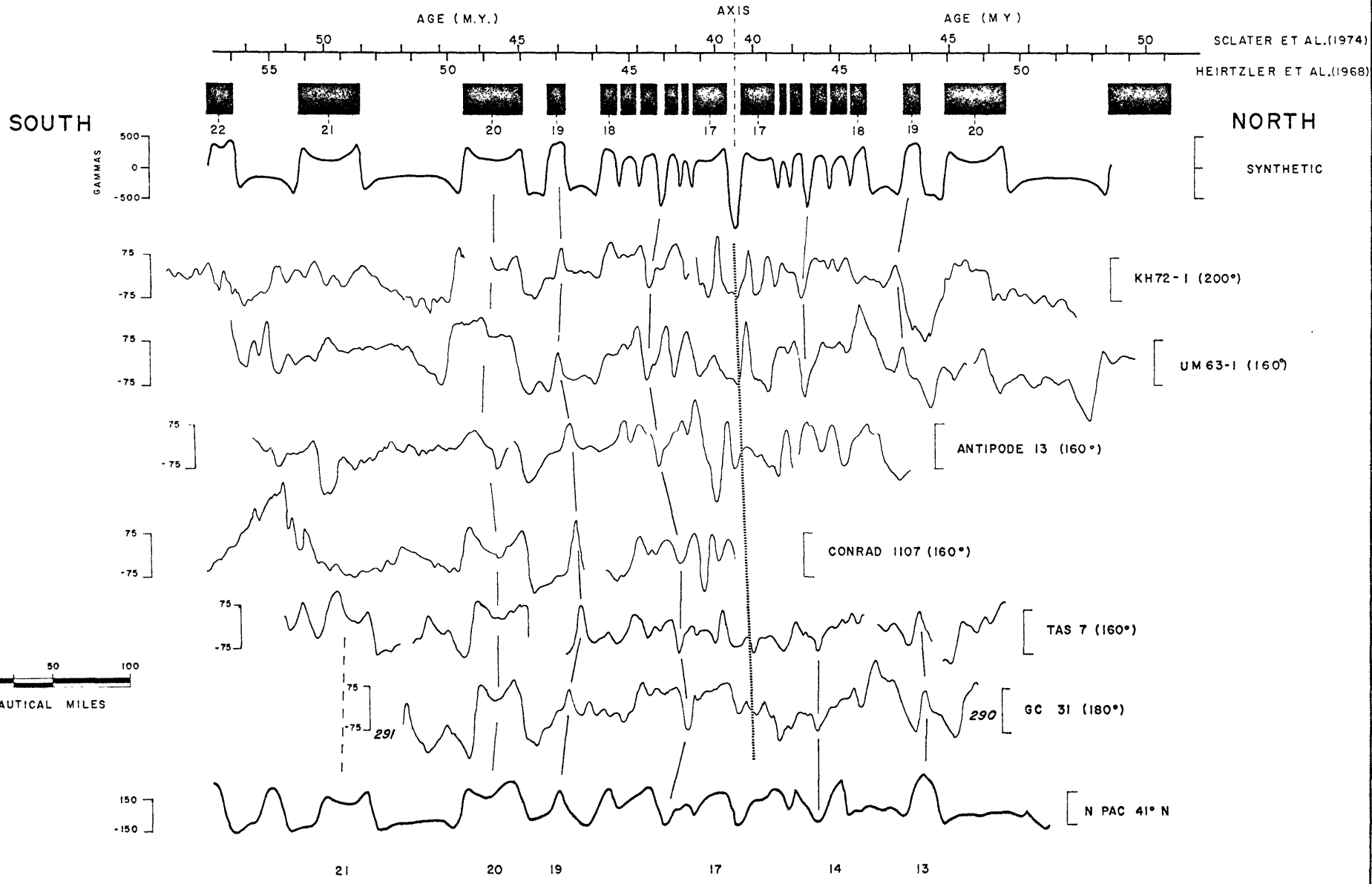
Thus I'_r can range from $-10°$ to $-30°$ according to eq. (1).
If α has remained constant, then these anomalies were formed
between $-4.5°$ and $-15°$ latitude; if α has changed, the value
of the paleolatitude could range from $0°$ to $-16°$. These
results disagree with earlier solutions given by Ben-Avraham
et al. (1972) which predict formation north of the equator.
It is unfortunate that we cannot determine if α has changed
since these anomalies were formed. Changes in α near the
equator affect the amplitude of the anomalies (the value of
C in eq. (3)) rather than their skewness (Schouten, 1971),
and too little is known regarding the predicted amplitudes of
magnetic anomalies for us to use that as a criterion (Cande
and Schouten, in prep.).

Identification of Anomalies

The nannofossil ages reported from leg 31 of the Glomar
Challenger (JOIDES, 1973) were all in the Eocene or younger,
except for hole 294/295 which was reported to be Paleocene.
This last date has been recently revised and now seems to be
much the same as the others (Karig, personal communication).
At first these dates were thought to rule out the possibility
of symmetric spreading from the Central Basin Fault (JOIDES,
1973; Karig et al., 1973). We do not subscribe to such a
conclusion. These dates do rule out a speculation by Ben-Avraham
et al. (1972) that his Philippine anomalies might be part of the

Mesozoic. But beyond telling us in what age province to look for matching our anomalies to standard reversals, they tell us little. Spreading rates must have been large, but the direction of spreading is not clearly indicated. We must therefore assume that the anomalies get younger as they approach the Central Basin Fault from the south, so as not to rule out the symmetric model from the outset. We cannot say a priori whether this is solid ground upon which to build further analysis. If we assume this nonetheless and then look at sea-floor spreading anomalies of 50 m.y.b.p., we find that there exists from anomaly numbers 22 to 17 a progression from longer wavelengths to shorter. This fits the general trend of long to short to long wavelengths observed in the anomalies of Figure 3 as one crosses the Central Basin Fault. By using the standard North Pacific profile at 41°N (Pitman et al., 1968), shifting it to remove its slight skewness and changing its horizontal scale to form a best fit, we produce the model at the bottom of Figure 4. This is a non-symmetric model starting at anomaly number 21 and ending at number 13, where only the direction of spreading has been assumed. To contrast it with the symmetric model, we have constructed the top model of Figure 4 from a standard magnetics program (McKenzie and Sclater, 1971). It adheres to the same fit in the region south of the Central Basin Fault as does the non-symmetric model. Notice however that they are not

identical reproductions. The synthetic anomalies include some additional short reversals not found in the Pacific data. This is to be expected since the reversal history for that age is not known with great precision.

Except for these few short reversals, both models are the same south of the Central Basin Fault. If we now look at the north side where the models should differ, it appears that the symmetric model forms a better match to our lineations. The primary basis for this is the presence of some positive events that do not appear in the non-symmetric model. It should be noted however, that both models show the same general trend from long to short to long wavelengths already noted in the real data. We therefore cannot be absolutely certain which model to discard on the basis of anomaly matching alone.

Testing the Models

The location of JOIDES sites 290 and 291 occur at either end of the anomalies presented in Figure 4. This allows us to use the dates of these sites for confirmation of our identifications to the south of the Central Basin Fault, and as a test for the age that each model would predict to the north. In order to do this we must: (1) analyze the fossil record for sites 290 and 291 to determine their range of possible

ages, and (2) date our anomalies by the use of a standard time scale.

Table I presents the JOIDES data for sites 290, 291, 19 and 32. The latter two are sites of simlilar age to the former but taken from other ocean basins. They were used by Sclater et al. (1974) to revise the Heirtzler et al (1968) time scale, which was found to predict progressively older ages than the fossil record. We will refer to their revision as the modified Heirtzler scale. Notice that this revision still does not account for all of the discrepancies between fossil and magnetic ages. Site 19 has a magnetic anomaly age based on the modified Heirtzler scale of 1-6 m.y. older than its nannofossil age as determined according to the Berggren (1972) Cenozoic time scale. A similar discrepancy appears in the ages for site 291, where we predict a magnetic anomaly age 3-10 m.y. older than the nannofossils allow. Since site 19 has well defined magnetics but still shows a similar variance, we believe that this justifies our magnetic identifications to the south of the Central Basin Fault.

Let us now analyze what our two spreading models predict for site 290. The magnetic vs. fossil ages should exhibit a similar pattern as do those of site 32. This means that they should agree to within 3 m.y. At first glance this would preclude the symmetric model, but actually this evidence is not very convincing. In Figure 5, which is a graph of

SITE	LAT	LONG	CONTACT CORE	DIAGNOSTIC CALCAREOUS ZONE	NANNO-FOSSIL AGE[1]	MAGNETIC ANOMALY	HEIRTZLER et al.(1968) AGE	SCLATER et al.(1974) AGE
19	28°32.1'S	23°40.6'W	12	Chiphragmolithus quadratus	46-48	Just be-fore 21	53-56	49-52
291	12°48.4'N	127°49.9'E	5	Discoaster barbadiensis Cyclococcolithus formosus	38-43	End of 21	50-52	46-48
32	37°07.6'N	127°33.4'W	14	Coccolithus bisectus	34-37.5	13	37-39	35-37
290	17°44.9'N	133°28.1'E	9	Reticulofenestra hillae	36-38	Just before 19	47-49	44-46
				R. umbilica		Just after 13	36-38	34-36

1 From Berggren (1972) and Bukry (1974)

TABLE I

Anomaly	DISTANCE FROM CBF (NM)						Average		AGE (MY)	
	KH 72-1	UM 63-1	ANT 13	C 1107	TAS 7	GC 31	N.M.	K.M.	Heirtzler	Sclater
Beginning of 21					277		277	513	54.2	50.7
Beginning of 20	183	189	177	180	180	183	183±6	339±11	49.6	46.4
19	114	117	114	109	109	120	114±6	211±11	47	44
Between 17 & 18	54	57	54	26*	46	43	51^{+6}_{-8}	95^{+11}_{-15}	44.1	41.4
End of 17	14	14	31*		17	14	15^{+2}_{-1}	28^{+4}_{-2}	42.3	39.7
Between 15 & 14 or Between 17 & 18	-43	-46	-34		-46	-43	-43^{+3}_{-9}	-80^{+5}_{-17}	39.5 / 44.1	37.1 / 41.4
19 or 13	-100	-109			-112	-112	-109^{+3}_{-9}	-202^{+5}_{-17}	47 / 38	44 / 35.8
Beginning of 20	-166	-160					-163±3	-302±5	49.6	46.4
JOIDES Site 290					-149		-149	-276		
JOIDES Site 291					229		229	424		

* Not included in average

TABLE II

FIGURE 5

Graph of distance from the Central Basin Fault

vs. age, taken from values measured in figure

4 and listed in Table II. Symmetric vs. non-

symmetric models for ages given by the revised

Heirtzler time scale (Sclater et al., 1974) are

compared to nannofossil ages for JOIDES sites

290 and 291. Arrows indicate ages adjusted to

better represent the basement contact.
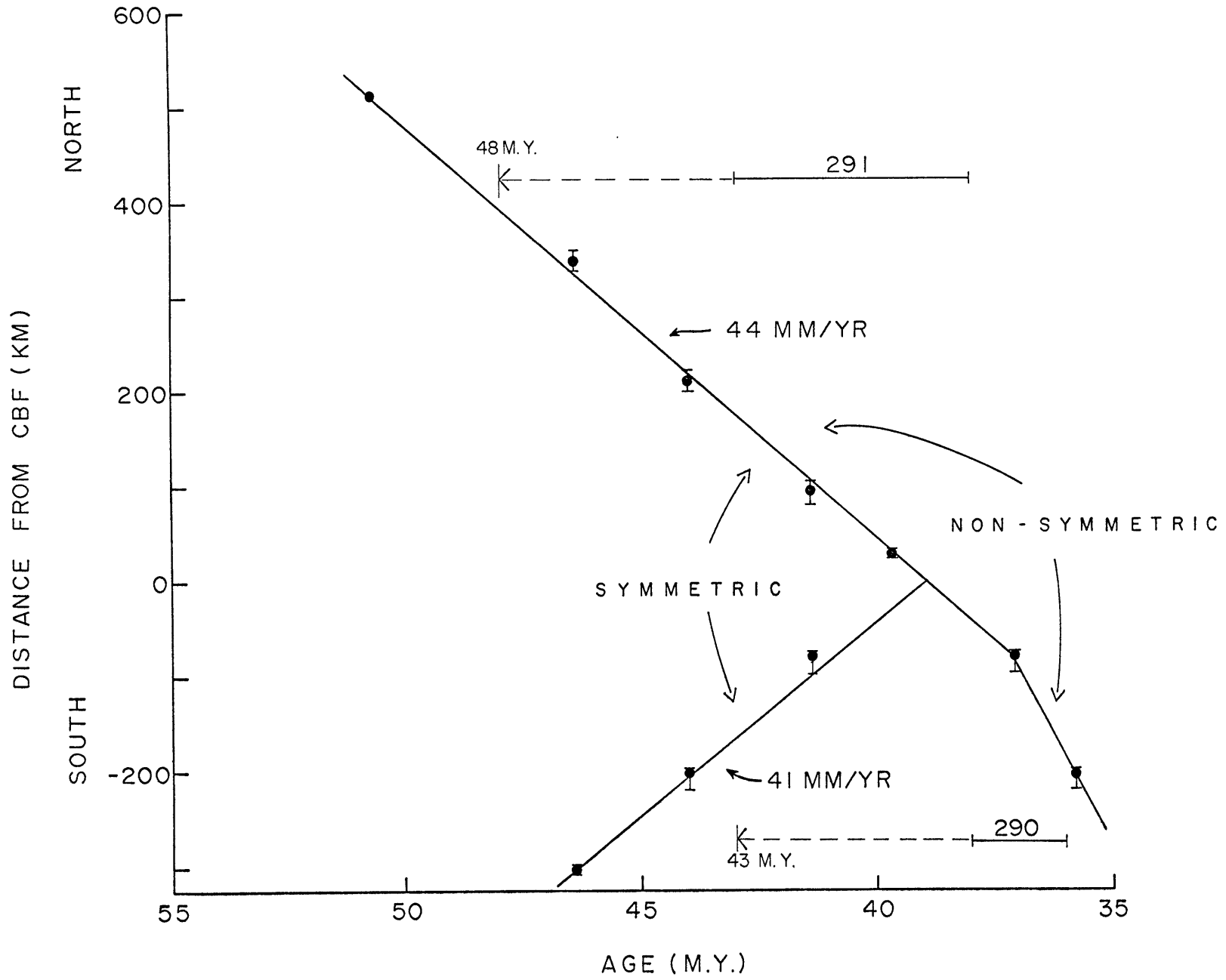
measurements taken from Figure 4 and tabulated in Table II,
neither the symmetric nor the nonsymmetric models uniquely
fit the JOIDES data. The primary reason for this is the
difficulty in dating the JOIDES holes due to a lack of fossils
close to basement for site 291 and failure to hit basement
for site 290. If sedimentation rates are extrapolated to
the basement of site 291, one obtains an age 5 m.y. older
than the lower most nannofossils indicate (Ingle et al., in
press). If one does the same for site 290, an age in excess
of 43 m.y.b.p. results.

These paleontological ages, once corrected to better
represent true basement (dotted arrows in Figure 5), have now
become much more definitive. Site 291 becomes an even better
fit to our magnetic identifications. Site 290 now adds further
evidence in favor of magnetic symmetry across the Central Basin
Fault, since it is unreasonable to suggest that magnetic
basement could be younger than the age of the earliest sediments.

BATHYMETRIC DATA

A summary diagram (Figure 6) shows our magnetic lineations and their possible interpretation. The lineations of Figure 4 are mapped onto the anomalies of Figure 2 for several specific reversals. We also include the bathymetric trace of the Central Basin Fault indicated in Figures 4 and 7. Notice that in this limited area it runs at a 20° angle to its overall trend, and is nearly parallel to our magnetic lineations. It seems highly unlikely that this would occur unless both magnetics and bathymetry are genetically related. This could only mean that this section of the Central Basin Fault was a former spreading center. Further confirmation is seen in Figure 7, which includes profiles of bathymetry projected along the same direction as the magnetics of Figures 3 and 4. We observe that:

(1) In all but the Tasaday 7 profile the Central Basin Fault is a sharp trough bounded by two peaks, which bottoms at a depth equal to that of the outer flanks. The Tasaday 7 profile has this same sharp trough but also has a broad trough next to it, which somewhat distorts the pattern.

(2) If a smooth average is drawn through the profiles, the area immediately adjacent to the Central Basin Fault is elevated relative to the flanks. This can be observed even though the flanks of several profiles are distorted by the outer rise of the Philippine Trench (Watts and Talwani, 1974)

FIGURE 6

Map of magnetic lineations (heavy lines) and

their possible interpretation according to

the symmetric   spreading

model . Less certain identifications are dotted.

Heavy dashed line indicates the central valley

of the Central Basin Fault which occurs

between peaks on either side. Total extent

from peak to peak is indicated by shaded

region.

20°N

2000

LUZON

290

19

19

3000

292

2000

17

17

15°N

20

19

19

20

291

21

10°N

120°E   125°E   130°E   135°E

F1
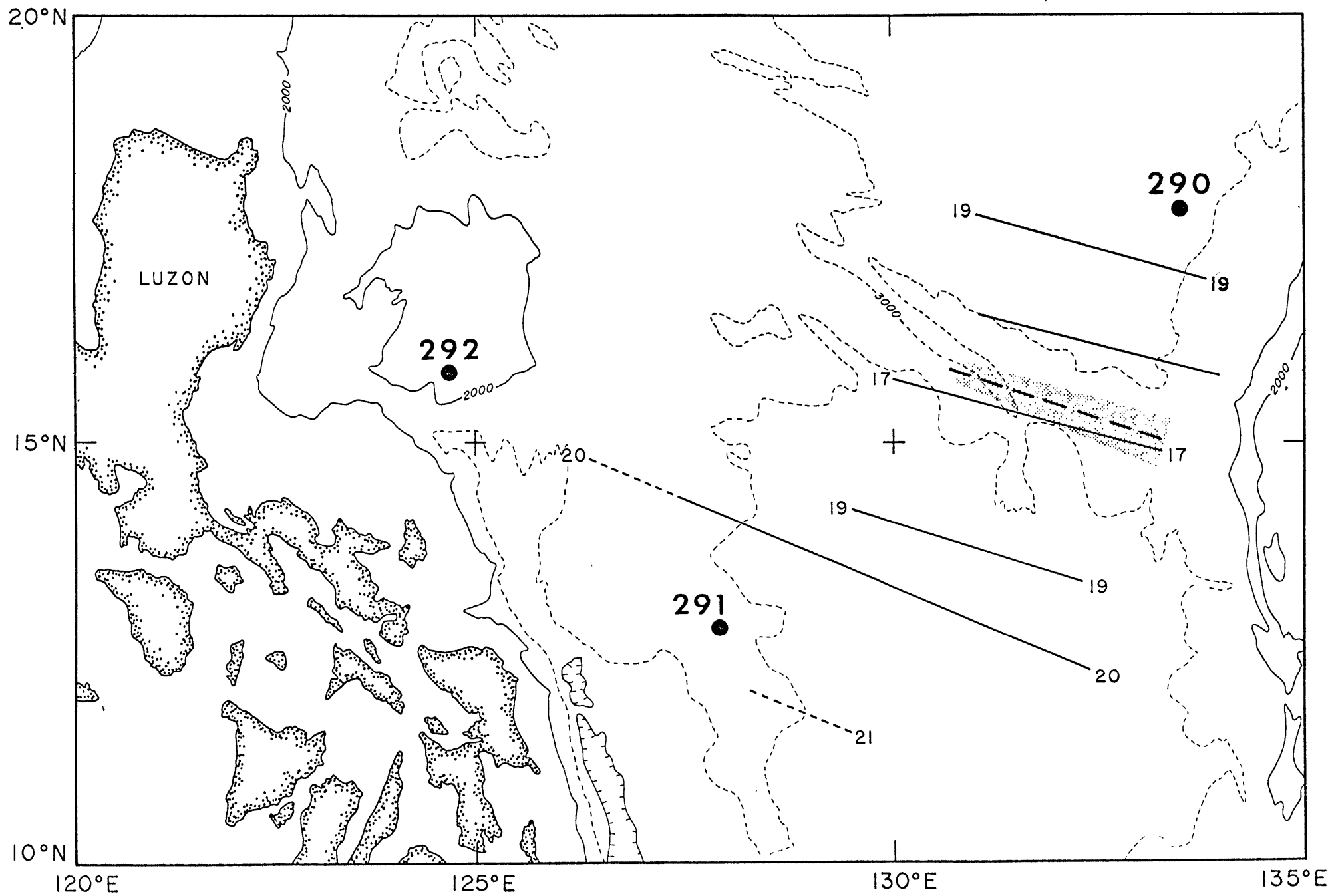
FIGURE 7

Bathymetric profiles across the Central Basin

Fault projected along a direction of N 21°E.

Dashed line represents visual smoothing of

overall topographic trends.

SOUTH
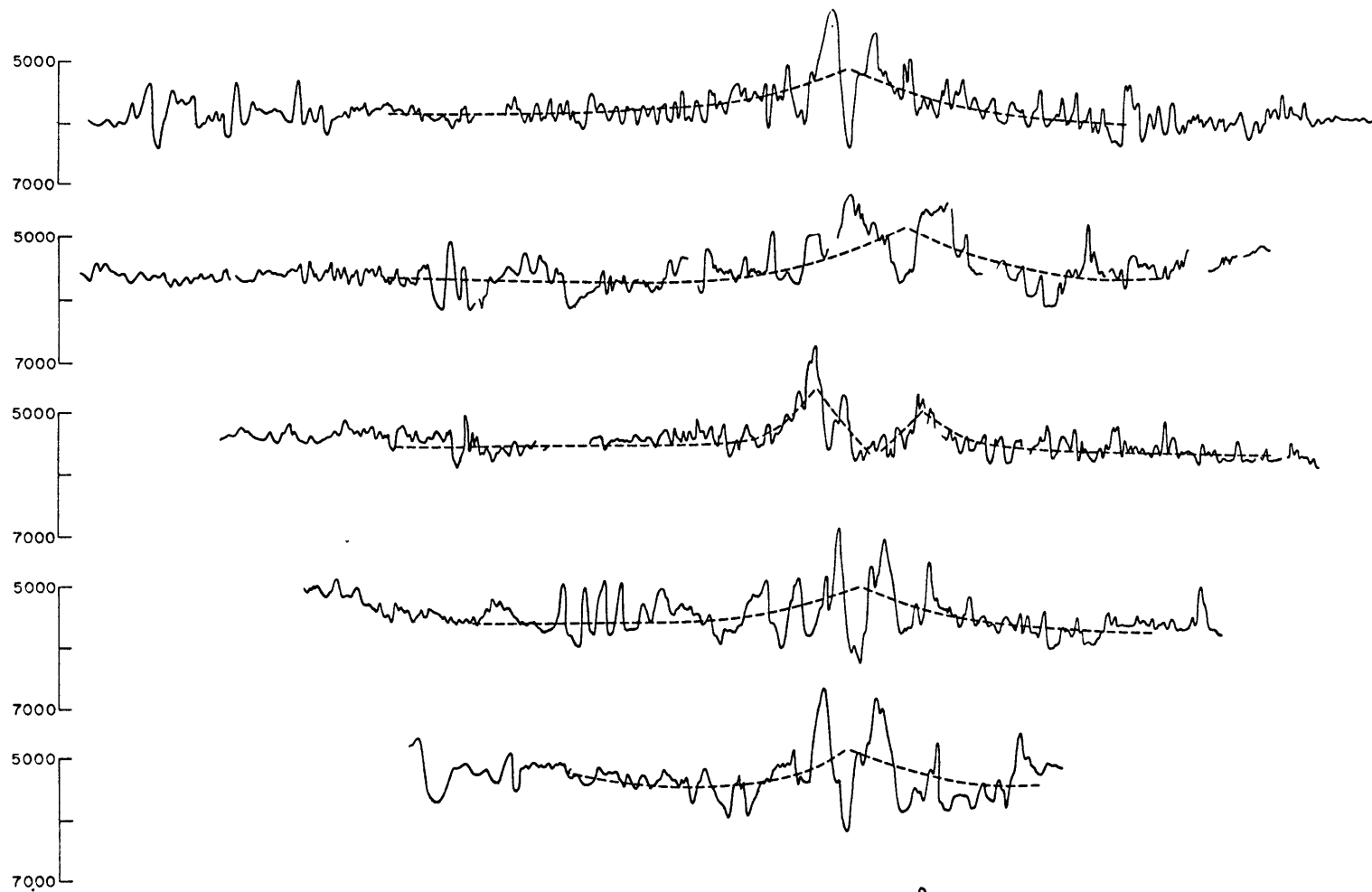
NORTH
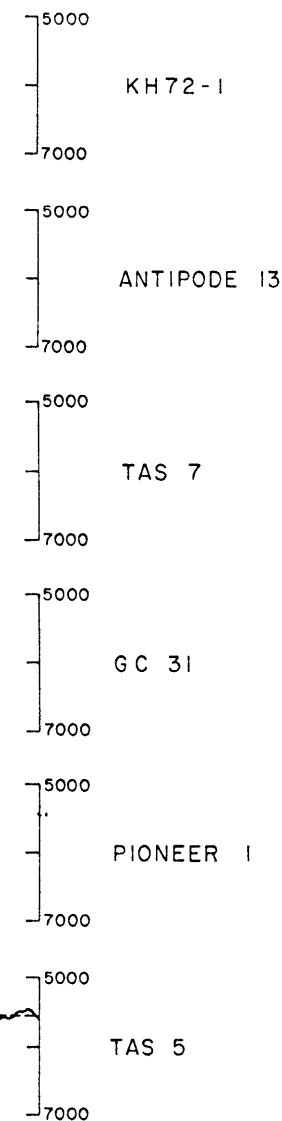
DEPTH (UNCORRECTED METERS)

5000

7000

5000

7000

5000

7000

5000

7000

5000

7000

5000

7000

KH72-1

ANTIPODE 13

TAS 7

GC 31

PIONEER 1

TAS 5

0   50   100

NAUTICAL   MILES
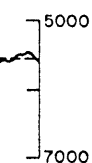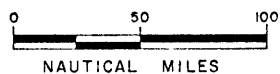
(southern sections of profiles ANT 13, TAS 7, GC 31 and
PIONEER 1) and the Palau-Kyushu Ridge (northern sections of
profiles ANT 13 and PIONEER 1). However, the rate of drop
in elevation differs for each profile. In the GC 31 profile
it is somewhat obscurred by large amplitude, short wavelength
fluctuations. The TAS 5 line which is located to the north
of the magnetic lineations (Figure 2) shows a slight drop
that is not well determined. The Central Basin Fault has an
anti-symmetric shape in this profile which differs from those
to the south.

A detailed survey during leg 5 of cruise Tasaday indicates
that at that point the Central Basin Fault is a N-S en eschalon
feature which appears highly fractured (Karig, personal
communication). This could have occurred during a later
tectonic activity postdating its spreading history and thereby
changing its original character. If such activity was strongest
to the north, it might explain why the bathymetry and magnetic
patterns become more confused there. The remaining question
is whether our region of study to the south represents a
small remainder of the original configuration of the entire
Central Basin Fault or whether the West Philippine Basin
was always a collection of distinct tectonic provinces.
Unfortunately the answer is at present beyond the limits of
our data to decide.

The profiles south of the TAS 5 track suggest two

further complications. First, the deep trough at the axis
of the Central Basin Fault is morphologically similar to
slow spreading ridges ($v_{1/2}$ < 20 mm/yr) which contradicts
our magnetic anomaly evidence (Fig. 5) of a faster spreading
rate ($v_{1/2}$ = 41-44 mm/yr). The faster spreading rate is
also supported by the sediment pattern which shows a thin
(<200 m) and uniform layer. Perhaps we can explain this
conflict by suggesting that the spreading decreased just
before it stopped, thereby producing a limited extent of
greatly elevated and rifted topography. This would also
help explain why the magnetic pattern changes so drastically
from one profile to the next in the vicinity of the Central
Basin Fault. Second, if we plot depth vs. age, we see from
table III and Figure 8 that all the depths, both for JOIDES
ages and for ages based on our magnetic anomalies, are
universally greater than for the North Pacific (Sclater et
al., 1971). Thus according to these plots, the age of this
basin should be greater than 80 m.y.b.p.

We do not believe that the depth of this basin gives a
true indication of age for the following reasons:

(1) Nowhere in JOIDES cores 290-295 are there sediments
older than the Paleocene (Ingle et al., in press).

(2) The correspondence of the younger sediment ages for
JOIDES cores 290 and 291 to a plausible magnetic anomaly
identification seems too coincidental to be an artifact. In
our view this rules out the older "depth" age even if possible
magnetic anomaly identifications could be found in the Mesozoic.

CRUISE ID	SMOOTHED BATHYMETRIC DEPTHS (uncorrected km)		
	South Flank	Ridge Crest	North Flank
KH 72-1	5.8	5.1	6.0
ANT 13	5.7	4.8	5.7
TAS 7	5.6	4.7	5.7
GC 31	5.6	5.0	5.8
PIONEER 1	—	4.9	—
TAS 5	5.3	4.9	5.6
AVERAGE	5.6±0.3	4.9±0.2	5.8±0.2

TABLE III

FIGURE 8

Depth of smoothed topography vs. age. Data for

the North Pacific (circles between heavy lines)

is from Sclater et al. (1971) and is compared

to values for JOIDES sites 53, 54, 290 and 291

(JOIDES, 1969, 1973). We also plot values treating

the Central Basin Fault as a symmetric spreading

ridge (triangles) taken from Table III and figure

5. Dashed line connects ridge crest to flank.
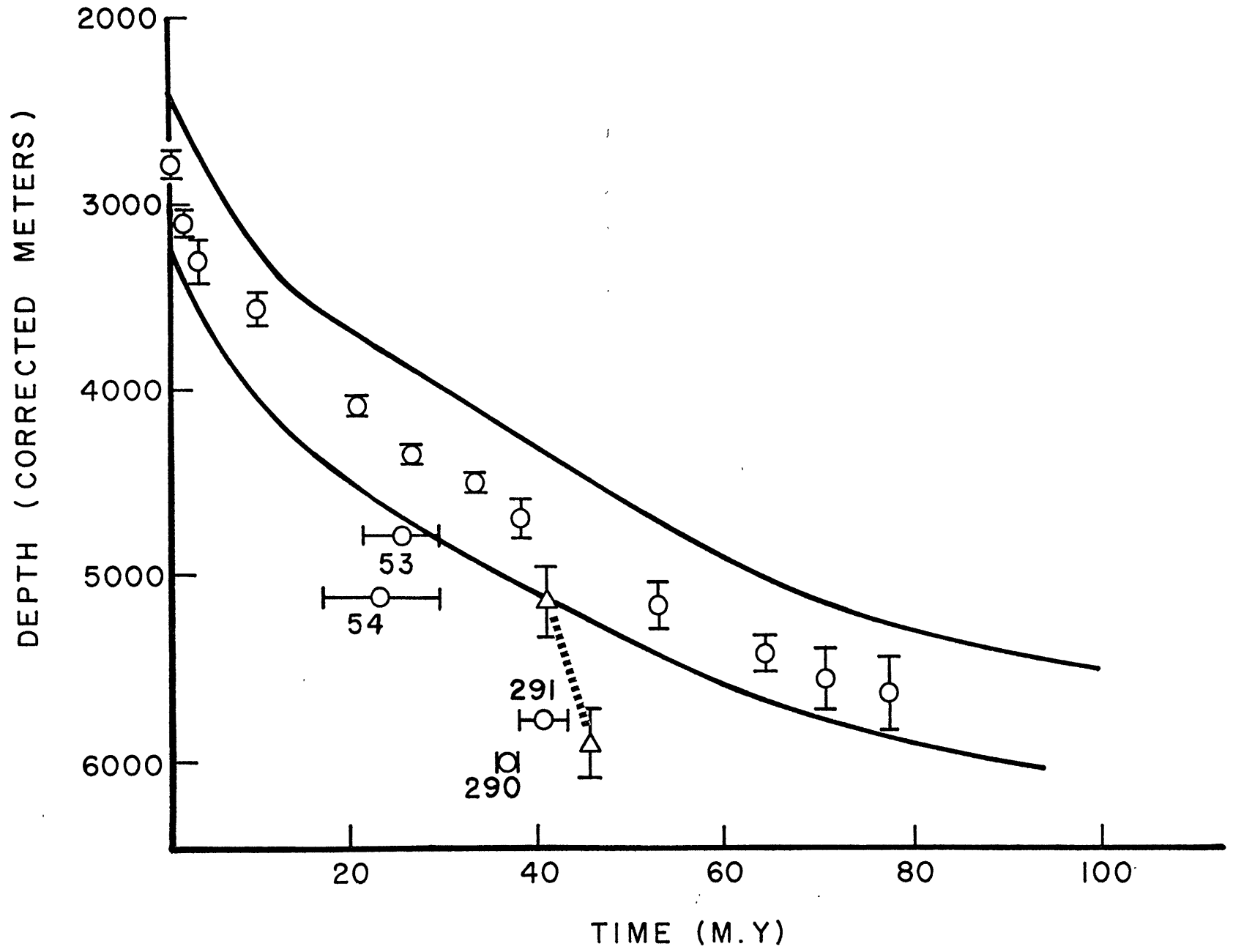
(3) There are recent seismic studies which indicate that the crust in the West Philippine Basin is not similar to North Pacific crust (Shimamura et al., 1975; Henry et al., in press). In particular, the thin "oceanic" crust suggested by the refraction studies of Henry et al. (in press) can help to explain the occurrence of a 1 km negative anomaly without a correspondingly large negative gravity anomaly (Sclater et al., in prep.).

CONCLUSIONS

All of the data presented in this paper can be accounted for by treating the Central Basin Fault as a spreading center that slowed and stopped 40 m.y. ago. The ridge-like bathymetry and symmetry in the magnetic lineations are the strongest support for such a conclusion. The ages of JOIDES sites 290 and 291 also can be explained with this model, but because of the incomplete agreement between fossil ages and magnetic time scales for this period, coupled with the limited extent of our lineations and the fast spreading rates needed to match the anomalies, they cannot remove all uncertainty in our identifications

It is very tempting to go beyond the limit of such a conclusion and propose a comprehensive tectonic model that connects the formation of this basin with a proto-Pacific reconstruction. Such an attempt has already been made by Uyeda and Ben-Avraham (1972) and Uyeda and Miyashiro (1974). They propose that the Philippine Ridge (Central Basin Fault)

was connected by means of a long transform fault to the
Kula-Pacific ridge system. When the Pacific plate changed
its direction of motion from north to north-west 42-44 m.y.
ago (Claque and Jarrard, 1973), the transform fault became a
subduction zone, leading to the start of inter-arc spreading
and the formation of the Parece Vela Basin. There are several
specific problems with such a model:

(1) The Palau-Kyushu Ridge is asserted to be the current
expression of the transform fault between the Kula-Pacific
and the Philippine Ridges. If so, the fault must have extended
for several thousand kilometers. This is much greater than
for most presently active transform faults. The only purely
oceanic transform fault of such a large extent that has been
magnetically documented is the Ninety-east Ridge (Sclater and
Fisher, 1974), which is no longer active. There are also
other interpretations of the origin of this feature (Bowin,
1973). Other long transform faults are either on continental
crust (San Andreas Fault) or are not yet supported by unequivocal
data (the connecting link between the South Atlantic Ridge and
the West Indian Ocean Ridge). It is possible that the mechanics
of ocean floor spreading make the possibility of such a long
transform fault lasting over an extended period of time
unlikely (Lachenbruch, 1973).

(2) The magnetic anomalies identified in this paper appear
to have originated near to or just south of the equator. This

invalidates the location of the ridge in its present latitude
when spreading ceased, which is central to the Uyeda and
Ben-Avraham (1972) model. Their model also predicts very
different subsequent motions between the Philippine and
Pacific plates. It is interesting to note, however, that
our results (formation of anomalies from 0° to -16°) can be
explained by using the same pole of "absolute" rotation for
the Philippine plate as has been determined for the Pacific
plate by the hot-spot theory (Claque and Jarrard, 1973). A
pole at 72°N, 83°W and a rate of 13.10^{-7} deg/yr yield a
paleolatitude of -10° for 50 m.y.b.p.

(3) The elevation of the West Basin is depressed by
1 km from standard oceanic depths of corresponding ages taken
from the North Pacific (Sclater et al., 1971). Such a negative
residual depth anomaly should produce a negative gravity anomaly
of 30 ± 10 mgals if it follows a similar relationship as the
North Atlantic (Sclater et al., in press). This is not observed.
It indicates that the crustal structure of the West Basin is
different from that of the North Atlantic and possibly from
other ocean basins. It follows that it could not have originated
in an identical process.

References

Barazangi, M. and J. Dorman, World seismicity map of ESSA coast and geodetic survey epicenter data from 1961-1967, Bull. Seismol. Soc. Am., 59, 369-380, 1969.

Barker, P.F., A spreading center in the East Scotia Sea, EPSL, 15, 123-132, 1972.

Ben-Avraham, Z., J. Segawa and C. Bowin, An extinct spreading center in the Philippine Sea, Nature, 240, 453-455, 1972.

Berggren, W.A., A Cenozoic timescale - some implications for regional geology and paleobiogeography, Lethaia, 5, 195-215, 1972.

Bowin, C., Origin of the ninety-east ridge from studies near the equator, J. Geophys. Res., 78, 6029-6043, 1973.

Bukry, D., Coccolith and silicoflagellate stratigraphy, Eastern Indian Ocean, in Von der Bosch, CC., J.G. Sclater, et al., Initial reports of the DSDP, 22, 601-605, Washington, D.C., (U.S. Govt. Printing Office), 1974.

Cande, S. and J.L. LaBreque and K. McCamy, Application of Linear filtering to marine magnetic anomalies, Paleo - poles and ridge crest processes (Abstract), Trans. Am. Geophys. Union, 54, p. 252, 1973.

Cande, S. and H. Schouten, Paleomagnetic poles from sea-floor spreading anomalies (Abstract), Trans. Am. Geophys. Union, 53, 362, 1972.

Cande, S. and H. Schouten, Paleomagnetic poles from sea-floor spreading anomalies, in preparation.

Chapman, S. and J. Bartels, Geomagnetism, Oxford Press, 1940.

Chase, T.E. and H.W. Menard, Bathymetric atlas of the Northwest Pacific Ocean, 1969.

Clague, D.A. and R.D. Jarrard, Tertiary Pacific plate motion deduced from the Hawaiian-Emperor chain, BGSA, 84, 1135-1154, 1973.

Fitch, T.J., Plate convergence, transcurrent faults, and internal deformation adjacent to Southeast Asia and the Western Pacific, J. Geophys. Res., 77, 4432-4460, 1972.

Gay, S.P., Standard curves for interpretation of magnetic anomalies over long tabular bodies, Geophysics, 28, 161-200, 1963.

Hayes, D.E. and J. Ringis, Sea-floor spreading in the Tasman Sea, Nature, 243, 454-458, 1973.

Heirtzler, J.R., G.O. Dickson, E.M. Herron, W.C. Pitman and X. LePichon, Marine magnetic anomalies, geomagnetic field reversals, and motions of the ocean floor and continents, J. Geophys. Res., 73, 2119-2136, 1968.

Henry, M., D.E. Karig, and G.G. Shor, Two seismic refraction profiles in the West Philippine Sea, in the Initial reports of the Deep Sea Drilling Program, 31, edited by Ingle, Karig et al., U.S. Govt. Printing Office, Washington, D.C., in press.

Hess, H.H., Major structural features of the western and north Pacific, BGSA, 59, 417-446, 1948.

Ingle, J.C., D.E. Karig, H.H. Bouma, C.H. Ellis, N. Haile, I. Koizumi, H.Y. Ling, I. MacGregor, C. Moore, H.

Ujiie, T. Watanabe, S.M. White, and M. Yasui, Initial reports of the Deep Sea Drilling Program, 31, U.S. Govt. Printing Office, Washington, D.C., in press.

Isezaki, N. and S. Uyeda, Geomagnetic anomaly pattern of the Japan Sea, J. Marine Geophys. Res., 2, 51-59, 1973.

JOIDES, Scientific staff, Deep-Sea Drilling Project, Leg 31, Geotimes, 18, 22-25, 1973.

Karig, D.E., Ridges and basins of the Tonga-Kermedec island arc system, J. Geophys. Res., 75, 239-254, 1970.

Karig, D.E., Structural history of the Mariana island arc system, BGSA, 82, 323-344, 1971a.

Karig, D.E., Origin and development of marginal basins in the Western Pacific, J. Geophys. Res., 76, 2542-2561, 1971b.

Karig, D.E., Evolution of arc systems in the Western Pacific, Annual Review of Earth & Planetary Sciences, 2, 51-75, 1974.

Karig, D., J.C. Ingle, A.H. Bouma, H. Ellis, N. Haile, I. Koizumi, I.D. MacGregor, J.L. Moore, H. Ujiie, J. Watanabe, S.M. White, M. Yasui, and H. Yi Ling, Origin of the West Philippine Basin, Nature, 246, 458-461, 1973.

Lachenbruch, A.H., A simple mechanical model for oceanic spreading centers, J. Geophys. Res., 78, 3395-3417, 1973.

Larson, R. and C.G. Chase, Late Mesozoic evolution of the Western Pacific Ocean, BGSA, 83, 3627-3644, 1972.

Larson, R. and W.C. Pitman, World-wide correlation of Mesozoic magnetic anomalies, and its implication, BGSA, 83, 3645-3662, 1972.

Matsuda, T. and S. Uyeda, On the Pacific-type orogeny and
its model-extension of the paired belts concept and
possible origin of marginal seas, Tectonophysics, 11,
5-27, 1971.

McKenzie, D.P. and J.G. Sclater, Heat flow inside the island
arcs of the Northwest Pacific, J. Geophys. Res., 73,
3173, 1968.

McKenzie, D.P. and J.G. Sclater, The evolution of the Indian
Ocean since the late Cretaceous, Geophys. J. Roy. Astr.
Soc., 25, 437-528, 1971.

Pitman, W.C., III, E.M. Herron, and J.R. Heirtzler, Magnetic
anomalies in the South Pacific Ocean and sea-floor spreading,
J. Geophys. Res., 73, 2069-2085, 1968.

Schouten, J.A., A fundamental analysis of magnetic anomalies
over ocean ridges, Mar. Geophys. Res., 1, 111-144, 1971.

Sclater, J.G., Heat flow and elevation of the marginal basins
of the Western Pacific, J. Geophys. Res., 77, 5705-5719, 1972.

Sclater, J.G., R.N. Anderson, and M.L. Bell, Elevation of ridges
and evolution of the Central Eastern Pacific, J. Geophys.
Res., 76, 7888-7915, 1971.

Sclater, J.G. and R.L. Fisher, Evolution of the East Central
Indian Ocean with emphasis on the tectonic setting of the
ninety-east ridge, BGSA, 85, 683-702, 1974.

Sclater, J.G., R.D. Jarrard, and S. Gartner, Comparison of the
magnetic and biostratigraphic time scales since the late

Cretaceous, in von der Borch, J.G. Sclater, et al.,

Initial reports of the Deep-Sea Drilling Project, 22,

Washington, D.C., (U.S. Govt. Printing Office), 1974.

Sclater, J.G., L.A. Lawver, and B. Parson, Comparison of long

wavelength residual elevation and free-air gravity anomalies

in the North Atlantic and possible implications for the

thickness of the lithospheric plate, in press, J. Geophys.

Res.

Shimamura, H., Y. Tomada and T. Asada, Seismographic observation

at the bottom of the Central Basin Fault of the Philippine

Sea, Nature, 253, 177-179, 1975.

Uyeda, S. and Z. Ben-Avraham, Origin and development of the

Philippine Sea, Nature Phys. Sci., 240, 176-178, 1972.

Uyeda, S. and A. Miyashiro, Plate tectonics and the Japanese

Islands: a synthesis, BGSA, 85, 1159-1170, 1974.

Vestine, E.H., Main geomagnetic field, in physics of geomagnetic

phenomena, ed. S. Matsushita and W.H. Campbell, Academic

Press, New York, 1967.

Vogt, P.R., C.N. Anderson, and D.R. Bracey, Mesozoic magnetic

anomalies, sea-floor spreading and geomagnetic reversals

in the southwestern North Atlantic, J. Geophys. Res.,

76, 4796-4823, 1971.

Watts, A.B. and M. Talwani, Gravity anomalies seaward of deep-sea

trenches and their tectonic implications, Geophys. J.R.

Astr. Soc., 34, 1-34, 1974.

ACKNOWLEDGEMENTS

SECTION III

PALEOMAGNETISM OF DSDP SEDIMENTS AND BASALT, PHASE

SHIFTING OF MAGNETIC ANOMALIES, AND ROTATIONS OF THE

WEST PHILIPPINE BASIN

ABSTRACT

A paleomagnetic study of sediments from DSDP sites 290, 292 and 294 suggests that the West Philippine Basin originated between 5°S and 10°S. Results for site 292 are particularly consistent; a group of 20 closely spaced samples at the sediment-basalt interface has a mean paleolatitude and 95% confidence interval of ±4.9°±2.0°. This is much more definitive than a group of 36 basalt samples from the same site which shows a possible range of ±11.4°±21.0°. This large interval is due to an incomplete sampling of secular variation which is not a problem for groups of sediment samples. The basalt is less stable than the sediment and may be contaminated by viscous components, although a study of VRM acquisition during 1000 hrs. in both a 1.0 and 0.5 oe field suggests that laboratory measurements may overestimate the actual viscous growth which occurs in geologic time.

Crustal origin of the West Philippine Basin in southern latitudes is also consistent with the phase shifting of marine magnetic anomalies which must be inverted to be matched with a set of world-wide Eocene reversals. Two well-defined paleomagnetic pole positions are determined if the low amplitude of these East-West anomalies, when compared to similarly oriented anomalies in the Pacific and Indian oceans, is due to a rotation of this plate. One of these is consistent with paleopoles calculated from the "absolute" motion of the Pacific and directions of relative motion between the Philippine and Pacific plates. This suggests a clockwise rotation of 60°

between the Philippine plate and the magnetic pole and is similar to results from the study of Miocene rocks on Guam. This may imply that both Guam and the West Philippine Basin have undergone the same past plate motion and that the rotation of Guam is not due to a simple bending of the Mariana arc.

INTRODUCTION

There are essentially four methods by which we can
determine the rotations of the plates relative to an external
frame of reference. These are: (1) the paleomagnetic study
of basalts and sediments, (2) the phase or shape analysis of
linear, sea-floor spreading and seamount magnetic anomalies,
(3) the bathymetric mapping of hot-spot traces, and (4) the
location of deep water regions of high sedimentation, which
are assumed to be produced within $\pm 5°$ of the paleoequator.
If it is then assumed that the earth's paleomagnetic field
has time-averaged over 10^4 to 10^5 years to an axially geocentric
dipole concordant with the spin axis [Opdyke, 1972], and
that hot spots have remained fixed with respect to this same
axis, then each of these measurements are directly comparable.
Such 'absolute' motions have been determined in this manner
for the South Atlantic [Phillips and Forsyth, 1972; Lowrie
et al., 1973b], North Pacific [Francheteau et al., 1970;
Claque and Jarrard 1973; Harrison et al., 1975] and Indian
oceans [McKenzie and Sclater, 1971; Blow and Hamilton,
1975], and results based on the different techniques are
generally consistent [Peirce, in press]. These studies have
been particularly successful in recording the degree of
northward motion since the Cretaceous, which is an especially
important characteristic of the Pacific and Indian plate
motions.

It is the attempt of this paper to use some of these
same techniques for placing constraints on the early history

and subsequent motion of the Philippine plate. A comparison
of the 'absolute' motions of the Pacific and Philippine
plates can hopefully lead to some understanding of how these
two plates have moved relative to each other. This is
important since the nature of relative motions produced by
inner-arc spreading is not well understood. Determinations
of instantaneous motion are based almost entirely on fault
plane solutions [Katsumata and Sykes, 1969; Fitch, 1972],
and the results are only poorly constrained as evidenced by
the many different locations of possible Philippine-Pacific
poles [Karig, 1975]. Almost nothing certain is known about
motions over a finite length of time.

The primary reason for this is the absence of easily
identifiable magnetic anomalies in both active (young) and
inactive (old) basins of the Philippine Sea. Recently,
however, Louden (1976) has identified some anomalies in the
West Philippine Basin across the Central Basin Fault (Figure
1 and 16). This region is one of the older sections of the
Philippine Sea, but controversy still exists over its exact
age and origin. One theory forms the West Philippine Basin
by inner-arc spreading during an Eocene pulse similar to,
but in a different direction from, that which later opened
the more eastern Parece Vela and Shikoku basins [Karig,
1975]. Another explains it as a remanent of the Mesozoic
Kula-Pacific ridge system which was trapped when the 'absolute'
motion of the Pacific changed direction 40 m.y. ago [Uyeda

FIGURE 1

Bathymetric map of the Philippine Sea from

Chase et al. (1969) with uncorrected thousand

fathom contours and selected DSDP site locations.

The dashed line encloses area of Figure 16.
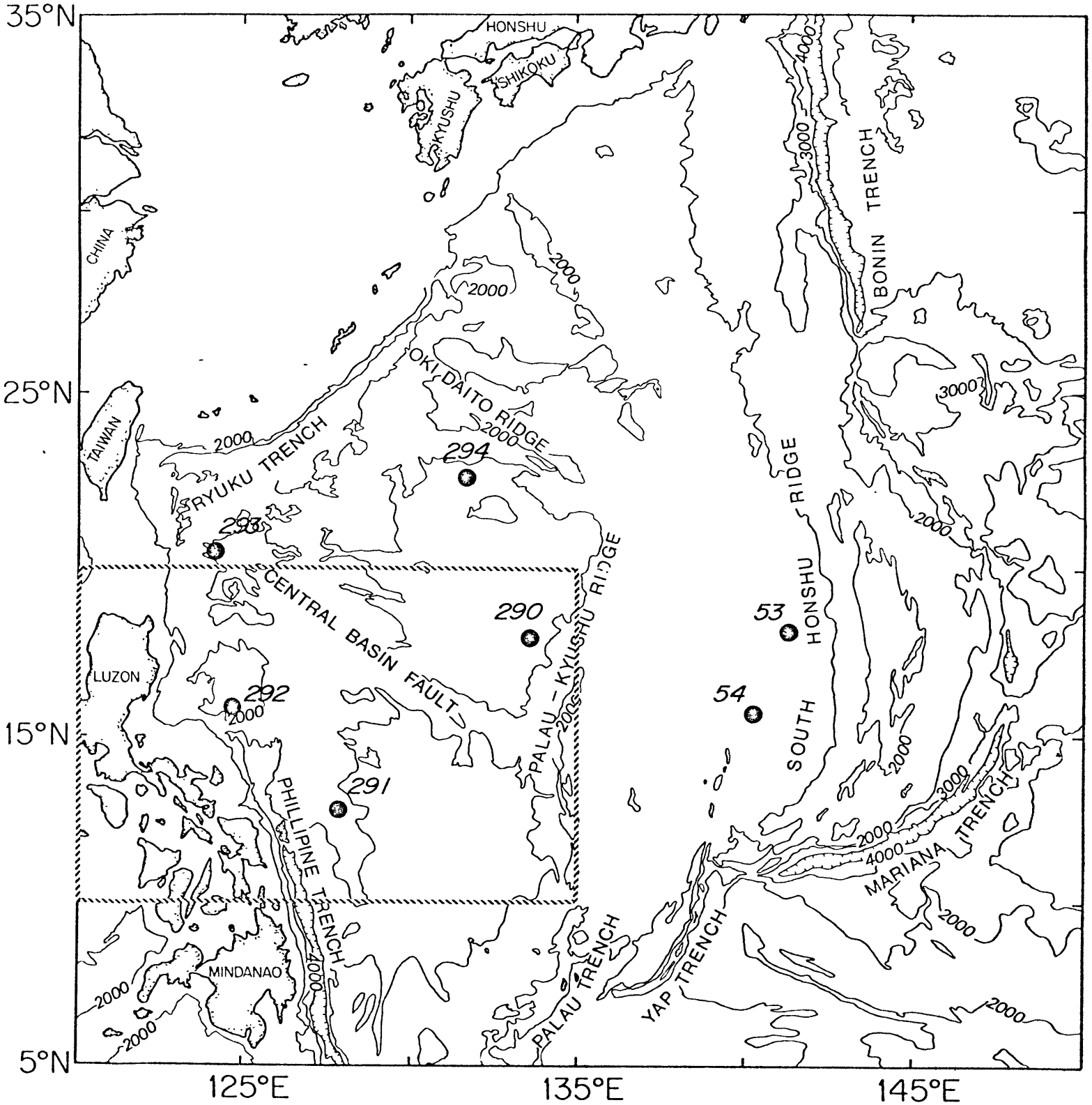
FIG 1

and Ben-Avraham, 1972]. This later theory is inconsistent
with ages based on JOIDES cores, magnetic anomaly identifications
and heat flow averages, which all indicate an Eocene age
[Louden, 1976]. Only the 6 km depth of the basin which
gives a minimum age of 80 m.y. from the depth vs. age curves
of the Pacific [Sclater et al., 1971], is consistent with
this interpretation; but it is not certain whether depth vs.
age curves for major ocean basins can be applied to marginal
basins [Sclater et al., 1976].

Initial analysis of the skewness of the magnetic anomalies
indicated that they must have been formed 0-16° south of the
equator. The total amount of northward motion is very
similar to that of the Pacific plate over the same time
period (40-50 m.y.). In this paper we will add to these
results a study of paleolatitudes derived from sediments
taken at three DSDP sites (290, 292 and 294) and basalt from
one site (292). We also have reanalyzed the magnetic anomalies
using a slightly larger data set. These two analyses (phase
shifting and paleomagnetics) can be combined to determine
geomagnetic pole positions well constrained in latitude but
not in longitude. In addition, the low amplitudes of our
magnetic anomalies suggest that they must have undergone
significant declinational change since they were formed, if
their origins are similar to those of anomalies in other
ocean basins. One of the two possible pole positions that
are consistent with these magnetic anomaly phase and amplitude
criterion plus the paleomagnetic inclinations which we

measure in DSDP sediments and basalt, would require significant
rotations (80-100°) about a relative Pacific-Philippine
pole similar to those determined from present day motions.
Paleomagnetic results for basalts from Guam [Larson et al.,
1975) can also be explained by the same "polar wandering"
curve.

PALEOMAGNETISM OF SITE 292 BASALTS

Introduction

Previous studies of DSDP basalts often show well grouped
inclinations which are consistent with plate reconstructions
[Lowrie, 1974; Blow and Hamilton, 1975; Peirce, in press].
These results have not, however, been nearly as useful as
paleomagnetic data from land basalt upon which the reconstructions
are based, because they lack declination control and often
do not sample separate flow units. This means that they may
not record pole positions for a time interval long enough to
average out non-dipole and dipole fluctuations away from the
spin axis. Angular standard deviations of such variations
can be as large as 20° [Baag and Helsley, 1974]. Another
complication is that many DSDP basalts show a large amount
of viscous remanent magnetization (VRM), which in several
cases has made their inclinations unreliable [Lowrie et al.,
1973a; Peirce et al., 1975].

The only land based paleomagnetic measurements relevant
to the Philippine Sea are those of Larson et al. [1975]

for Miocene volcanic rocks on Guam. Their results suggest

that Guam has not changed latitude since the Miocene, but

has rotated clockwise by 50°. This may record the buckling

of the island arc as the Parece Vela Basin opened and does

not necessarily apply to the earlier history of the West

Philippine Basin. Guam is situated on the boundary between

the Pacific and Philippine plates and its motion may represent

distortions in that boundary rather than the actual plate

motions themselves. It is therefore necessary to look at

the paleomagnetic record of DSDP basalts in the West Philippine

Basin, keeping in mind the probable limitations.

Site 292 on the Benham Rise is the only large volume of

basalt recovered during DSDP leg 31: 76 m of basalt was

cored of which 72 m were recovered. This is a uniform

intersertal to subophitic tholeite with plagioclase and

augite phenocrysts. Some sections show a slightly greenish

color due to alteration effects. Although a few individual

units can be distinguished, there are no major discontinuities

and the entire 72 m probably represents a single flow unit

[Ingle et al., 1975]. The following sections describe the

results of our paleomagnetic study of 36 samples of this

basalt. Measurements of basalt magnetization were made on a

PAR spinner magnetometer operating at 15 Hz.

Alternating Field Demagnetization

Eleven of our 36 samples with a wide range of NRM

intensities (12.0 to $1.8*10^{-3}$ gauss) and inclinations

(+13° to -77°) were subjected to alternating field (AF)

demagnetization of up to 200 oe. peak field. In most cases

measurements were repeated once again at each field value.

We used a two-axis tumbler and a 60 Hz alternating field

which decreased from peak field to zero in 2.5 min. Results

are shown in figures 2 and 3. By 200 oe inconsistent directions

or intensities under double demagnetization made results at

higher fields suspect. Median destructive fields (figure

2) ranged from 42 to 139 oe; 8 of 11 values fell between 75

and 95 oe. This loss of intensity with increasing demagnetization

is much less variable from sample to sample than were the

changes in direction of magnetization (fig. 3). Some directions

varied little from NRM to fields of 200 oe while others had

large variations. Symons and Stupavsky (1974) have suggested

a stability index, PSI, for such cases in which the variation

in magnetization direction is of greatest interest. The PSI

is a measure of the angular change (in millidegrees) per

oersted increase in demagnetizing field; the lower this

value is, the more stable is the remanence. Figure 4 shows PSI

vs. peak demagnetizing fields for our 11 pilot samples. Low

values are reached around 50-75 oe and most fall within the

moderate to low stability range of Symons and Stupavsky [1974].

One disadvantage of the PSI calculation is that it does

not account for inconsistencies between multiple measurements

at the same demagnetizing field. For instance, samples 42-

3-123 and 42-5-121 show low PSI readings at 200 oe (figure

4), but the stereo-net plots (figure 3) show large angular

TABLE I continued:

ID	J_0	J_{75} (10^{-3} Gauss)	J_{100}	D_0	D_{75} (Deg)	D_{100}	I_0	I_{75} (Deg)	I_{100}	λ_{75} (Deg)	d	k (10^{-3} Gauss/oe)	Q_n
45-1-76	3.19	1.28	.725	53.1	44.4	43.5	-13.1	-8.9	-10.9	(-4.5)	14.1	1.34	2.38
45-2-28	5.67	2.57	1.61	65.0	52.8	54.3	-20.0	-16.9	-22.5	-8.6	3.9	1.29	4.40
45-2-78*	.900	.478	.306	172.4	170.5	167.8	-33.4	-22.8	-22.1	-11.9	2.6		
45-2-132	8.90	6.53	4.83	164.2	174.6	175.3	-24.5	-24.9	-24.0	-13.1	1.8	1.26	7.06
45-3-7	9.69	7.50	6.32	38.8	33.3	32.7	-14.6	-18.1	-18.2	-9.3	0.57	1.01	9.59
45-3-126	13.9	11.7	10.1	44.6	44.0	42.9	-31.8	-33.6	-34.2	-18.4	1.1	1.33	10.5
46-1-25	2.70	1.95	1.35	154.0	163.3	164.3	-18.5	-17.9	-22.3	-9.1	2.6	.83	3.25
46-1-136	1.04	.714	.323	46.9	37.0	41.1	-18.6	-16.3	-11.3	(-8.3)	13.1	.82	1.27
46-2-116	2.00	1.42	1.11	13.4	357.5	354.6	-21.5	-10.8	-13.2	-5.4	4.4	1.32	1.52
47-1-47	6.06	1.46	.880	93.9	90.4	82.8	-22.2	-32.5	-36.4	(-17.7)	5.4	1.20	5.05
47-2-31	3.75	.734	.447	97.4	135.9	107.1	-1.9	-4.3	-43.7	(-2.2)	46.9	1.16	3.23
47-2-130	2.81	.943	.489	44.3	23.3	22.0	-15.7	-27.2	-38.4	(-14.4)	7.1	1.27	2.21
	6.32									mean -11.4 (-10.3)		1.28	5.26
										σ 3.8 (6.4)			
										σ/√N 0.8 (1.1)			

The ID gives the core no., section no. and position in cm. from the top of the section to the top of the sample. Each sample is approximately 10 cm^3. Subscripts refer to fields of peak AC demagnetization. λ_{75} is the paleolatitude after 75 oe demagnetization. d is a measure of the reliability as defined in the text. Values in parentheses are only included in the bracked mean and standard deviation. Underlined values represent one measurement; all other values are averages of two separate measurements.

* volume is not measured, but is assumed to be 10 cm^3.

TABLE I: Summary of Remanent Magnetic Properties for DSDP Site 292 Basalts.

ID	J_0	J_{75}	J_{100}	D_0	D_{75}	D_{100}	I_0	I_{75}	I_{100}	λ_{75}	d	k	Q_n
		$(10^{-3}$ Gauss)			(Deg)			(Deg)		(Deg)		$(10^{-3}$ Gauss/oc)	
40-1-103	11.8	6.60	4.29	194.2	197.8	198.6	12.7	13.8	14.0	7.0	1.4	1.17	10.1
41-3-32	3.55	1.84	.959	348.2	333.3	322.5	-21.5	-25.2	-20.1	(-13.2)	9.1	1.52	2.34
41-3-127	4.99	3.27	2.06	217.9	221.1	219.3	-22.1	-21.5	-14.7	-11.1	2.9	1.13	4.42
41-4-51	5.81	2.34	2.09	129.7	130.1	128.0	-13.4	-14.7	-14.6	-7.5	2.0	1.27	4.57
41-5-8	17.2	13.4	10.3	156.2	157.7	157.6	-17.1	-17.2	-17.7	-8.8	0.87	.85	20.2
41-5-117	14.1	12.0	10.2	321.7	320.1	320.5	-17.2	-18.6	-18.0	-9.6	0.57	1.66	8.49
42-2-12	2.44	1.43	.905	119.9	115.1	110.8	-3.4	-7.8	-6.5	-3.9	4.5	1.43	1.71
42-2-144	2.15	1.22	.602	288.9	275.9	271.9	-26.1	-26.2	-23.4	(-13.8)	14.3	1.34	1.60
42-3-123	3.97	2.40	1.79	340.6	321.0	332.0	15.5	24.0	25.0	(12.6)	10.1	1.64	2.42
42-4-62	9.03	6.42	4.18	298.1	295.4	294.3	-20.8	-20.6	-22.3	-10.6	1.5	.89	10.1
42-5-22	10.7	9.38	8.66	294.7	292.2	290.6	-29.2	-28.7	-29.0	-15.3	1.1	1.18	9.07
42-5-121	12.0	10.4	8.72	223.9	225.9	226.4	-29.7	-29.3	-30.3	-15.7	1.2	1.06	11.3
43-2-41	7.10	4.61	3.15	120.2	124.9	127.0	-10.5	-12.0	-8.5	-6.0	2.9	1.21	5.87
43-2-120	5.69	2.02	1.47	31.8	349.4	350.2	-28.9	-27.2	-27.7	-14.4	4.6	1.52	3.74
43-3-90	5.43	2.33	1.15	206.5	214.0	219.6	-25.0	-33.1	-34.9	-18.0	3.9	1.26	4.31
43-4-50	4.39	2.18	1.42	76.2	72.6	71.6	-19.9	-22.5	-18.1	-11.7	4.5	1.36	3.23
43-4-102	6.05	2.09	1.30	82.3	72.6	71.1	-16.2	-18.8	-16.1	(-9.6)	9.7	1.63	3.71
44-2-19	4.02	2.51	1.65	146.2	154.7	153.4	-26.9	-21.3	-21.4	-11.0	3.8	1.19	3.38
44-2-138	3.71	3.03	1.93	197.0	217.0	215.6	-17.2	-27.3	-24.6	-14.5	4.4	1.44	2.58
44-3-128	6.34	4.39	2.97	244.5	246.0	247.6	-30.9	-27.0	-26.5	-14.3	2.3	1.06	5.98
44-4-23	7.55	4.44	2.71	162.1	169.6	166.8	-32.6	-28.9	-27.4	-15.4	1.6	1.49	5.07
44-4-141	5.25	2.12	1.30	151.2	162.8	162.7	-25.5	-29.0	-33.0	-15.5	4.3	1.87	2.81
44-5-121	1.80	1.23	.769	321.5	258.8	258.7	-76.8	-32.6	-33.3	(-17.7)	13.2	1.49	1.21

FIGURE 2

Demagnetization curves for selected site 292

basalts. All repeated values are plotted

except in a few cases where they are identical.

ID	J_{nrm} $(10^{-3}gauss)$	MDF (oe)
□ 42-5-121	12.0	139
● 44-4-23	7.55	85
△ 45-3-7	9.69	128
○ 43-4-50	4.39	75

ID	J_{nrm}	MDF
□ 41-4-51	5.81	82
△ 45-2-78	9.00	79
● 42-2-12	2.44	85

ID	J_{nrm}	MDF
□ 44-5-121	1.80	93
● 42-3-123	3.97	92
△ 40-1-103	11.8	83
■ 47-2-31	3.75	42

AVERAGE NRM

%

PEAK ALTERNATING FIELD (oe)
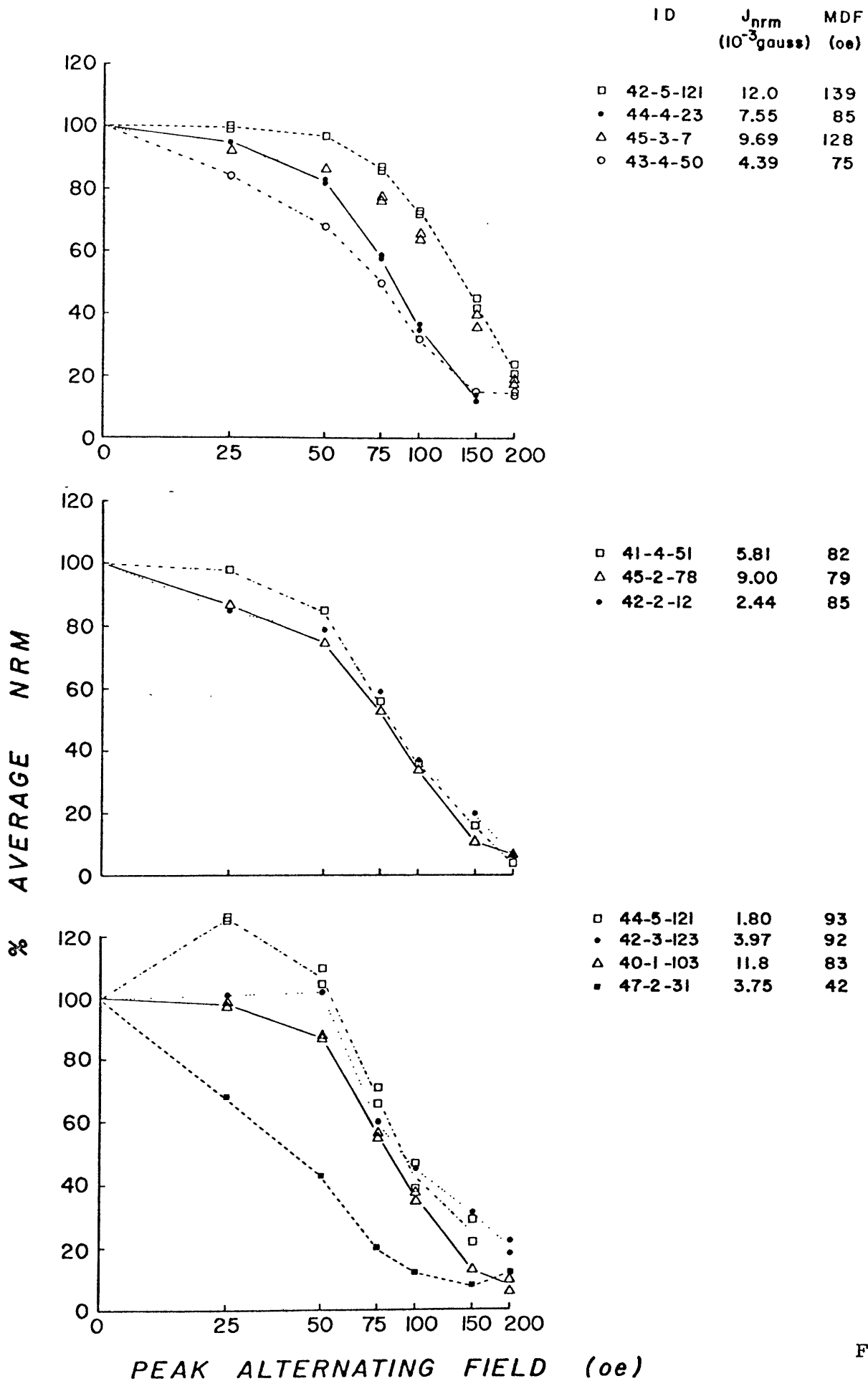
FIG 2

FIGURE 3

Stereonet plots of relative magnetization

directions for the same samples as in Figure

2. All repeated measurements are shown and

joined by dotted lines where greatly different.

Parentheses enclose values of positive inclin-

ation except for samples 42-3-123 and 40-1-103

which have all positive inclinations (indicated

by the + next to their ID number). All other

inclinations are negative. Solid lines and

arrows outline the path that magnetization

directions follow after demagnetization at pro-

gressively higher fields.
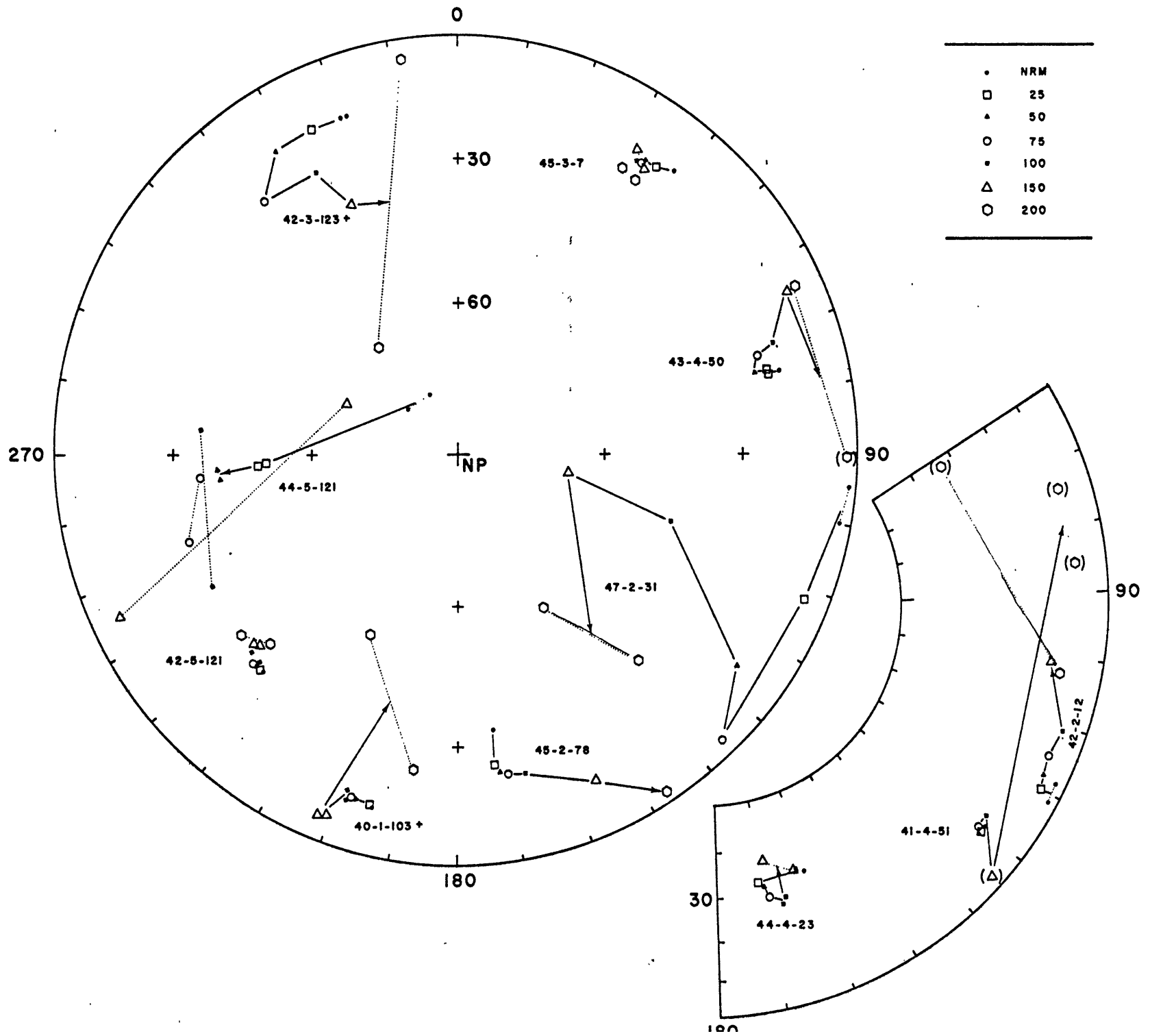
FIG 3

FIGURE 4

PSI values as a function of demagnetizing field
for the same site 292 basalts as in figures 2
and 3. The PSI index is a measure of stability
as defined by Symons and Stupavsky (1974).
Lowest values fall between 75 and 100 oe demag-
netizing field and lie in the range of low to
moderate stability.
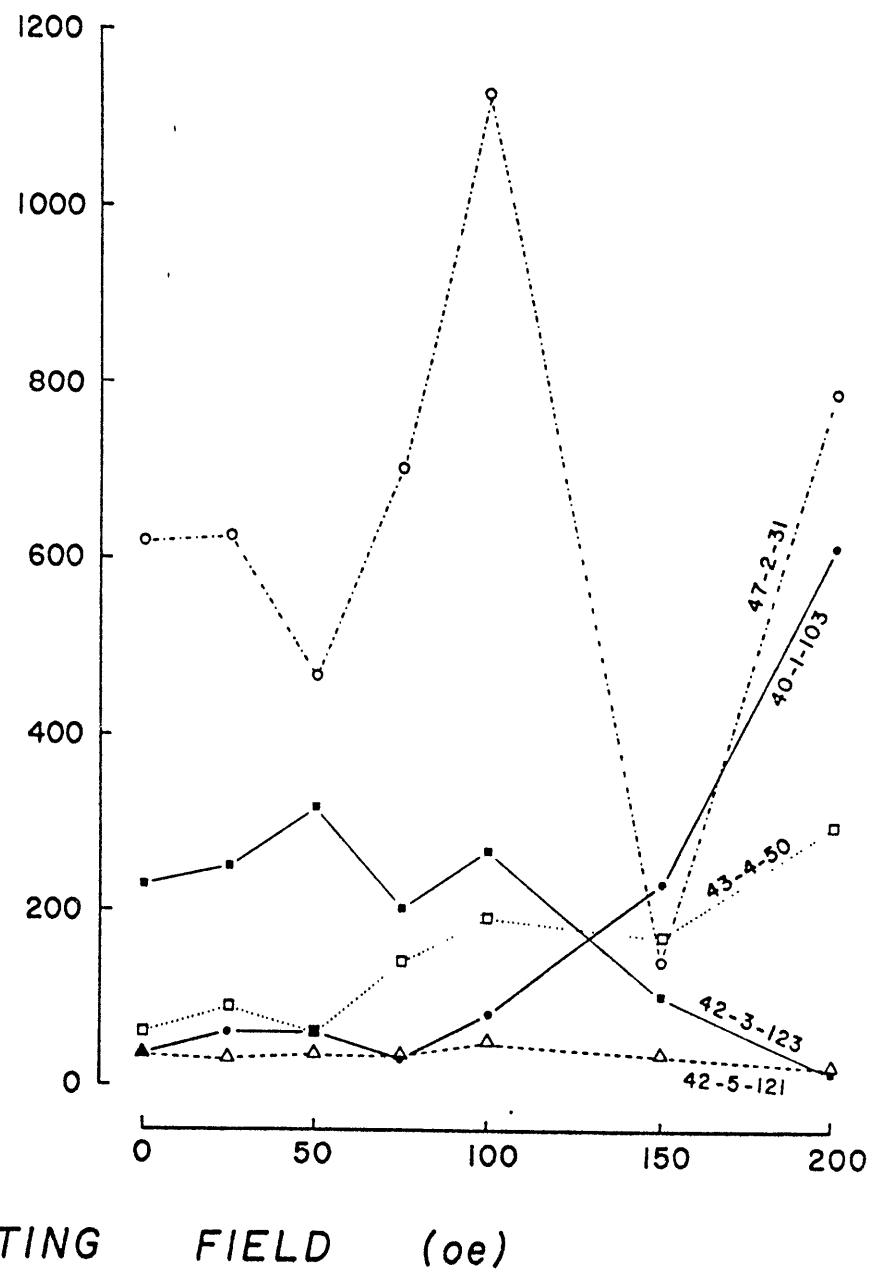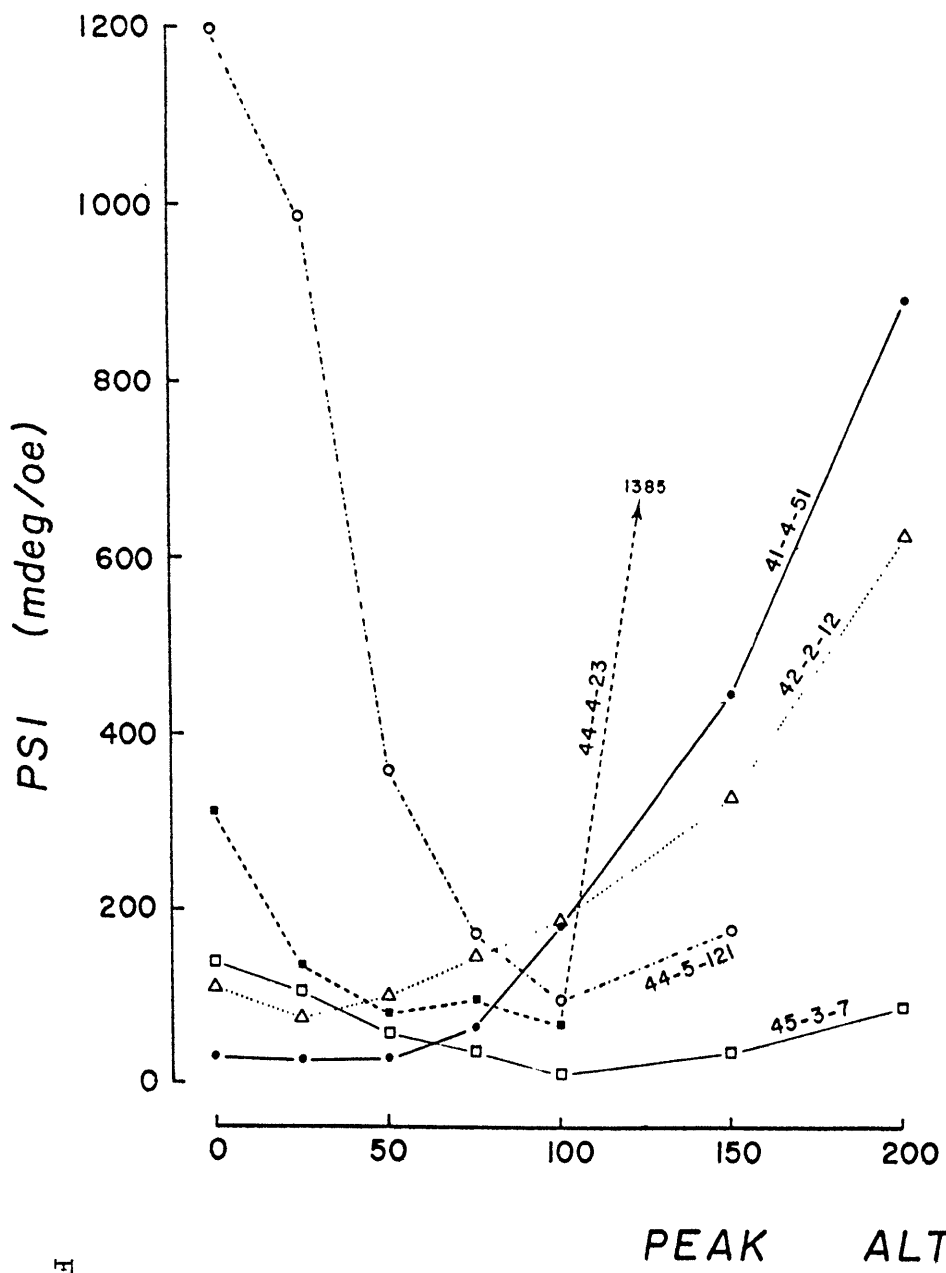
FIG 4

differences between the two separate determinations of the
magnetization vector. In order to include this additional
information about the consistency of magnetization direction,
we calculate a stability index, d, given by the following
equation:

$$d = (\alpha_{75-100} + \alpha_{75} + \alpha_{100})/3 \qquad (1)$$

where, α_{75-100} is the angular change between average magnetization
directions at 75 and 100 oe, and α_{75} and α_{100} are the angular
changes between repeated magnetization measurements at 75
and 100 oe respectively. Low values of d represent small
angular changes in magnetization direction between 75 and
100 oe (as do the PSI values for these fields) in addition
to small changes in repeated measurements at each field. We
use an average of the three separate angular changes because
repeated measurements were not always taken.

A plot of d vs. NRM intensity (J_{nrm}) is given in figure
5. It appears that there is a general increase in stability
(i.e. lower values of d) for samples with higher values of
J_{nrm}. Acquisition of viscous magnetization might be one
explanation for this. All but two of our samples are reversely
magnetized, with inclinations close to, but of opposite sign
from that of the present field. This means that viscous
components acquired since the beginning of the Bruhnes epoch
would reduce the amplitude of the originally reversed magnetization.
We know that it is difficult to remove VRM by AF demagnetization

FIGURE 5

Stability index d (defined in the text) vs.

NRM intensity J_{nrm} for all site 292 basalts.

Low stability (high values of d) at low J_{nrm}

suggests that viscous components may be a partial

cause of their instability.

FIG 5
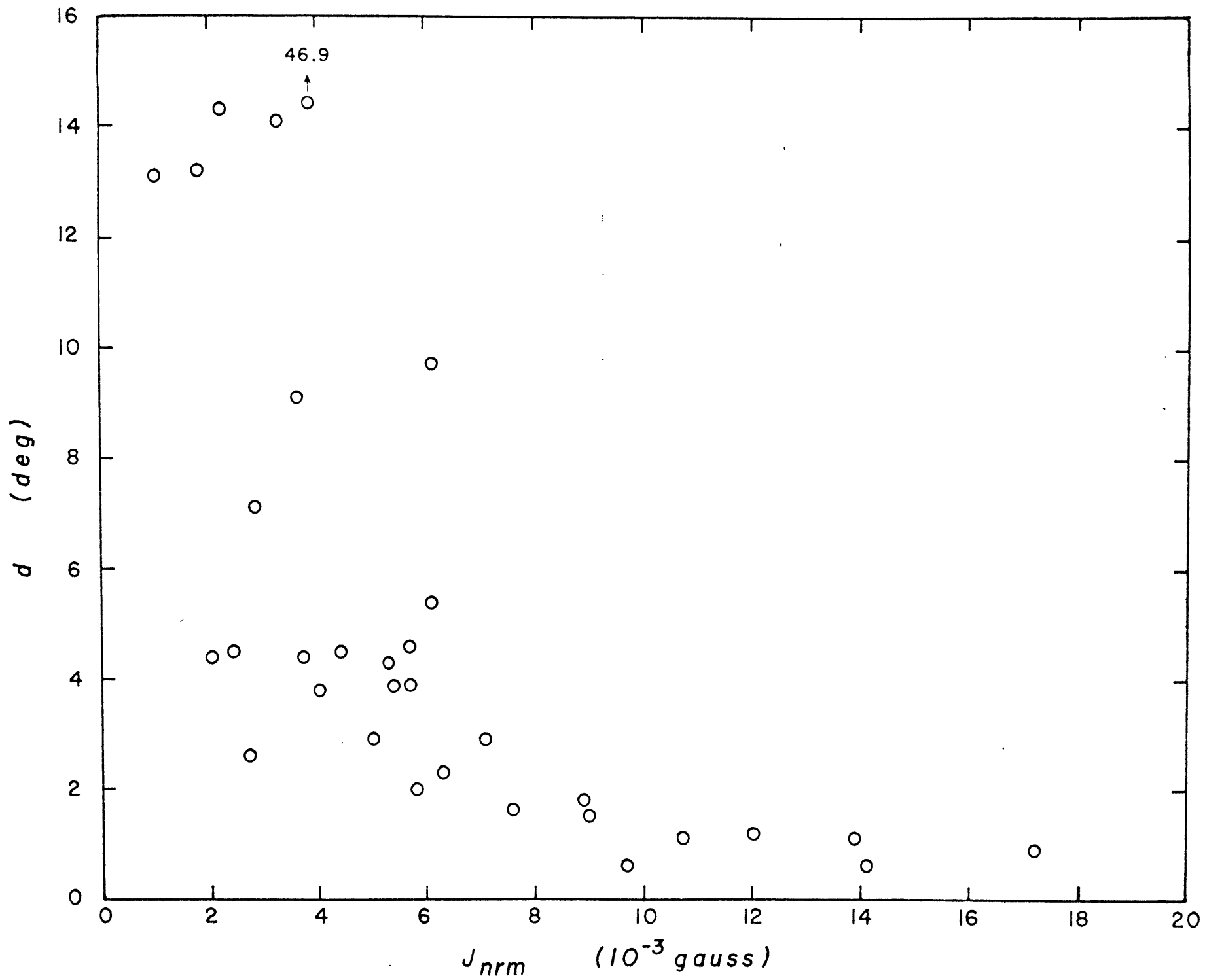
[Biquand and Prevot, 1971], so it is quite possible for it
to contaminate even our demagnetized results. If, however,
we can show that there is a relationship between the degree
of VRM acquisition and our stability parameter d, then we
might be able to confidently reduce the effects of VRM in
our paleolatitude determination by using only those samples
with small d.

Acquisition of Viscous Remanent Magnetization

The predominant feature of viscous remanent magnetization
(VRM) is its acquisition in an applied field H as a function
of the logarithm of time:

$$J(t) = J_o + S (\log t - \log t_o) \qquad (2)$$

where J is the magnetic intensity, t is the time spent in the
field H, and S is the magnetic viscosity coefficient. Such
behavior is predicted by all theories of thermally activated
magnetic viscosity, primarily due to Neel [1950] and Stacey
[1963], and has been observed in both single and multi-domain
terrestrial materials. Lowrie [1973] has shown that it is
also an important factor in the instability of some DSDP
basalts. On the basis of laboratory VRM growth during 1000
hours, he extrapolated values of J(t) to 0.69 m.y. as an
estimate of the viscous growth during the Bruhnes normal epoch.
If such a value is a large portion of the total NRM, this
indicates that an initial remanence may have been destroyed
by the later accumulation of viscous components.

There are several additional features of VRM acquisition which complicate the significance of such an extrapolation. First, the log t relationship is critically dependent on the nature of the grain distribution $f(v, H_{co})$ for non-interacting SD grains, where v is the volume and H_{co} the microscopic coercive force (Dunlop, 1973). Consequently, if a sample contains discontinuities in $f(v, H_{co})$, the slope S may change with time. Grain sizes and coercivities affected during 1000 hours are quite different from those affected over 10^6 years, and extended extrapolations in time based on constant S could become inaccurate. Second, the temperature at which acquisition occurs has an important influence on S through its effect on the relaxation time by which an initial magnetic moment decays. This relaxation time τ depends exponentially on the thermal energy, and if the temperature changes from T_1 to T_2, τ will shift from τ_1 to τ_2 according to the relationship

$$T_1 \ln(C\tau_1) = T_2 \ln(C\tau_2) \qquad (3)$$

where $C=10^{10}$ sec^{-1} [Neel, 1950]. A change from oceanic bottom water (T=275°K) to laboratory (T=293°K) conditions decreases $C\tau$ to $(C\tau)^{0.94}$, which will have the effect of increasing S. Third, our measured values of S may not correspond to the real geological acquisition rate. Our laboratory procedure, in which we first demagnetize the sample in an alternating field, may activate VRM susceptibility by rearranging domain walls into less durable positions, from which subsequent VRM is more

easily acquired. All of these effects are not well understood and we should proceed with caution when using laboratory VRM studies in analysis of NRM measurements.

We have conducted some traditional VRM experiments to determine the extent to which 6 samples acquired magnetization during a period of up to 1000 hours after initial demagnetization in a field of 500 oe. Two experiments were conducted on the same samples, the first using a field of 1.0 oe to produce the VRM and the other using a 0.5 oe field. Results are shown in figure 6. For each sample the shape of the best fitting curve (using the least squares fit of a 3rd order polynomial) differs between the 1.0 oe and 0.5 oe cases. In most instances there are significant changes in slope during the 1000 hours, with the 1.0 oe results showing increasing slopes similar to those reported by Creer et al. [1970], and the 0.5 oe showing a three stage pattern previously observed by Lowrie [1974]. Such changes in slope have been attributed to the dependence of the viscosity coefficient S on grain size distribution. The region of large slope is thought to be due to growth of VRM by single domain grains; the smaller slopes due to larger grains, possibly in the region of pseudo-single domains. But the fact that the shapes of our curves depend on the field strength acting on the samples suggests that the true reason for this behavior does not lie entirely with the grain size distribution.

After 30-50 hours the 1.0 oe slopes have become approximately twice the 0.5 oe slopes, as determined by a least squares straight line fit (see figure 6 and Table II). This confirms

FIGURE 6

Acquisition of viscous remanent magnetization

as a function of the logarithm of time for

selected site 292 basalts. Solid circles

represent acquisition in a 0.5 oe field and

open circles in a 1.0 oe field. Curves are the

best least squares fit by a 3rd order polynomial

to all of the points; dashed lines are the best

linear fit to values for large t. Numbers

indicate slopes of these straight line segments.
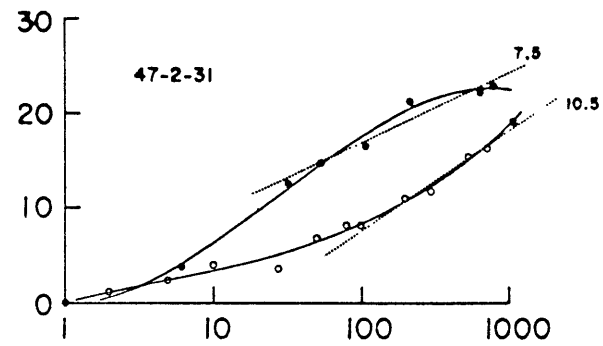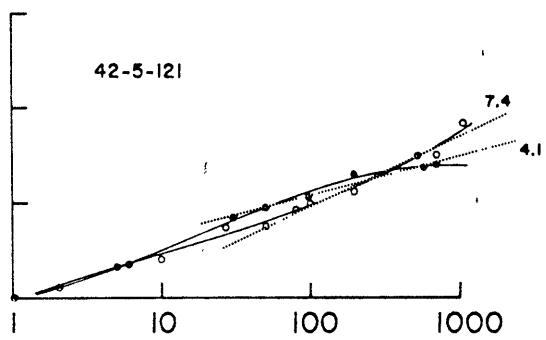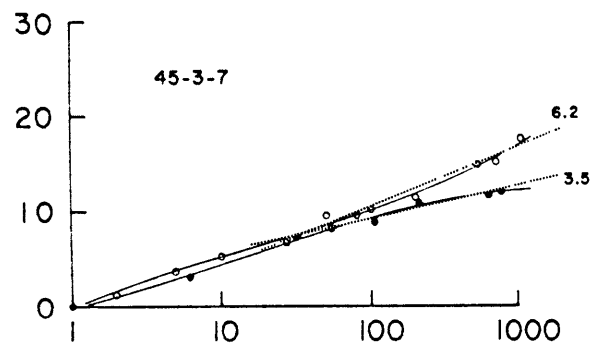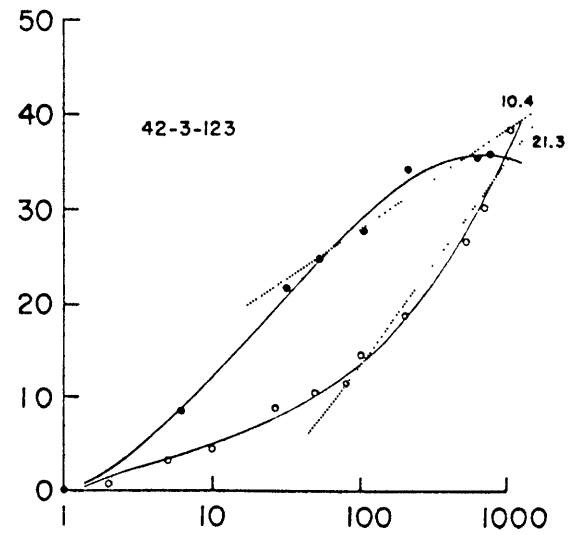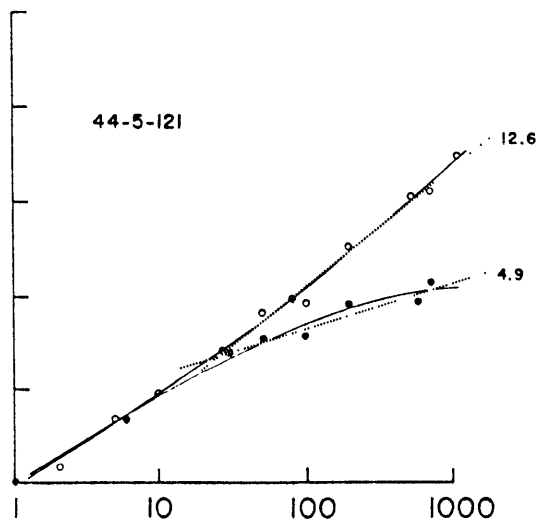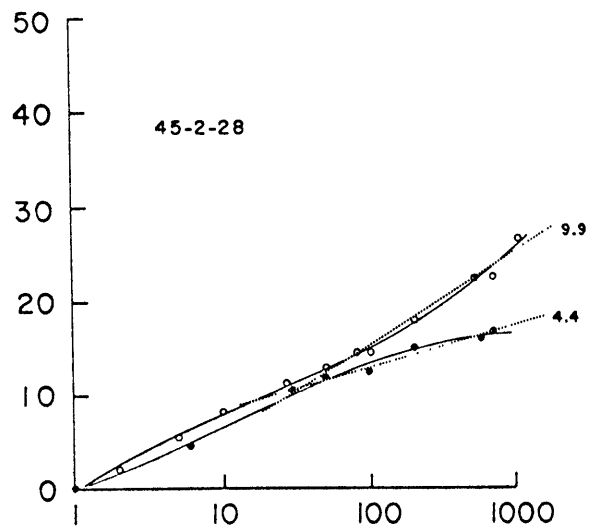
FIG 6

TABLE II: Summary of Viscous Magnetic Properties for DSDP Site 292 Basalts

ID	$H_{1000}^{(1)}$	$H_{700}^{(2)}$	$H_{0.69}^{(2)}$	H_{nrm}	$S^{(1)}$	$S^{(2)}$	$M_{700}^{(2)}$	$M_{0.69}^{(2)}$	M_{nrm}	d
			(oe)				(10^{-4} Gauss-cm^3)			(deg)
42-5-121	19	28	96	139	7.39	4.10	14.0	42.4	118.	1.2
45-3-7	37	28	96	128	6.22	3.54	12.2	36.7	93.	0.6
42-3-123	18	27	93	92	21.3	10.4	35.7	108.	37.	10.1
44-5-121	16	19	65	93	12.6	4.93	21.3	55.5	17.5	13.2
45-2-28	21	26	89	66	9.91	4.43	16.9	47.6	53.4	3.9
47-2-31	45	24	83	42	10.5	7.46	22.8	74.5	35.2	46.9

$H_{1000}^{(1)}$, median destructive field (MDF) of viscous magnetization acquired in 1000 hours in a 1.0 oe field; $H_{700}^{(2)}$, MDF of viscous magnetization acquired in 700 hours in a 0.5 oe field; $H_{0.69}^{(2)}$, calculated MDF for a linear extrapolation of $H_{700}^{(2)}$ to 0.69 my; H_{nrm}, measured MDF.

$S^{(1)}$ and $S^{(2)}$, viscosity coefficient in 1.0 and 0.5 oe fields respectively; $M_{700}^{(2)}$, magnetization acquired after 700 hours in a 0.5 oe field; $M_{0.69}^{(2)}$, calculated magnetization after 0.69 my using a linear extrapolation of $M_{700}^{(2)}$ with a slope of $S^{(2)}$; M_{nrm}, measured NRM magnetization.

d, stability index as defined in the text.

previous results [Creer, 1957], which show that the magnitude
of S depends upon H, in the Rayleigh region of small field
strengths (<20-50 oe). To test whether the magnitude of
these slopes is related to the instability of our samples
under AF demagnetization, we plot S vs. log d and S vs. J_{nrm}
in figure 7. We find that in both 1.0 oe and 0.5 oe fields,
the larger values of S are associated with more unstable
rocks (larger d) and with lower NRM intensities. The one
exception is sample 42-3-123, but this specimen has a normal
inclination and would not represent removal of a reversed
magnetization by a positive field as would the others.

The extent to which an original remanent intensity
might be destroyed by such rates of VRM growth are calculated
in Table II. Using extrapolations based on magnetizations
at 1000 hours in the 1.0 oe field (M_{1000}) and 700 hours in
the 0.5 oe field (M_{700}), together with our linear determinations
of S, we can calculate magnetizations acquired over the
duration of the Bruhnes epoch ($M_{0.69}$ m.y.). In Table II we
only calculate $M_{0.69}$ for a 0.5 oe field which should be
closer to the actual Bruhnes earth's field acting on the
ocean crust [McElhinney, 1973]. In two cases (47-2-31 and
44-5-121) $M_{0.69}$ was larger than M_{nrm} although I_{nrm} was still
reversed. This may indicate that our extrapolations are too
large and that true viscous effects are smaller than indicated
by our laboratory experiments. This is not surprising since
the lack of a simple log t relationship during the 1000
hours of our experiment, makes a linear extrapolation out to

FIGURE 7

Viscosity coefficient S of selected site 292

basalts as a function of (a) stability index d,

and (b) NRM intensity J_{nrm} for viscous acquisition

in 1.0 and 0.5 oe fields. The direct relation-

ship in (a) between S and d suggests that samples

with low d are the least affected by viscous

components. The inverse relationship in (b)

suggests, as does figure 5, that acquisition of

VRM causes decreased NRM intensities. This would

be expected for samples such as these, whose

inclinations are opposite in sign to that of the

present field. The only dissimilar points in

both (a) and (b) are for sample 42-3-123 which is

the only one with positive inclination.
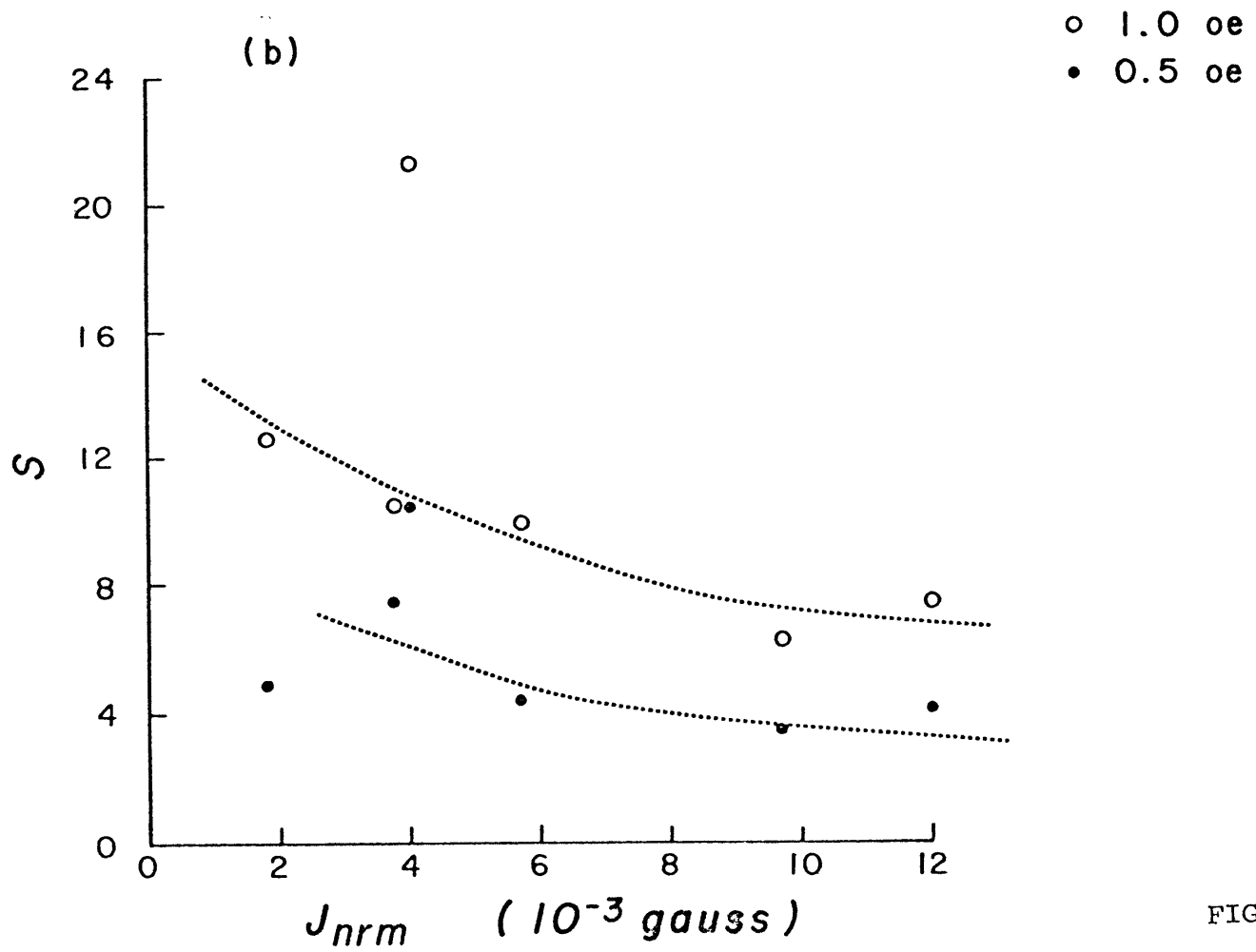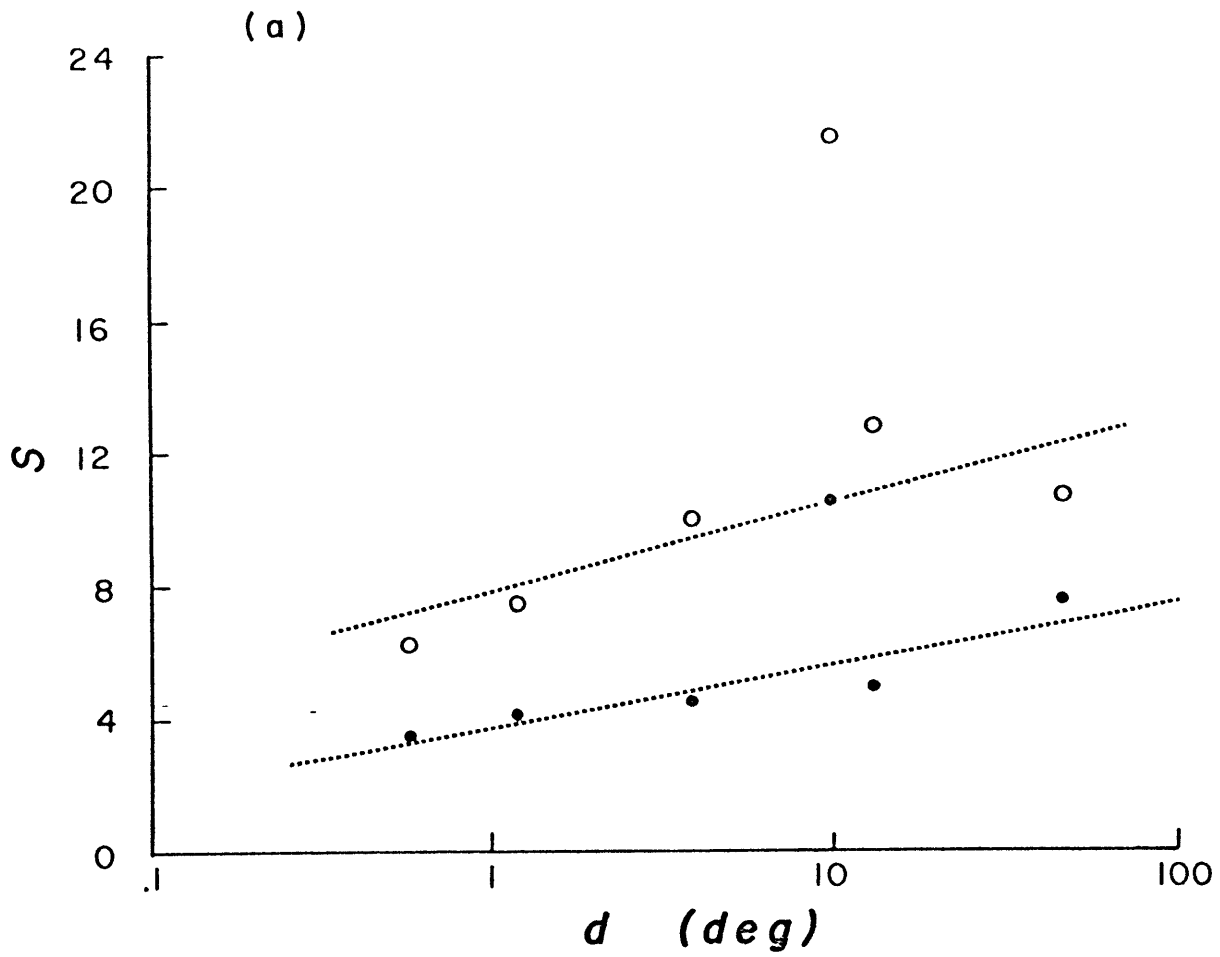
FIG 7

0.69 m.y. highly questionable. We still are not certain of
the extent that viscous effects have hindered accurate
determinations of remanent inclinations, but we do have some
justification for expecting that samples with low values of
d may be the least effected. The large values of S as
measured in the laboratory must, however, add a certain
skepticism as to the true meaning of our basalt inclinations.

Paleolatitudes

In Table I we calculate a paleolatitude for each paleoinclination
after AF demagnetization in 75 oe. We only consider values
for d<5 and also have disregarded our one positive inclination
with small d (sample 40-1-103). This serves to reduce the
scatter in the result, but does not greatly shift the average
paleolatitude calculated using all the data (Table I). Our
result is that the mean paleolatitude is ±11.4°. We use the
arithmetic mean even though our numbers should actually be
treated by the statistics on a sphere when only inclinations
are known. Theoretical analysis of borehole data indicates
that for high latitudes (particularly above 50°) the true
spherical mean should be as much as 20° higher than that
given by the arithmetic average of the paleolatitudes, but
that for low latitudes simple averaging of the paleolatitudes
gives the same result as when they are treated on a sphere
[Briden and Ward 1966; Cox, in preparation].

The southern latitude is consistent with the author's
previous analysis of magnetic anomalies in the West Philippine
Basin [Louden, 1976], but it is not unique because we do not

know whether the field was reversed or normal during the formation of these rocks. They do not lie on an identifiable magnetic anomaly. Also, we must add onto the experimental variance (given by the square of the standard deviation of our numerical population), a variance determined from probable models for secular variation. Our samples only record a moment in time, and the standard deviation of the mean paleolatitude cannot contain information concerning the secular variation. We use the relationship,

$$S.E. = \sqrt{(\sigma_{sv}^2 + \sigma_{exp}^2)/N_i} = 10.5° \qquad (4)$$

where, S.E. = standard error in our mean paleolatitude,

$$\sigma_{sv} = 9.8° \text{ [Cox, 1970]},$$
$$\sigma_{exp} = 3.8° \text{ (from Table I), and}$$
$$N_i = \text{number of flow units} = 1.$$

The possible range of paleolatitudes,

$$\lambda_r = \pm 11.4° \pm 21.0°,$$

represents the interval of 95% confidence, and extends from +33.4° to -33.4°. This large range tells us that basalts which do not adequately sample secular variation must have paleolatitudes greater than 30° for either polarity to be unique.

We must look to the sediment record for more significant data. In that case, where groups of samples span time intervals greater than 10^4 years, σ_{exp} does contain information concerning secular variation, and it is not necessary to add the additional term σ_{sv} to it. N_i would be the total number of values contained in the mean (i.e. the number of samples in each group) rather than the number of flow units. These changes should significantly reduce the standard error.

PALEOMAGNETISM OF DSDP SEDIMENTS

Introduction

The paleomagnetic study of deep-sea sediment cores has led to significant advances both in our knowledge of the magnetic reversal stratigraphy over the last 20 m.y., and in understanding the nature of secular variation and excursions in the earth's magnetic field of much shorter duration [Opdyke, 1972; Harrison, 1974; Creer et al., 1972]. The major advantage of sediments is that, unlike the basalts, they can offer a semi-continuous record of the magnetic field direction and intensity. The detail of such a record depends directly upon the rate of sedimentation. Low rates (0.1 cm/10^3 yr) will average out most of the secular variation in a standard sample 2.54 cm thick, whereas samples with high sedimentation rates (10 cm/10^3 yr) can record the details of variations over several hundred years.

Successful studies of the sediment paleomagnetic record are possible even though there is relatively little known

about the mechanisms by which the magnetic pattern is recorded.
The slow deposition of sediment grains on the ocean floor
(DRM), post-depositional mixing such as caused by bioturbation
(PDRM), and chemical alteration (CRM) may all play a role.
Measurements on many cores of differing lithologies show
that some offer coherent patterns in agreement with results
from land basalts and sea-floor spreading anomalies, while
others are scattered with unrecognizable patterns. We do
not understand why this happens. Our confidence in the
reliability of any particular sediment record is based more
on macroscopic properties, such as the statistics of the
scatter in inclination and declination directions, than it
is on any fundamental paleomagnetic properties of the minerals
which carry the signal. This poses a significant problem
for the analysis of DSDP cores. Because of probable rotations
during the drilling process, declination values are always
highly scattered, and reversal chronologies can only be
determined by changes in sign of the inclination which may be
unreliable for low latitudes. Results often have not been
easy to interpret and attempts at utilizing these cores to
extend the sequence of reversals back through the Tertiary
have made only slow progress.

Recently there have been attempts at using the JOIDES
data for mapping changes in paleolatitude back in time
[Sclater and Cox, 1970; Hammond et al., 1975; Peirce, in
press]. Results can become particularly useful when averages

are taken of many closely spaced samples, with the standard
deviation of the mean forming one measure of our confidence in
the result [Green and Brecher, 1974]. Collections of high
density sampling can be taken in several locations down core
to give averages of paleolatitude as a function of age.
With such a relationship we can hope to distinguish between
origins north and south of the equator. A pattern of steep
to shallow to steep inclinations should define an equatorial
crossing even though the polarity of the inclination averages
alone are not significant. Such a pattern has been observed
in equatorial Pacific piston cores by Hammond et al. [1974].
We only must assume that the plate motion is continuous and
that abrupt reversals in its direction do not occur. The
two fundamental limitations in our basalt analyses (i.e. the
large uncertainties produced by secular variation and the
non-uniqueness of the polarity) can be overcome by detailed
analysis of sediment cores.

Site 292

Drill cores from site 292 contain the most complete
sediment section to basement of any of the JOIDES holes in
the West Philippine Basin. The lithology of this sediment
is a uniform calcareous ooze/ chalk rich in nannofossils,
indicating that the bottom (now at 2943 m) has remained
above the carbonate compensation depth (CCD) throughout its
history [Ingle et al., 1975]. Sedimentation rates as determined
by these fossils are fairly uniform at approximately 1.0 cm/10^3yr.

Levels of bulk magnetization (0.3 to $4.0*10^{-4}$ gauss-cm^3) are relatively high due to the large ash content, which probably owes its origins to nearby island arc volcanoes. All of these factors plus the undisturbed nature of many of the cores, makes this a most promising site for paleomagnetic study.

We selected six relatively undisturbed areas at different locations down core for detailed sampling. These positions together with their associated paleontological ages are shown in Figure 8. At each position we took a suite of 10-20 samples of approximately 10 cm^3 each. If the sediment was sufficiently indurated, as it was in cores 31-33, 34-38 and 39, we could sample by diamond drilling, just as for the basalts; if not, we took an oriented sample by pressing a non-magnetic plastic tube (approximately 1 in. by 1 in.) into the core by means of a small piston apparatus. The ends of the tube were sealed by epoxy to avoid later disturbances. A total of 94 samples were taken by these techniques and later studied with the use of C.E. Helsley's cryogenic magnetometer amd 400 Hz demagnetizer at the University of Texas at Dallas.

We selected 5 of our samples for detailed AF demagnetization experiments, results of which can be seen in figures 9 and 10. The PSI stability index indicates moderate to high stability at a demagnetization field of 88 oe. Median destructive fields (MDF) range from 135 to 310 oe. On the

FIGURE 8

Lithological and paleontological stratigraphy

for DSDP site 292 sediment from Ingle et al.

(1975). Shaded areas locate positions of recovered

sediment. Numbers identify the location and age

of cores which were densely sampled. Paleomagnetic

measurements were made on 10-20, 10 cm^3 samples

as closely spaced as possible in each of these

6 locations, for a total of 93 individual samples.

AGE (MY)

SITE 292

DEPTH (M)

7-10 MY

8

18   24 MY

23   28 MY

32-34 MY

31-33   35-40 MY

34

38

39   41 MY
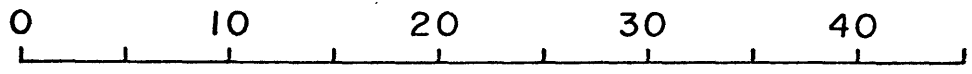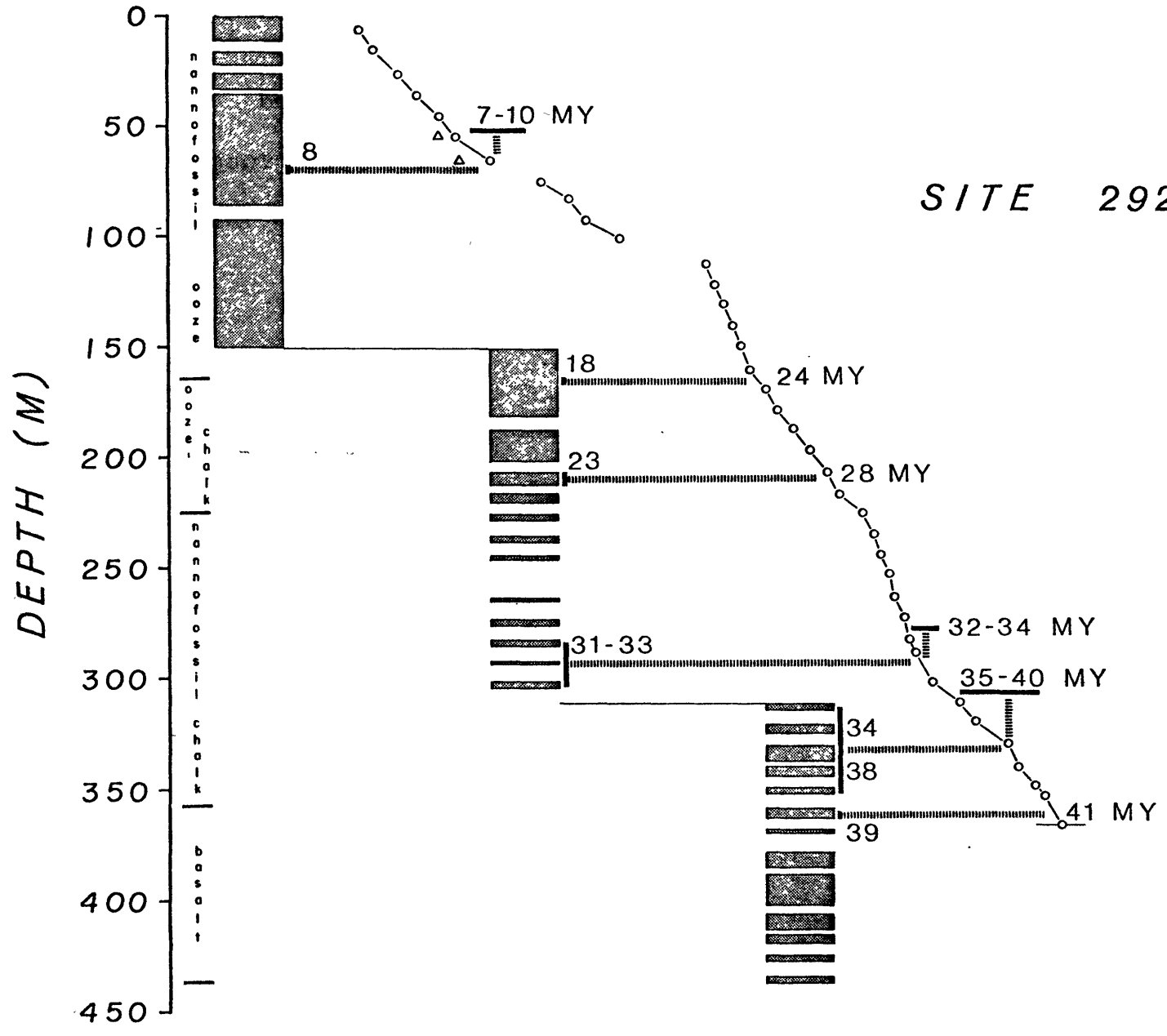
FIG 8

FIGURE 9

Demagnetization curves and stereonet plots for

selected site 292 sediment intensities and

directions. Higher MDF values and well grouped

directions indicate higher stability than for

the site 292 basalts of Figures 2-4.
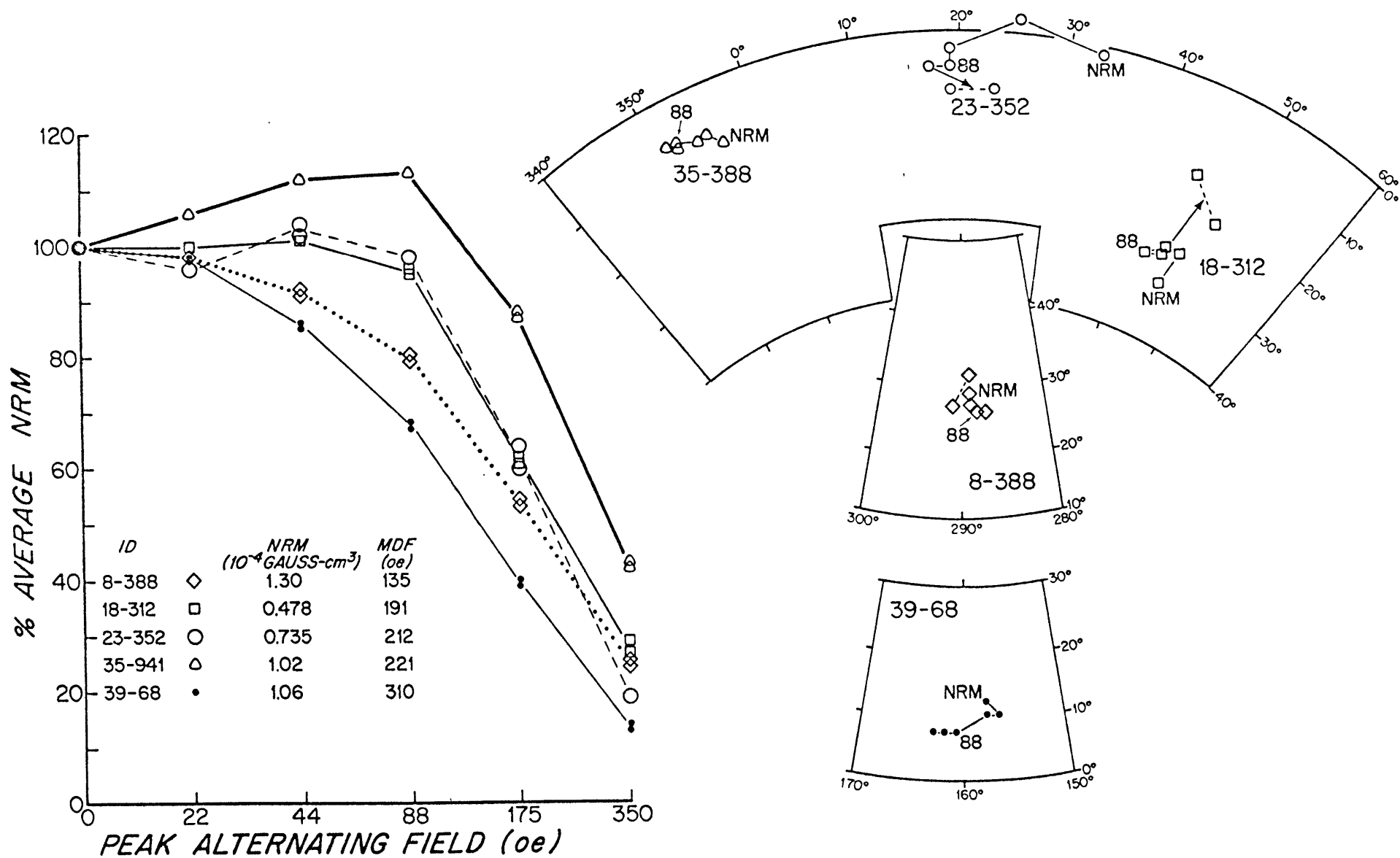
FIG 9

FIGURE 10

PSI stability index as a function of demagnetizing field for the same selected site 292 sediments as in Figure 9. Low values at 88-175 oe indicate moderate to high stability.
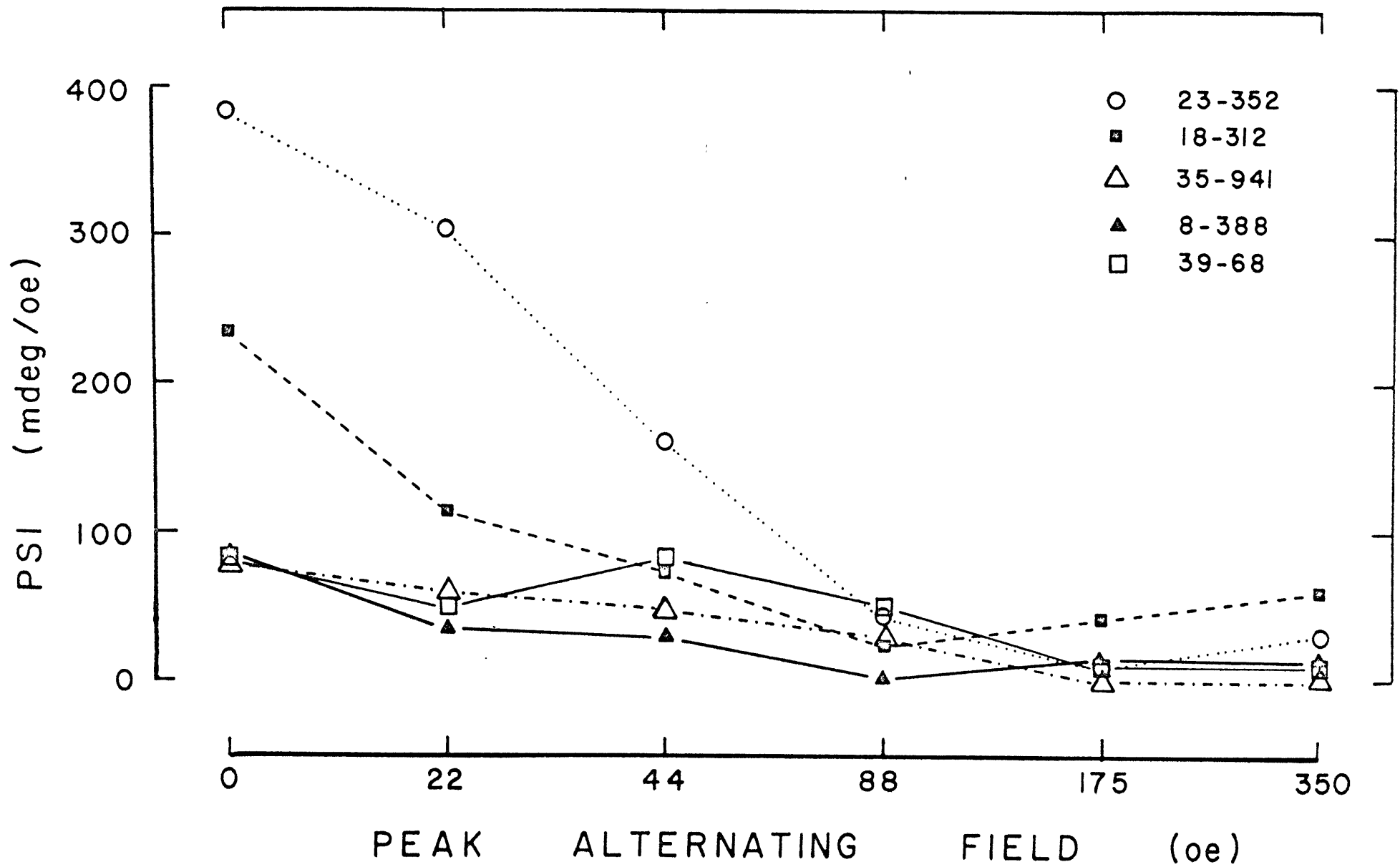
FIG 10

basis of these results we demagnetized all samples at 88 oe

(see Table III for a listing of all our paleomagnetic measurements).

Figure 11 is a graph that shows all the demagnetized inclinations

in 5 of our 6 groups of samples. Values for cores 34-38

were omitted because they span a depth range much greater

than do the others. Histograms of inclinations in each

group show a marked decrease from core 8 to 33, followed by

an increase from 33 to 39. This is precisely the pattern

that we hoped might be associated with an equatorial crossing.

A more statistical analysis can be accomplished by

determining means and their deviations for each group of

samples. So as not to bias our averages we first want to

discard any results which are either very different from the

others or represent more unstable behavior. Unfortunately,

we cannot calculate as detailed a stability index as we

could for the basalts, since we only know two magnetization

vectors (NRM and 88 oe). We do notice that many samples

with extreme inclinations also have magnetization directions

which change greatly under demagnetization from NRM to 88

oe, whereas most samples show little change. We quantify

this by calculating the angular change between magnetizations

at NRM and 88 oe. This number, Δ, is not a strictly valid

criterion of stability although in general higher values of Δ

correspond to higher values of PSI. We utilize it only as a

means of limiting our results so that they all represent

similar magnetic behavior. A histogram of Δ values (Fig.

TABLE III: Remanent Magnetic Properties for DSDP Site 292 Sediments

292-8
N=13

Depth below sea floor: 66.67 m   Age: 7-10 mybp

DEPTH (CM)	M (10^{-4} GAUSS-CM^3)	M88	I (DEG)	I88 (DEG)	D (DEG)	D88 (DEG)	Δ (DEG)	λ88 (DEG)
0	0.518	0.486	22.3	21.1	25.4	23.5	2	10.9
53	1.06	0.821	21.0	18.8	269.7	280.4	10	9.7
152	0.652	0.607	-9.7	-8.6	352.8	354.0	2	-4.3
170	1.04	0.735	19.5	19.0	186.1	185.8	1	9.8
187	0.629	0.531	28.7	30.4	90.1	83.7	6	16.4
226	1.20	0.978	30.1	31.7	119.5	117.0	3	17.2
251	1.43	1.18	17.0	17.1	290.7	297.7	7	8.7
273	0.996	0.768	1.8	0.7	227.8	232.2	5	0.4
291	0.332	0.244	-26.9	(-36.5)	209.3	254.3	39	(-20.3)
328	0.469	0.348	11.4	9.8	245.7	255.5	10	4.9
388	1.30	1.04	27.0	26.4	109.0	106.7	2	13.9
424	1.37	1.13	17.9	20.4	78.2	77.6	3	10.5
470	1.29	1.10	9.5	9.8	335.9	338.5	3	4.9
496	1.05	0.820	21.7	23.0	116.8	115.9	2	12.0

mean   8.8   (6.8)

σ 5.9   (9.4)

$\sigma/\sqrt{N}$ 1.6   (2.5)

TABLE III continued:

292-18
N=14

Depth below sea floor: 163.35 m Age: 24 mybp

DEPTH (CM)	M_0 (10^{-4} GAUSS-CM^3)	M_{88}	I_0 (DEG)	I_{88} (DEG)	D_0 (DEG)	D_{88} (DEG)	Δ (DEG)	λ_{88} (DEG)
0	1.00	0.876	14.8	11.7	128.0	133.1	6	5.9
30	1.55	1.14	16.2	13.9	157.4	161.8	5	7.1
58	0.842	0.789	9.8	4.2	213.1	213.2	6	2.1
109	0.564	0.427	-9.6	-8.6	199.1	191.1	8	-4.3
138	0.265	0.225	4.8	-2.3	161.4	135.9	26	-1.2
176	0.102	0.104	0.5	(-2.0)	327.4	212.9	115	(-1.0)
191	0.244	0.139	48.6	(67.8)	210.6	166.1	29	(50.8)
209	0.078	0.124	20.1	(-7.5)	217.4	240.3	36	(-3.8)
222	0.192	0.119	-31.7	(-53.4)	169.2	110.9	47	(-34.0)
241	0.313	0.261	-21.3	-18.8	175.9	164.0	12	-9.7
256	1.30	1.14	-15.5	-13.4	172.7	172.9	2	-6.8
288	0.657	0.715	-11.9	-16.6	213.2	206.9	8	-8.5
312	0.480	0.461	-30.4	-27.7	225.6	222.6	4	-14.7
342	0.612	0.644	-18.8	-26.9	263.9	245.1	19	-14.2

							mean	-7.4 (-4.5)
							σ	4.3 (17.3)
							$\sigma/\sqrt{N}$	1.4 (4.6)

TABLE III continued:

292-23
N=14

Depth below sea floor: 206.03 m   Age: 28 mybp

DEPTH (CM)	M_0 $(10^{-4}$ GAUSS-CM$^3)$	M_{88}	I_0 (DEG)	I_{88} (DEG)	D_0 (DEG)	D_{88} (DEG)	Δ (DEG)	λ_{88} (DEG)
0	0.832	0.513	4.7	−8.8	340.4	324.4	21	−4.4
6	0.627	0.701	−16.4	−19.9	297.6	313.9	16	−10.3
18	0.638	0.500	3.7	−13.7	307.3	277.7	34	−7.0
31	0.893	0.884	−5.1	0.0	79.2	69.3	11	0.0
95	1.70	1.51	0.1	−1.5	186.3	184.3	3	−0.8
115	0.621	0.636	−18.7	−21.7	55.9	77.7	21	−11.3
125	1.30	1.16	−8.7	−13.1	147.3	138.7	10	−6.6
219	0.552	0.654	−8.2	4.4	72.8	60.5	18	2.2
261	1.07	1.24	−4.7	−6.6	349.5	347.0	3	−3.3
282	0.762	0.735	−19.3	(−27.4)	116.5	95.3	21	−14.5
352	0.733	0.722	0.8	−4.2	212.0	198.6	14	−2.1
426	0.749	0.727	3.1	2.2	290.9	295.3	5	1.1
471	1.21	1.04	−25.8	(−28.5)	172.9	173.3	3	−15.2
539	0.422	0.379	22.1	4.2	61.3	81.1	26	2.1

mean −5.0

σ 5.7

$\sigma/\sqrt{N}$ 1.5

TABLE III continued:

292-31 to 33
N=19

Depth below sea floor: 283.69 m . Age: 32-34 mybp

DEPTH (CM)	M_0	M_{88}	I_0 (DEG)	I_{88} (DEG)	D_0 (DEG)	D_{88} (DEG)	Δ (DEG)	λ_{88} (DEG)
	(10^{-4} GAUSS-CM^3)							
0	0.683	0.738	7.1	(−21.6)	322.4	321.6	29	(−11.2)
70	0.850	0.819	−8.0	−7.7	263.7	265.1	1	−3.9
154	0.334	0.347	−30.3	(−34.8)	33.4	35.5	5	(−19.2)
241	1.27		11.1		52.7			5.6*
283	1.63	1.57	−5.4	−5.3	4.7	3.4	1	−2.7
288	1.57	1.50	−9.2	−9.0	14.2	12.7	2	−4.5
292	0.875	0.854	−2.2	−4.8	166.1	164.8	3	−2.4
297	0.905	0.877	−6.8	−6.7	160.0	160.4	0	−3.4
302	0.783	0.770	−4.9	−5.5	159.8	158.8	1	−2.8
311	0.714	0.701	−2.3	−5.4	170.8	169.2	4	−2.7
317	0.836	0.832	−12.8	−12.4	261.5	260.8	1	−6.3
323	0.695	0.686	−4.9	−3.4	269.9	269.3	2	−1.7
328	0.559	0.537	−0.8	−1.0	37.8	36.3	2	−0.5
334	0.455	0.445	−8.4	−8.3	40.3	41.3	1	−4.2
343	1.14	1.17	−1.8	−4.3	129.9	131.2	3	−2.2
394	0.197	1.00	23.8	(3.6)	46.7	81.0	39	(1.8)
398	0.509	0.401	4.6	7.4	43.6	47.3	5	3.7
404	3.02	2.88	−5.5	−4.2	280.0	276.0	4	−2.1
408	3.98	3.79	−12.9	−10.6	280.5	280.4	2	−5.4
419	1.35	1.25	−0.6	−0.9	271.7	270.1	2	−0.5
423	0.835	0.802	4.7	2.9	57.1	61.0	4	1.5
428	0.932	0.905	4.0	5.6	51.9	52.3	2	2.8

mean −1.7 (−2.7)

σ 3.0 (5.0)

$\sigma/\sqrt{N}$ 0.7 (1.1)

TABLE III continued:

292-34 to 38

N=9

Depth below sea floor: 312.17 m   Age: 35-40 mybp

DEPTH (CM)	M_0 (10^{-4} GAUSS-CM^3)	M_{88}	I_0 (DEG)	I_{88} (DEG)	D_0 (DEG)	D_{88} (DEG)	Δ (DEG)	λ_{88} (DEG)
0	1.89	1.69	-2.6	-3.0	286.5	284.9	2	-1.5
106	1.11	1.04	2.5	2.8	97.4	96.3	1	1.4
941	1.02	1.15	-9.7	-6.4	355.6	351.8	5	-3.2
1044	0.358	0.461	-0.6	0.5	14.7	8.9	6	0.3
1929	1.18		8.2		111.7			4.1*
1964	2.39	2.41	0.4	-0.2	293.3	296.8	4	-0.1
2865	1.17	0.969	5.4	2.5	207.4	207.3	3	1.3
2918	0.956		9.1		61.1			4.6*
3794	0.442		0.0		274.3			0.0*
3897	0.0881		(29.2)		261.0			

mean	0.8
σ	2.3
$\sigma/\sqrt{N}$	0.8

TABLE III continued:

292-39
N=20

Depth below sea floor: 359.57 m   Age: 41 mybp

DEPTH (CM)	M_0 (10^{-4} GAUSS-CM^3)	M_{88}	I_0 (DEG)	I_{88} (DEG)	D_0 (DEG)	D_{88} (DEG)	Δ (DEG)	λ_{88} (DEG)
0	0.767		-7.6		99.6			-3.8*
11	0.806		0.5		256.9			0.3*
24	0.554		19.0		52.9			9.8*
35	0.825	0.543	17.7	13.2	59.2	65.1	7	6.7
45	0.688	0.413	22.9	20.7	61.6	68.1	6	10.7
68	1.05	0.719	11.9	8.3	158.0	160.4	4	4.2
83	0.675	0.427	17.7	12.5	162.7	168.3	8	6.3
101	1.25	0.801	14.6	9.2	98.2	101.8	6	4.6
117	1.15	0.778	24.5	19.9	94.3	93.6	5	10.3
130	1.26	0.843	11.0	8.4	106.1	100.6	6	4.2
147	0.645	0.361	0.0	-8.2	18.6	19.2	8	-4.1
154	0.478	0.346	1.8	-7.1	30.6	33.1	9	-3.6
169	1.24	0.842	8.2	6.6	290.8	286.0	5	3.3
185	1.13	0.799	12.2	9.6	17.2	21.0	5	4.8
205	1.59	1.14	11.4	14.0	288.6	292.6	5	7.1
211	1.46	1.11	11.1	13.0	292.9	292.9	2	6.6
228	1.05	0.803	15.6	14.6	0.0	3.4	3	7.4
236	0.653	0.481	22.0	20.5	355.9	8.3	12	10.6
258	0.665	0.447	15.4	15.3	327.3	343.2	15	7.8
266	0.732	0.417	8.3	9.0	339.1	346.5	7	4.5

mean 4.9

σ 4.5

σ/√N̄ 1.0

The depth is the distance from the top of the core. Each sample is
approximately 10-20 cm^3. Subscripts refer to fields of peak AC
demagnetization. Δ is a measure of the reliability as defined in
the text. λ_{88} is the paleolatitude after 88 oe demagnetization.
Values in parentheses are only included in bracked values for the
mean and standard deviation.

* NRM value

FIGURE 11

Paleoinclinations after demagnetization in 88

oe for site 292 sediments. Large numbers identify

the sampling location (see Figure 8) for each

group of closely spaced samples. The depth is

relative to the position of the top sample in

each group. Histograms show the decrease in

inclination from cores 8 to 33 and increase from

33 to 39 which we attribute to a crossing of the

paleomagnetic equator. Inclinations from cores

34-38 are not included due to the large depth

range which they span.
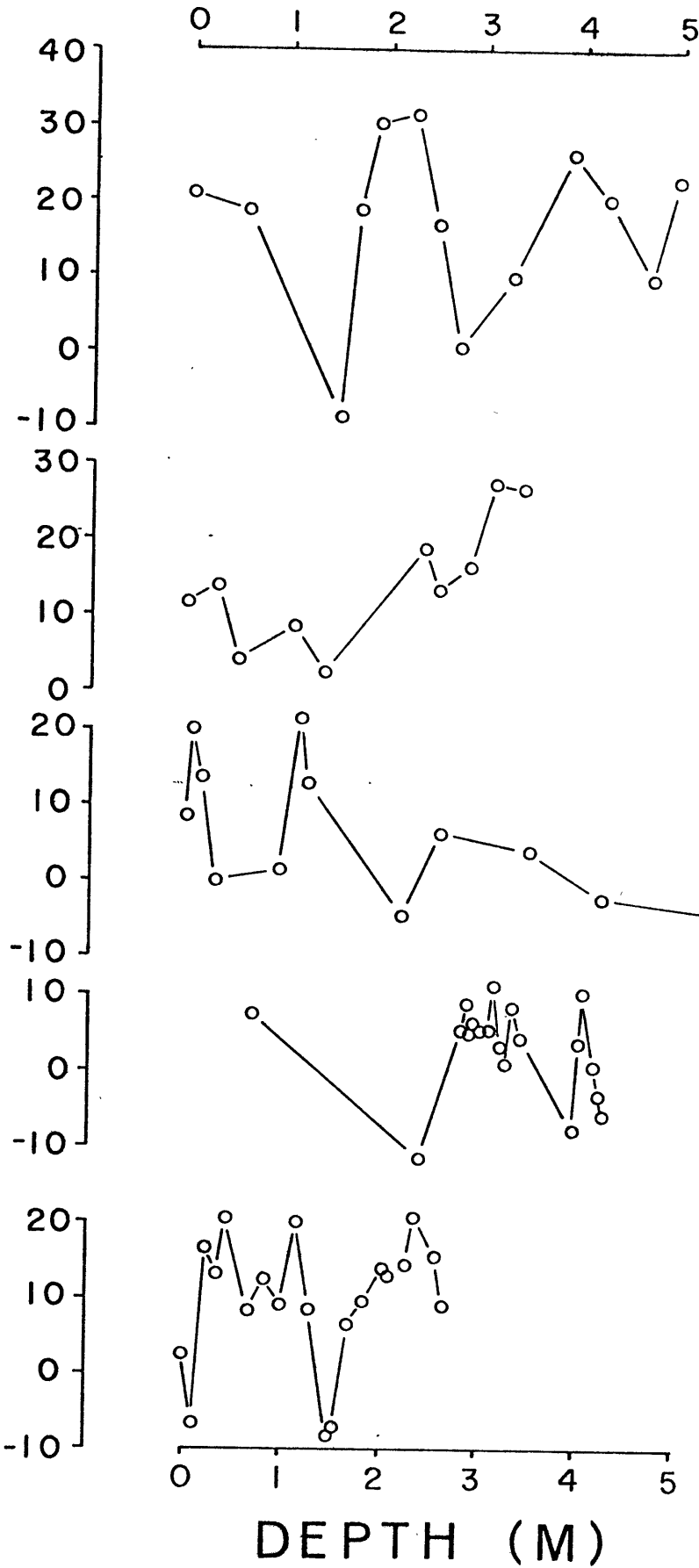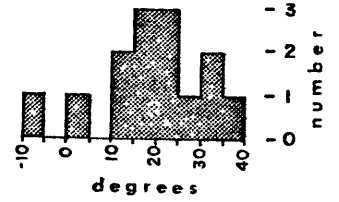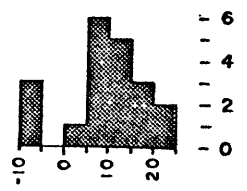
FIG 11

12) shows that most are small (<20°), although from table
III we can see that samples from different cores show different
behavior. Some, like those in core 8, have very low values
except for the few that also have extreme values of inclination;
others, like those from core 23, have all rather high values.
In general we have discarded data from samples with $\triangle$>25.
In only one case (sample 31-154) have we discarded an extreme
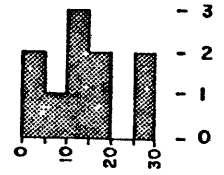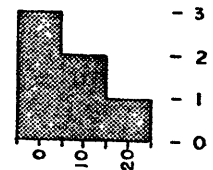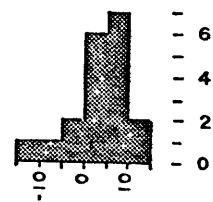inclination that also had low$\triangle$. Mean inclinations of these
selected samples are not greatly different from those which
include all our samples (Table III), but standard deviations
are in some cases greatly reduced. In all but one case we
use the actual sign of the inclinations, and assume that the
values in each group are not affected by reversals of the
earth's field. By so doing we produce distribution patterns
(Figure 11) more similar to Gaussian than if we took absolute
values and assumed that all changes in sign were caused by
reversals. The only exception to this is in core 18, where
a sequence of three positive inclinations shifts to negative
values. This we attribute to a reversal.

Mean paleolatitudes and their 95% confidence intervals
are plotted in figure 13 as a function of age. Here we can
clearly see the northward motion and equatorial crossing of
site 292. The two primary difficulties with our basalt
results are not present in this analysis of sediments.
First, the ability of the sediments to average out secular
variations in paleopole positions allows us in the best

FIGURE 12

Histograms of $\triangle$ (defined in the text) for
sediments of site 292, 290 and 294. Higher
values for sites 290 and 294 may indicate greater
instability in remanent magnetization than for
site 292. This is also evidenced by the larger
standard errors in mean paleolatitude deter-
minations for sites 290 and 294 (Figure 15)
than for site 292 (Figure 13).
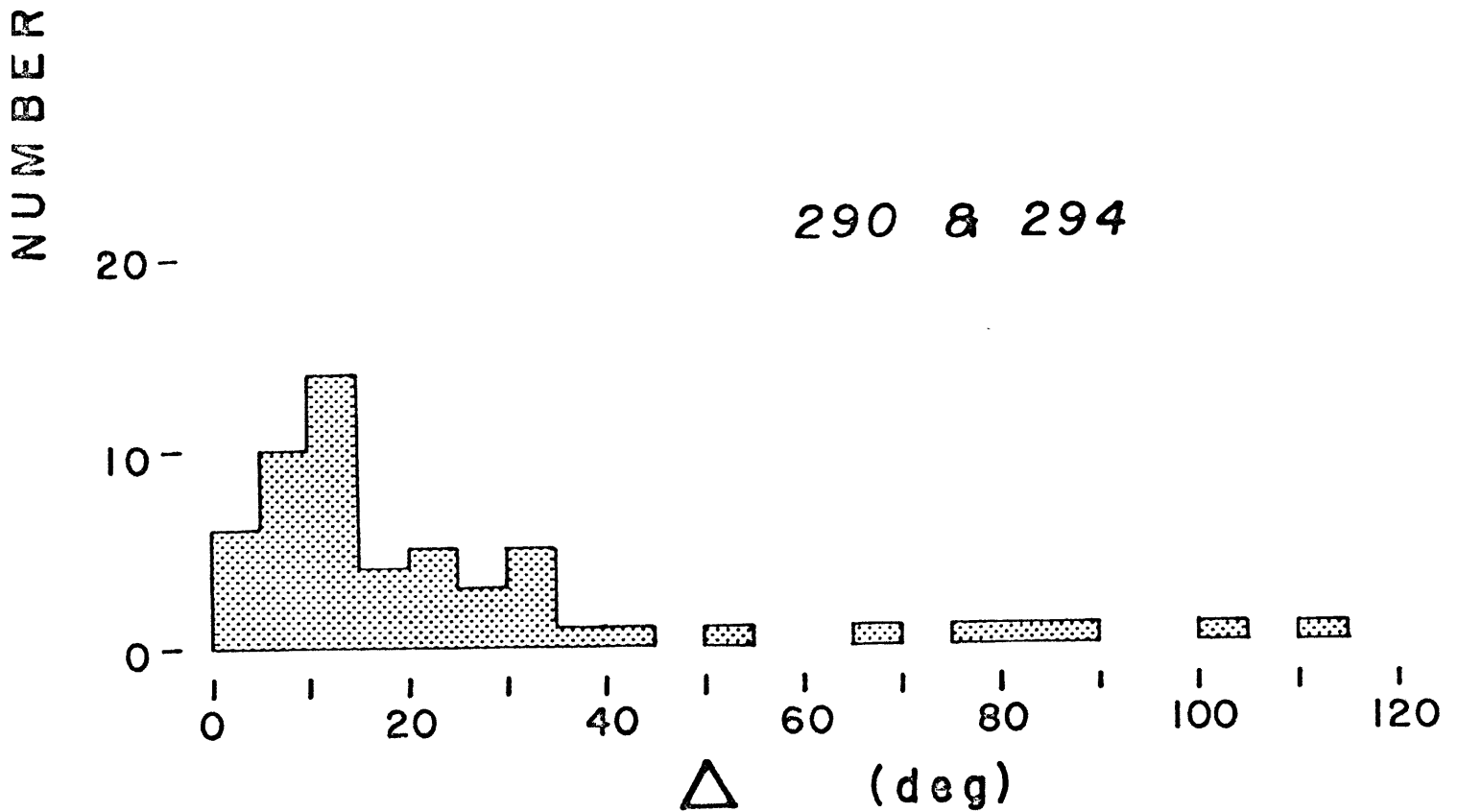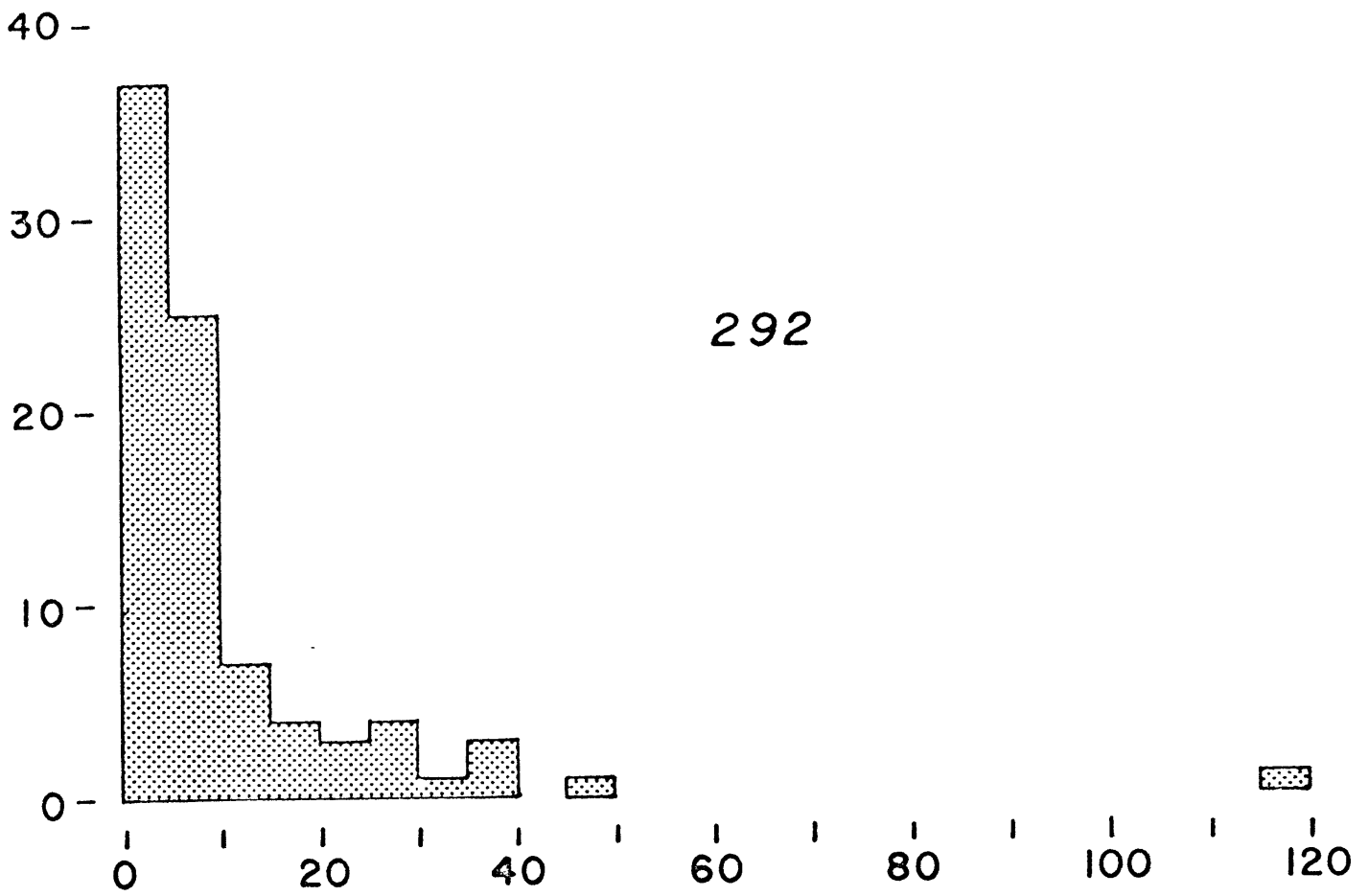
FIG 12

FIGURE 13

Age vs. mean paleolatitude for site 292 sediment

(circles) and basalt (triangles). Error bars

represent ±2 standard errors and include deviations

due to theoretical secular vatiation. Each mean

paleolatitude could be plotted on either side

of the equator as indicated by the two locations

for the basalt and the oldest sediment (core 39),

but a southern origin is suggested if plate motion

is to be uniform. Line A is a visual best fit

constrained to go through the present latitude

of site 292 (solid circle), while line B fits

only the 5 oldest sediment values. The large

range in basalt paleolatitudes is due to its

insufficient sampling of secular variation, and

shows that in the absence of multiple basalt flows

the sediment data can be much more conclusive.

SITE 292
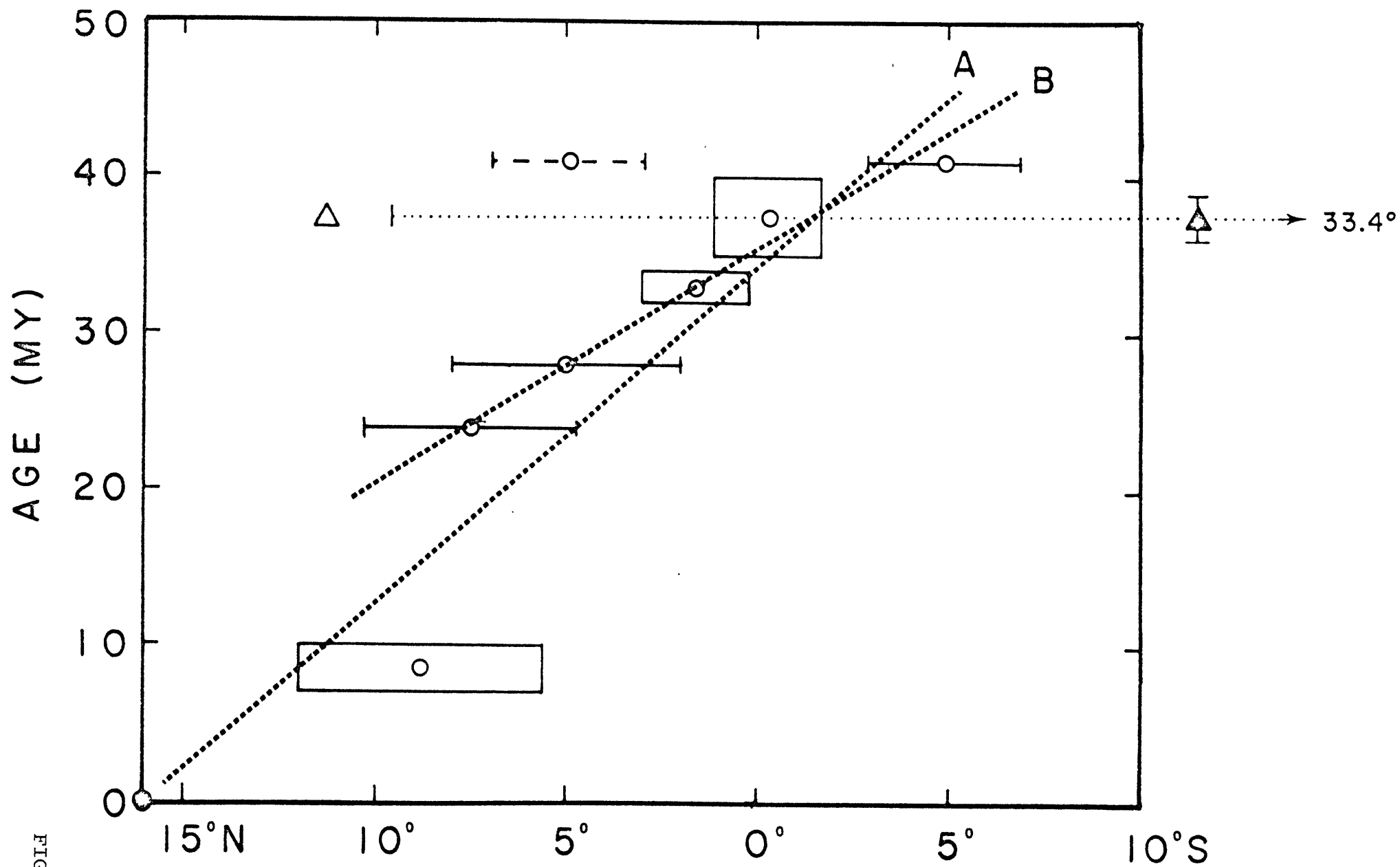
FIG 13

cases a 95% confidence interval of less than 5°. Second, we deal with the problem of non-uniqueness in paleolatitude sign by considering the trend as a function of age. Only if rather discontinuous plate motions occurred could the northern latitude location for core 39 be possible.

Of course, when we calculate paleolatitudes from our paleoinclinations, we use the equation for a geocentric dipole,

$$\tan I = 2 \tan\phi \qquad (5)$$

where I is the inclination and ϕ is the latitude. If the dipole is not geocentric, but has been shifted northwards in the past, as is suggested by several authors [Wilson, 1970; Wilson and McElhinny, 1974], then that shift would produce an apparent northward motion for a fixed site when analyzed with the geocentric equation. We should really use the equation for an offset dipole,

$$\tan I = \frac{2\cos\theta + 2\,r^2\,\cos\theta - r\,\cos^2\theta - 3\,r}{\sin\theta(1 + r\,\cos\theta - 2\,r^2)} \qquad (6)$$

where θ is the colatitude of our site and r is the northward offset in the dipole expressed as a fraction of the earth's radius. However, to produce as large enough an effect for θ fixed at 75° as to fit Figure 13 by increasing r, we would need a maximum offset larger than 1000 km. This is several

times as large as values which have recently been suggested
[Wilson and McElhinney, 1974]. Also, our purpose is to
compare our paleomagnetic results with those from magnetic
anomalies. Northward shifts in the dipole would affect both
results and would not interfere with such a comparison.

Sites 290 and 294

The one major assumption we do make in order to directly
compare our site 292 paleomagnetic results with those from
the phase shifting of magnetic anomalies is that they are
both part of the same rigid plate. They do lie near each
other, but this still does not make this assumption entirely
obvious. Site 292 is situated on an anomalous and unexplained
feature, the Benham Rise, while the magnetic anomalies are
all located in the deep water regions of the basin. We must
therefore show that our paleomagnetic analysis of site 292
is not unique to it, but is also valid for other sites in
the West Philippine Basin.

Sites 290 and 294 [Figure 1] offer the only other
relatively undisturbed sedimentary sections in the West
Philippine Basin, but these do not consist of as promising a
material as does site 292. Only a few cores were recovered
at each site, sedimentation rates are low ($0.2-0.3$ cm/10^3yr),
and the sediment contains few micro-fossils. The lithologies
are variable and quite different from site 292. Site 290
consists of a zeolite rich clay/ash in core 2 and a nannofossil
rich volcanic ash in core 7; site 294 contains a brown clay

in core 2 and a clay with palagonite ash in core 4. Most of
these differences are due primarily to the greater water
depths (6063 m at site 290 and 5784 m at site 294) which
places the sedimentary regime well below the CCD [Ingle
et al., 1975].

We collected a total of 58 samples from two cores in
each of sites 290 and 294. A pilot study of 8 of these
shows [Figure 14] that they are less stable than are the
site 292 samples, and that 175 oe may have been a better
choice for a standard field of demagnetization than the 88
oe which was our value for all non-pilot samples. Values
for Δ (Table IV) are higher than for site 292, and show a
different distribution in the histogram of figure 12. It is
therefore not surprising that we find the standard deviations
of mean paleolatitudes from these sites to be much larger
than those for site 292.

Figure 15 shows mean paleolatitudes for sites 290 and
294 as a function of time. The paleolatitudes themselves
are not very definitive owing to their large intervals of
95% confidence, but we can still use them as a test for
values predicted by the motion of site 292. These predictions
are based on the two lines A and B, which are determined in
figure 13. Line A is a visual best fit that is constrained
to go through the present latitude of site 292, while line B
fits only the oldest 5 paleolatitudes. These same lines,
plotted in figure 15 to go through the present latitudes of

TABLE IV: Remanent Magnetic Properties for DSDP Sites 290
and 294 Sediments

290-2
N=14

Depth below sea floor: 75.05 m   Age: 31-33 mybp

DEPTH (CM)	M_0	M_{88}	I_0 (DEG)	I_{88} (DEG)	D_0 (DEG)	D_{88} (DEG)	Δ (DEG)	λ_{88} (DEG)
	(10^{-4} GAUSS-CM^3)							
0	1.70	1.72	−6.8	−7.1	61.5	92.9	31	−3.6
21	0.865	0.643	16.6	−0.2	139.8	106.1	37	−0.1
41	1.31	0.930	−23.4	−25.8	240.6	256.0	14	−13.6
61	1.30	0.832	−5.7	−10.1	253.0	258.0	7	−5.1
81	1.85	1.32	15.2	13.1	240.9	252.5	11	6.6
101	1.10	0.664	1.0	−4.4	237.5	260.4	24	−2.2
121	2.38	1.91	−30.5	−31.9	239.2	252.2	11	−17.3
141	1.23	0.852	−16.9	−23.5	236.3	248.8	13	−12.3
151	0.288	0.370	39.8	28.6	155.2	107.5	41	15.3
174	0.332	0.314	−11.1	(−53.8)	177.5	109.3	68	(−34.3)
191	0.791	0.907	−6.8	−15.2	133.9	101.7	33	−7.7
211	0.688	0.780	−37.8	−34.6	143.2	102.0	33	−19.0
229	1.44	1.26	7.1	8.9	273.3	288.7	15	4.5
251	1.97	1.54	40.0	34.8	256.7	273.6	14	19.2
271	0.745	0.370	−39.9	−40.7	152.6	114.4	29	−23.3
							mean	−4.2 (−5.4)
							σ	12.1 (14.1)
							$\sigma/\sqrt{N}$	3.2 (3.8)

TABLE IV continued:

290-7
N=15

Depth below sea floor: 205.07 m Age: 45-46 mybp

DEPTH (CM)	M_0 (10^{-4} GAUSS-CM^3)	M_{88}	I_0 (DEG)	I_{88} (DEG)	D_0 (DEG)	D_{88} (DEG)	Δ (DEG)	λ_{88} (DEG)
0	0.359	0.523	40.3	37.6	274.4	206.8	51	21.1
15	0.636	0.613	-15.0	-8.9	268.6	248.6	21	-4.5
25	1.25	0.852	3.3	4.6	22.4	41.1	19	2.3
50	3.78	1.31	7.6	8.2	161.3	151.6	10	4.1
98	0.909	1.08	79.3	61.1	260.8	192.3	27	42.2
115	2.23	2.10	21.7	32.4	314.5	317.0	11	17.6
129	2.40	1.92	23.5	34.4	342.1	346.2	12	18.9
156	2.15	1.66	9.1	11.3	6.1	6.4	2	5.7
285	2.71	2.61	60.4	69.2	344.9	343.6	9	52.8
333	3.20	2.87	44.4	51.7	284.8	274.5	10	32.3
353	2.70	2.49	65.3	71.3	292.2	276.1	8	55.9
371	2.92	2.65	61.5	68.0	321.7	302.8	10	51.1
385	2.54	2.57	64.4	63.6	261.3	239.2	10	45.2
408	2.45	2.50	63.9	58.9	119.9	139.8	11	39.7
423	1.80	1.94	20.1	29.2	77.4	102.2	24	15.6

mean 26.7

σ 19.5

$\sigma/\sqrt{N}$ 5.0

TABLE IV continued:

294-2
N=11

Depth below sea floor: 47.39 m   Age: 24 mybp+

DEPTH (CM)	M_0 (10^{-4} GAUSS-CM^3)	M_{88}	I_0 (DEG)	I_{88} (DEG)	D_0 (DEG)	D_{88} (DEG)	Δ (DEG)	λ_{88} (DEG)
0	1.34	1.01	60.4	(72.5)	149.2	107.9	20	(57.8)
7	1.59	1.20	45.7	43.0	74.7	73.4	3	25.0
17	0.575	0.202	49.2	46.1	171.6	336.5	84	27.5
26	0.491	0.169	−14.3	(−77.4)	151.4	339.3	88	(−65.9)
35	0.360	0.177	12.3	4.8	213.9	224.7	22	2.4
40	0.717	0.616	−32.6	−39.0	147.7	105.8	34	−22.0
46	0.544	0.643	−21.3	−26.0	108.5	80.1	26	−13.7
57	1.03	0.736	−1.6	−18.2	11.5	2.1	19	−9.3
67	1.11	0.811	14.2	10.8	112.6	95.2	17	5.5
72	0.688	0.450	39.4	53.4	116.5	51.4	45	34.0
85	0.209	0.0762	0.0	15.1	261.5	13.0	111	7.7
93	0.556	0.378	19.6	25.1	168.2	81.7	79	13.2
99	0.443	0.190	10.3	29.0	194.4	301.7	100	15.5

mean 7.8 (6.0)

σ 16.9 (29.1)

$\sigma/\sqrt{N}$ 5.1 (8.1)

TABLE IV continued:

294-4
N=15

Depth below sea floor: 99.05 m   Age: 50 mybp[+]

DEPTH (CM)	M_0 (10^{-4} GAUSS-CM^3)	M_{88}	I_0 (DEG)	I_{88} (DEG)	D_0 (DEG)	D_{88} (DEG)	Δ (DEG)	λ_{88} (DEG)
0	1.58	1.21	2.1	-5.2	301.7	313.5	14	-2.6
5	1.63	1.06	-0.8	1.5	238.5	238.8	2	0.8
11	1.21	0.754	23.3	20.6	169.0	165.4	4	10.6
16	1.77	1.15	58.7	59.7	86.5	77.3	5	40.6
21	1.78	1.41	27.8	21.5	341.9	347.3	8	11.1
26	2.86	1.70	33.6	34.5	186.9	187.7	1	19.0
37	3.12	2.30	9.1	6.6	298.8	305.9	8	3.3
52	4.82	3.29	27.6	30.9	73.6	65.1	8	16.7
58	2.05	1.72	22.2	19.4	349.3	350.6	3	10.0
68	1.28	0.897	-2.6	-3.3	222.6	330.6	8	-1.7
78	2.39	1.66	56.2	51.8	70.4	58.7	8	32.4
88	0.733	0.475	2.0	-5.7	192.8	202.4	12	-2.9
98	0.328	0.200	47.3	48.5	128.7	80.0	32	29.5
108	0.366	0.0815	21.5	24.2	190.3	185.0	6	12.7
118	0.442	0.149	58.5	32.8	276.2	336.8	47	17.9

mean 13.2

σ 12.8

$\sigma/\sqrt{N}$ 3.3

The depth is the distance from the top of the core. Each sample is approximately 10-20 cm^3. Subscripts refer to fields of peak AC demagnetization. Δ is a measure of the reliability as defined in the text. λ_{88} is the paleolatitude after 88 oe demagnetization. Values in parentheses are only included in the bracked means and standard deviations.

+ assuming a sedimentation rate of 2.0 m/my.

FIGURE 14

PSI vs. field of demagnetization for selected
site 290 and 294 sediments. Lowest values at
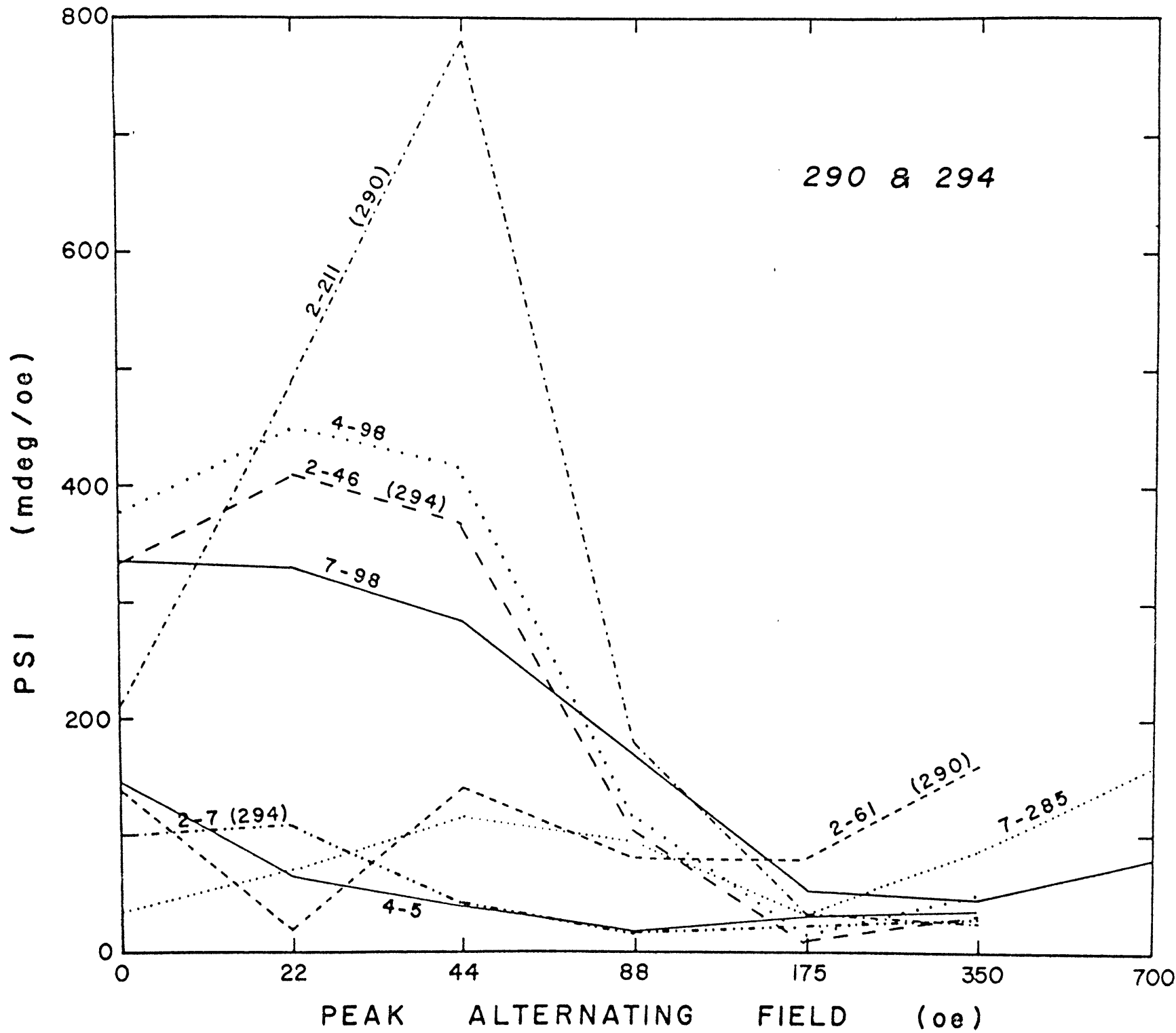175 oe indicate only moderate to low stability.

FIG 14

FIGURE 15

Paleolatitudes vs. age for sites 290 and 294.

Means and ±2 standard errors are plotted for

two groups of samples at each site. Values

on either side of the equator are equally possible

and both are plotted for each determination.

Origins south of the equator are consistent with

lines A and B defined in Figure 13 for the motion

of site 292. This agreement suggests that paleo-

latitude determinations for site 292 are not

governed by the possibly anomalous tectonic

setting of the Benham Rise.
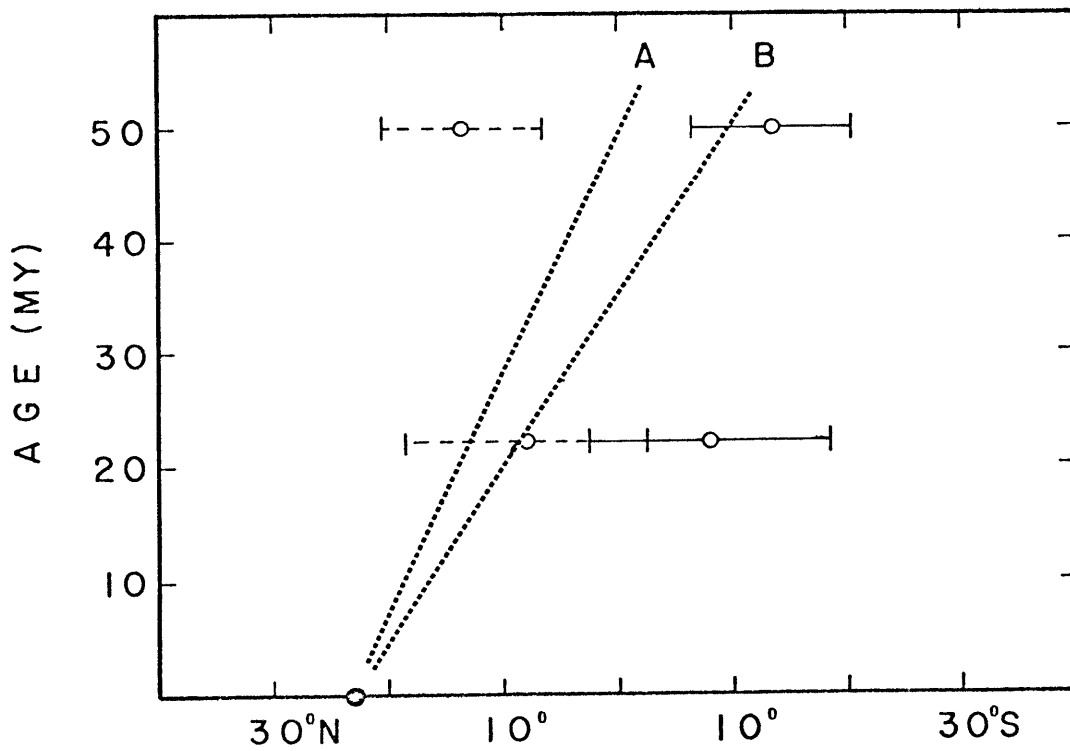
SITE 290
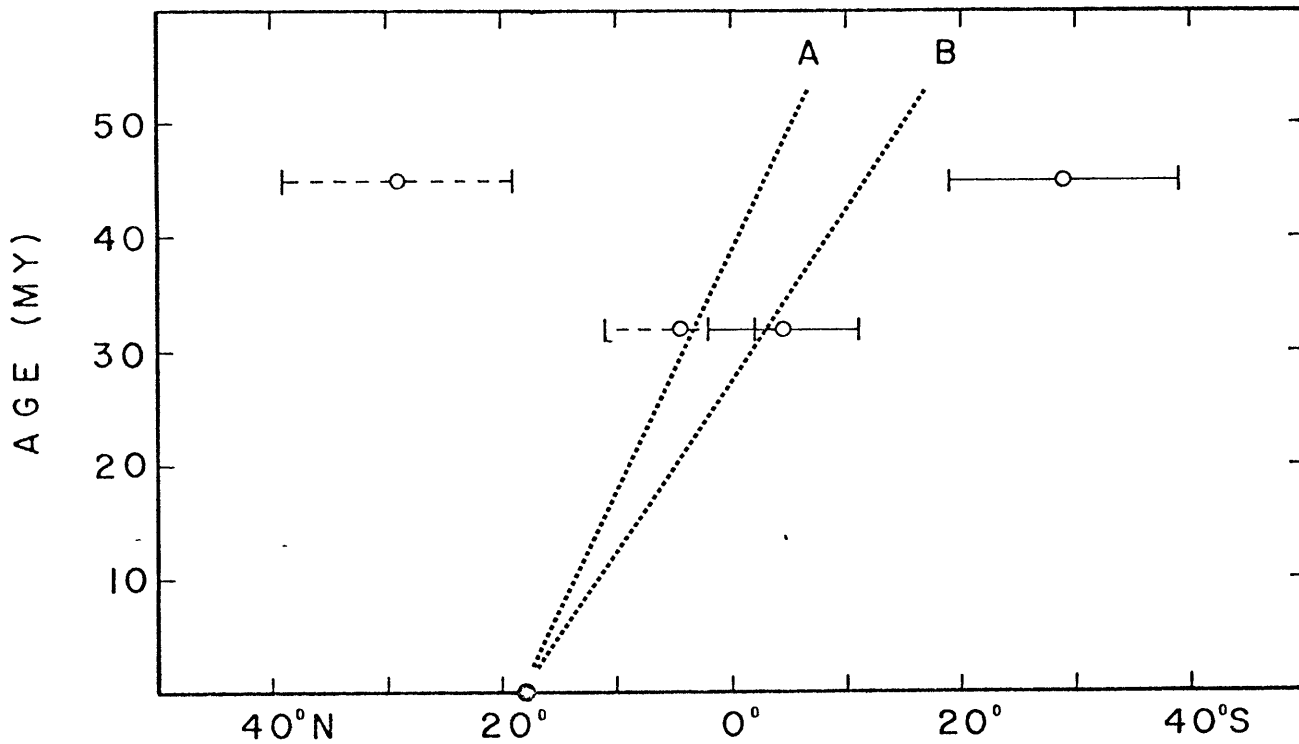
SITE 294

FIG 15

sites 290 and 294, also fit the older paleolatitude measurements.
The one exception is the oldest paleolatitude determination
for site 290, which is located further south than its prediction.

PALEOPOLES AND RELATIVE ROTATIONS

Paleopoles can be determined from the shape of sea-
floor spreading magnetic anomalies [Larson and Chase, 1972;
Schouten and Cande, 1976; Louden, 1976]. The technique is
to describe the anomaly in the wave number domain,

$$M(k) = C.J(k).E(k).e^{-i\theta}, \qquad (7)$$

where M(k) is the Fourier transform of the magnetic anomaly
m(x), C is a constant, J(k) is the transform of the magnetization
distribution j(x) and E(k) is the magnetic earth filter
[Schouten and McCamy, 1972]. The effect of phase filter $e^{-i\theta}$
can be removed by multiplying M(k) by $e^{i\theta}$ for the appropriate
value of θ, and a "deskewed" (i.e. squarewave looking)
pattern should result. This θ gives the set of all possible
remanent inclinations and declinations, which map as a great
circle on a stereonet plot of paleo-north poles (Schouten
and Cande, 1976).

We apply this technique on a short sequence of anomalies
in the West Philippine Basin first described by Louden
(1976). Figure 16 gives the location and identification of
these anomalies. These identifications are consistent with

FIGURE 16

Map of DSDP sites, ship tracks and magnetic

anomalies in the West Philippine Basin (see

Figure 1 for location). Alphabetic labels

identify ship track segments used in Figure 17.

Numbers identify anomalies as in Heirtzler et
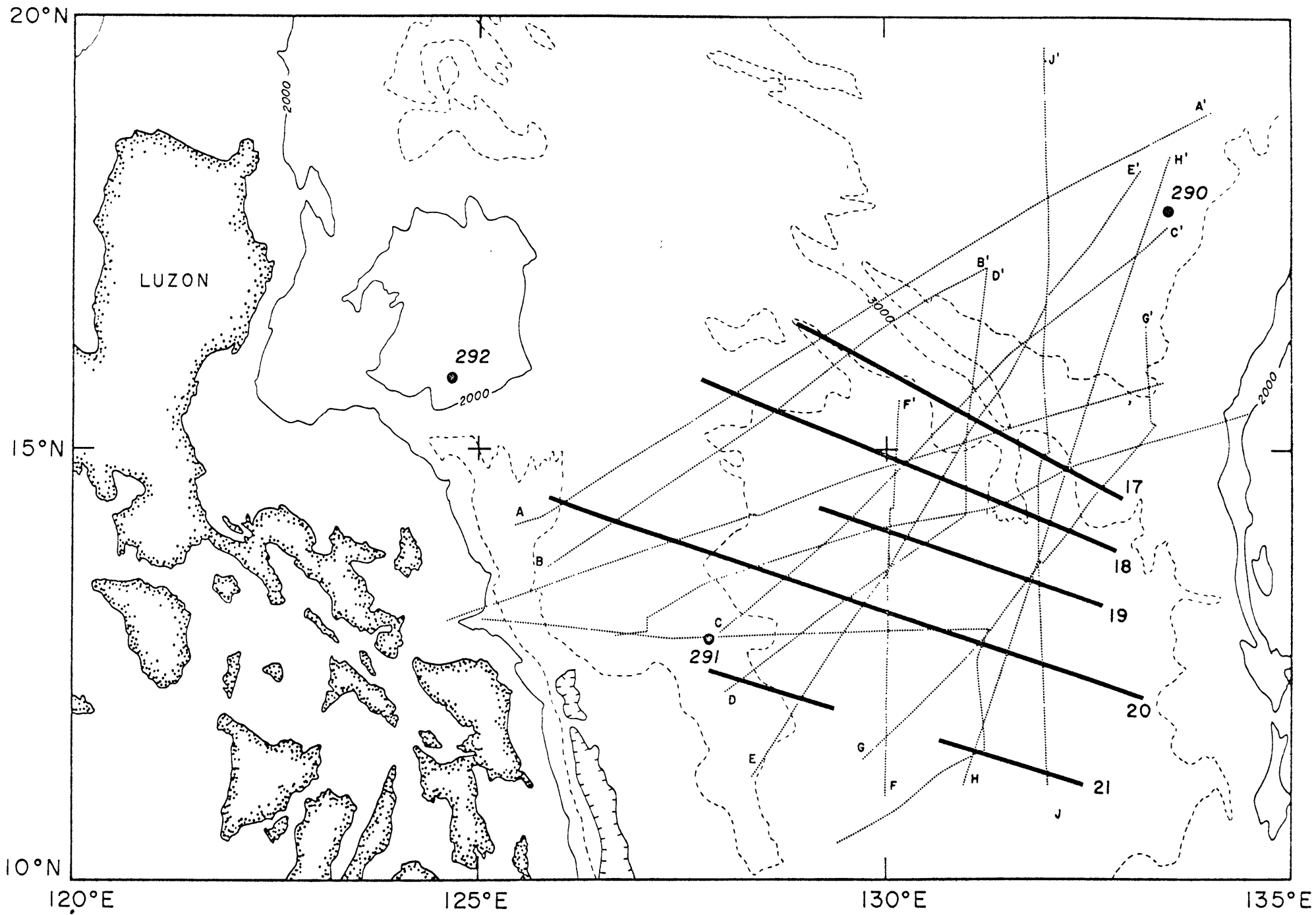
al. (1968)

FIG 1

the paleontological dates from DSDP Site 291 [Ingle et al.,

1975] and an origin south of the equator, which is supported

by the paleomagnetic measurements described in this paper.

The phase shifted anomalies and degree of phase shift are

shown in Figure 17. These values are little changed from

the previous estimates of Louden [1976] and range from 160°

to 200° for the various profiles. This range of θ is plotted

as a paleopole positions in figure 18a, and is consistent

with the sediment paleolatitudes for DSDP sites 292, 294 and

290, which plot as small circles of paleopole positions in

figure 18b. This means that the skewness of the magnetic

anomalies is not greatly effected by tectonic effects such

as can sometimes cause anomalous results [Cande, 1976],

but is a true indicator of the remanent magnetic field.

Unfortunately, we are still left a large uncertainty in

determining a unique paleopole position.

The one remaining parameter which also depends on the

remanent inclination and declination is the amplitude factor

C in eq (6),

$$C = (\sin I \sin I_r)/(\sin I' \sin I'_r), \qquad (8)$$

where $\tan I'_r = \tan I_r/\sin \alpha_r$. For the anomalies of figure

16 and 17, C can range from 0 to 0.94, depending on the

value of the remanent strike (α_r). Values of C along θ= 180°

are plotted in figure 18a. If we can assume that the magnetic

FIGURE 17

Phase shifted anomalies from tracks in Figure

16 projected along N 21°E. Degree of phase

shift is given in parentheses next to the cruise

identification for each track. Correlation of

anomalies is extended from the original identi-
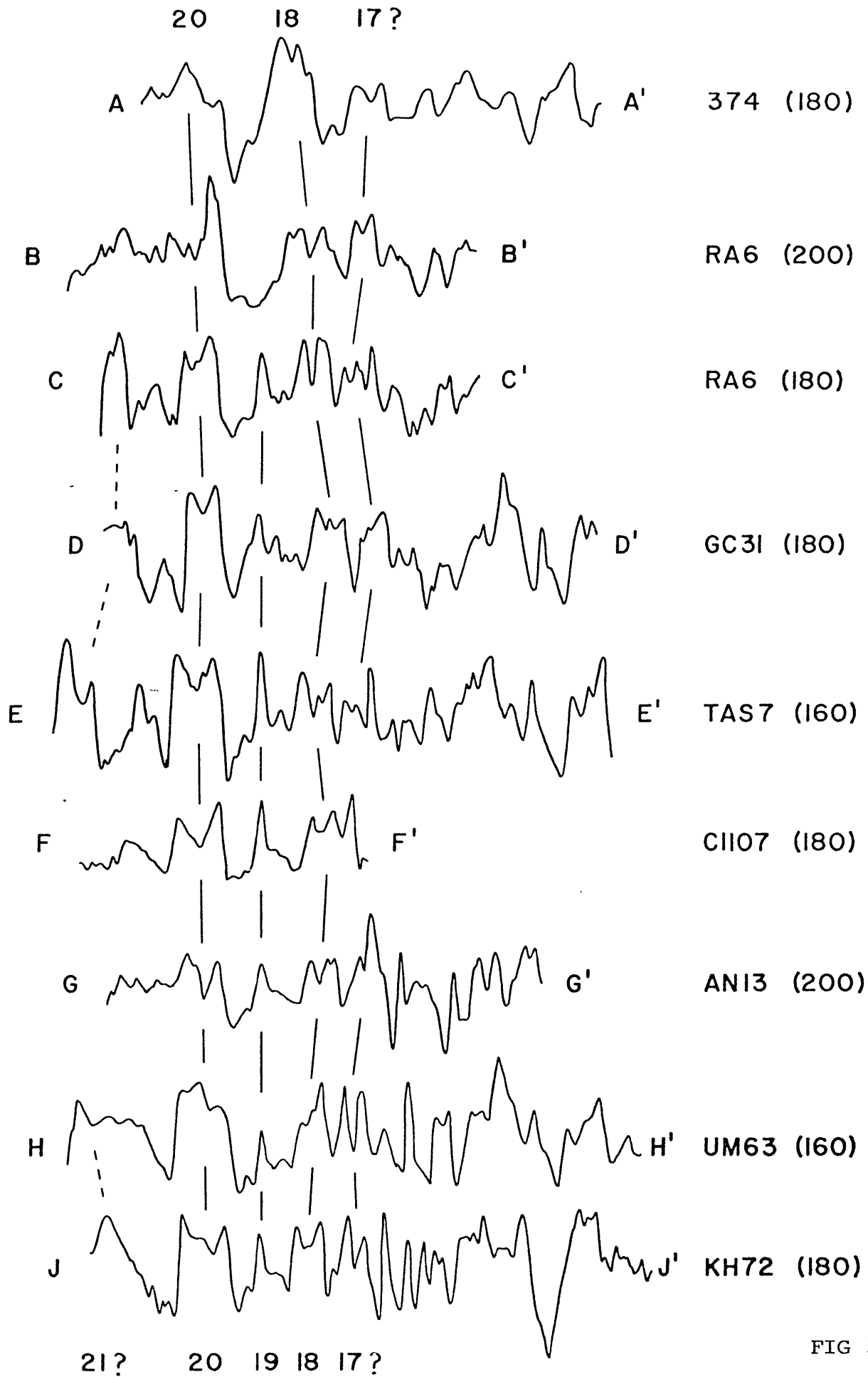
fications of Louden (1976).

FIG 17

origins of our anomalies are the same as for anomalies in
other ocean basins, then we can determine C by comparing the
amplitude of our anomalies to those where C is known. This
is done in Table V, where we list all of the major East-West
anomalies. Excepting one anomaly sequence in the Indian
Ocean, all amplitudes of East-West anomalies are large (700-
1000γ); and the small amplitudes (200-300γ) of our nearly
East-West Philippine Basin anomalies indicate that this
plate must have undergone significant rotations in the past.
Taking

$$0.2 \leq C \leq 0.6$$

limits our locus of pole positions in figure 18a to two
areas at either extreme of our great circles, both of which
are consistent with mean paleolatitudes for DSDP sites 292
and 294 (figure 18c).

We can compare our West Philippine Basin paleomagnetic
pole positions to predictions based on known plate rotations.
The rotation of the Philippine plate with respect to the
spin axis is the vector sum of rotations of the Pacific
plate relative to the spin axis and Philippine plate rotations
with respect to the Pacific:

$$\omega_{phil\ pole} = \omega_{phil\ pac} + \omega_{pac\ pole} \qquad (9)$$

Finite rotations of the Pacific with respect to the

TABLE V: Magnitude and Location of Major East-West Sea-Floor Spreading Magnetic Anomalies

ID	Anomaly No.	Site Lat	Site Long	Paleo- Lat	Peak to Peak Magnitude	C*	Reference
Phoenix	M1-M10	5°N	175°W	50°S	1000	0.9	Larson and Chase 1972
Wharton Basin	21	4°S	95°E	25°S	400	1.0	Sclater and Fisher 1974
	21	20°S	84°E	40°S	700	1.0	
North Pacific	27-32	50°N	170°W	30°N	1000	1.0	Cande 1976
Galapagos	3-5	3°N	87°W	1°N	700	1.0	Sclater and Klitgord 1973
Philippine Sea	20	15°N	130°E	5°S	200-300	?	Louden 1976

* $C = (\sin I \sin I_r)/(\sin I' \sin I'_r)$ where I is the inclination and I' is the effective inclination and r refers to remanent values.

FIGURE 18

Stereonet projections of paleomagnetic pole

positions: (a) Small circles determined from

paleolatitude measurements on sediments of DSDP

sites 290 (dashed lines), 292 (solid lines)

and 294 (dotted lines). Pairs of lines enclose

areas of 95% confidence. (b) Great circles

determined from the phase shifting of magnetic

anomalies (Figure 17). Individual circles

correspond to phase shifts of 160°, 180° and .

200°. Numbers correspond to magnetic anomaly

amplitude factors of 10.C as defined in the text.

(c) Combined plots of mean paleolatitude data

(lines) and phase shifting (shaded regions)

where $0.2 \leq C \leq 0.6$. The amplitude constraint is

determined from comparison with other east-west

anomalies (Table V). (d) Shaded region includes

region of (c) which falls between site 292 and

294 paleomagnetic data. ⬡ is the mean pole

FIG. 18 (cont.)

position for Guam Miocene volcanics (Larson et al.,

1974). Numbers indicate paleopole determinations

from the motion of the Pacific and Philippine

plates for various relative Phil-Pac poles:

(1) -5°, -52° and (2) -3°, -63° from Karig (1975);

(3) 26°, -37° and (4) -1°, 1° from Fitch (1972);

and (5) -7°, -38° from Katsumata and Sykes (1969).

Each successive number represents an additional

20° of relative Phil-Pac rotation away from the

Pacific paleopole for 50 m.y.b.p. (open circle)

which is calculated from motions of Minster et al.
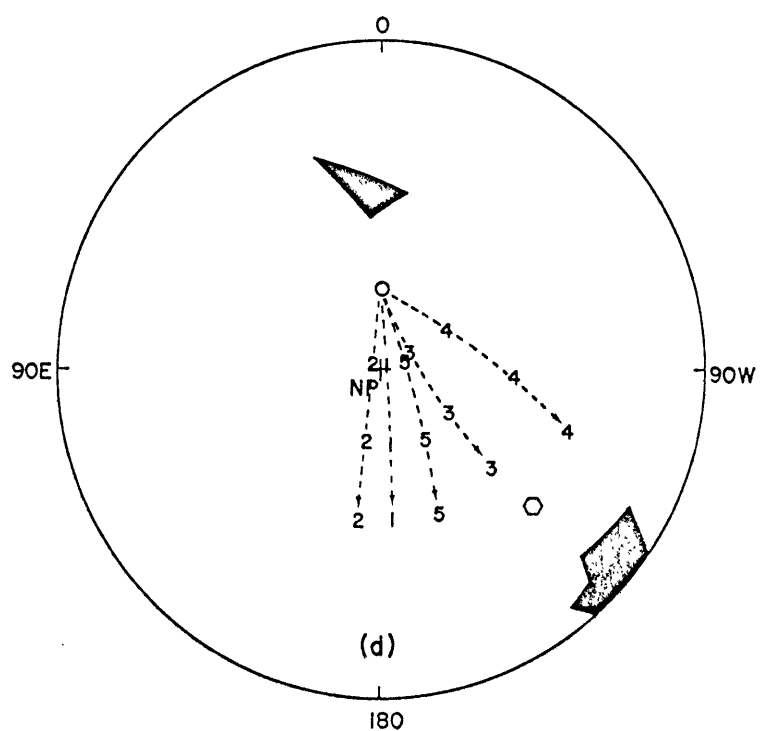
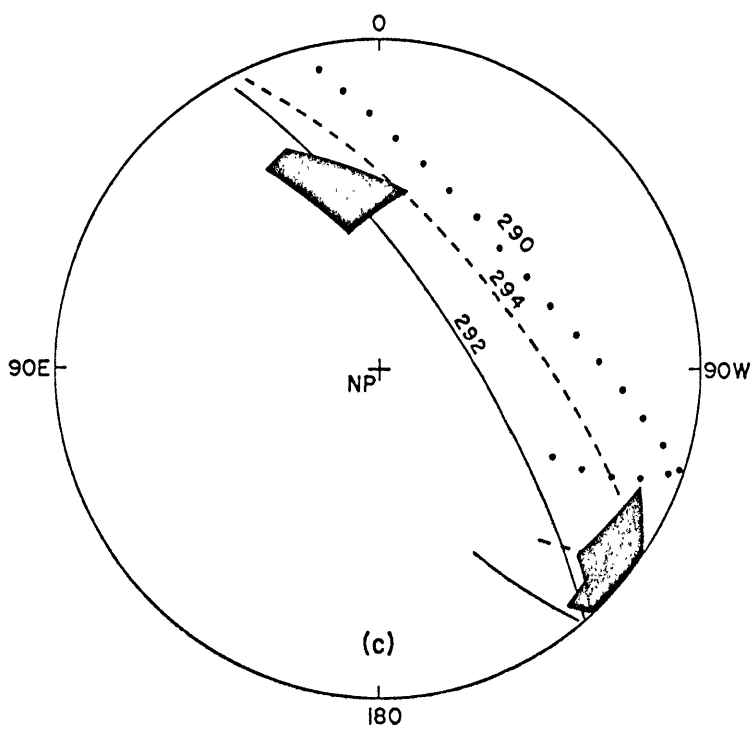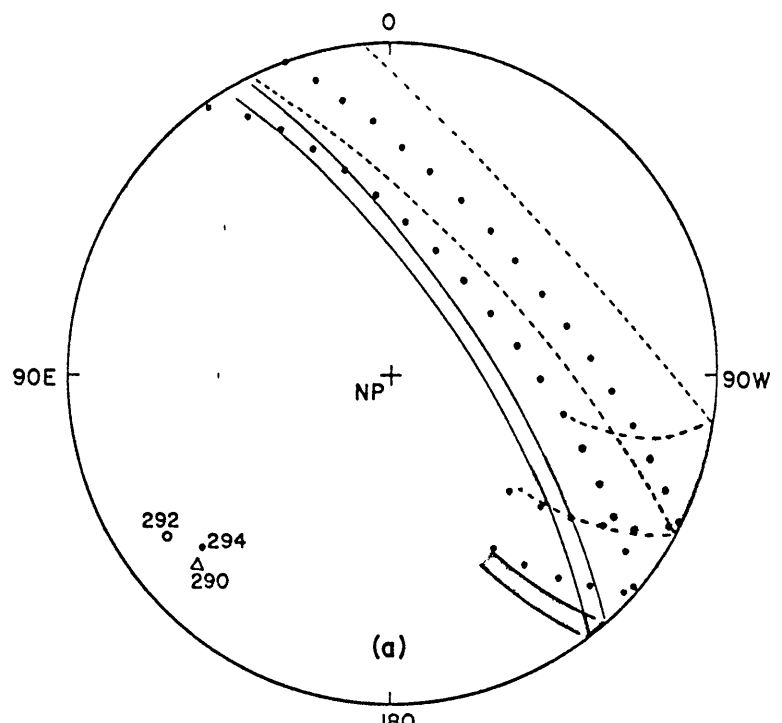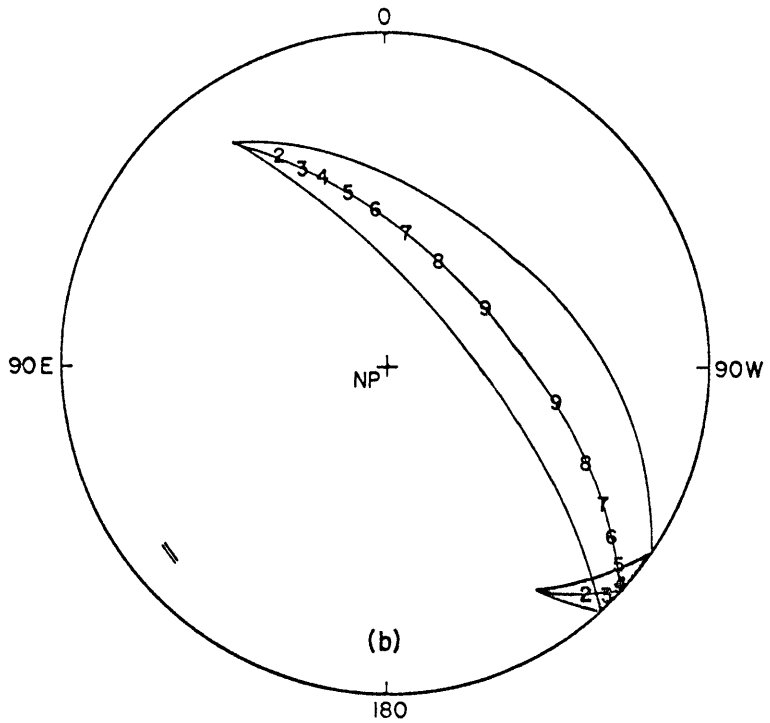(1974) and Clague and Jarrard (1973).

FIG 18

pole are recorded in bathymetric lineations such as the Emperor-Hawaiian seamount chain. Various determinations have been made of this pole for the past 40 m.y. (see Solomon and Sleep [1974] for a summary), but differences are not significant in this study. We use the Minster et al. [1974] pole (67°S, 121°E) and rate (8.10^{-7}deg/yr) over the past 40 m.y. Since our anomalies are as old as 50 m.y., we add to this a rotation of 10° (10^{-6}deg/yr over 10 m.y.) about the Clague and Jarrard [1973] pole (17°S, 73°E) determined from the Emperor seamount chain.

The only information concerning $_{phil}\omega_{pac}$ comes from fitting fault plane solutions for recent earthquakes on the margins of the Philippine plate. This has been done by Katsumata and Sykes [1969] for earthquakes on the Izu-Bonnin margin of the Pacific and Philippine plates, and by Fitch [1972] and Karig [1975] for earthquakes on the Japan-Ryuku margin of the Philippine and Eurasia plates. These latter solutions are then summed with Eurasia-Pacific rotations to get a Philippine-Pacific pole. These pole positions are not well constrained, are poorly located, and of course are only instantaneous and need not apply over a finite time period. We use them only as a point of reference.

Figure 18d shows the results of calculations based on equation 8. Paleomagnetic pole positions are calculated for varying amounts of rotation about the different Pacific-Philippine poles. Only one of our two possible pole positions

are compatible with these rotations. Plate motion between the Philippine and Pacific plates would have to have been the reverse of what it is today for the other paleopole to be possible. This is evidence for a large amount (60°) of clockwise rotation between the Pacific and Philippine plates , which conforms to the theory of Uyeda and Ben-Avraham [1972].

The same rotations can also explain the paleopole position for Miocene volcanic rocks on Guam [Larson et al., 1974]. This could mean that Guam has undergone the same rotations as has the West Philippine Basin, and that these rotations took place before Guam was separated from the West Philippine Basin by the opening of the Parece Vela Basin. In this case such a rotation would not be due to a deformation of the plate boundary alone but would be felt by the entire rigid plate. The other possibility is that these rotations have taken place continuously over the past 50 m.y. and that Guam and the West Philippine Basin have always remained fixed.

CONCLUSIONS

The following list is a summary of the major results of this study:

(1) Sediment cores taken by the Deep Sea Drilling Project can yield well grouped paleolatitudes, especially when results of closely spaced samples can be averaged

together at several separate locations down core. These

results can be of greater resolution than those from DSDP

basalts, which may not contain enough flow units to adequately

average out components of secular variation.

(2) The effect of viscous remanent magnetization in

destabilizing the original remanent magnetization in DSDP

basalts may be exaggerated by laboratory measurements of up

to 1000 hours. Site 292 basalts have large viscosity coefficients

while still retaining reversed polarities.

(3) Paleolatitudes for DSDP site 292 sediments indicate

that this site formed south of the equator, and results for

sites 290 and 294 can be explained in a similar manner.

This adds independent justification for our inversion of

magnetic anomalies in the West Philippine Basin with respect

to North Pacific anomalies, which is necessary in order to

identify them with world-wide Eocene reversals.

(4) Paleomagnetic pole positions determined from both

the phase shifting of magnetic anomalies and the paleomagnetics

of DSDP sites in the West Philippine Basin are consistent

with each other, and can be restricted to two relatively

well defined positions if the low amplitude of the anomalies

is due to a rotation of the Philippine plate. One of these

two positions, which includes a large amount of clockwise

rotation of the Philippine plate with respect to the magnetic

pole, is consistent with the finite "absolute" rotations of the Pacific plate and present Philippine-Pacific plate rotations. It is also consistent with paleopole positions for Guam and may mean that both have undergone the same motions since the early Miocene.

References

Baag, C. and C.E. Helsley, Geomagnetic secular variation model E, J. Geophys. Res., 79, 4918-4922, 1974.

Biquand, D. and M. Prevot, A.F. demagnetization of viscous remanent magnetization in rocks, Z. Geophys., 37, 471-485, 1971.

Blow, R.A. and N. Hamilton, Paleomagnetic evidence from DSDP cores of northward drift of India, Nature, 257, 570-572, 1975.

Briden, J.C. and M.A. Ward, Analysis of magnetic inclinations in bore cores, Pure App. Geophys., 57, 133-152, 1966.

Cande, S., Paleomagnetic poles from late Cretaceous marine magnetic anomalies in the Pacific, Geophys. J.Roy. Astron. Soc., 44, 547-566, 1976.

Clague, D.A. and R.D. Jarrard, Tertiary Pacific plate motion deduced from the Hawaiian-Emperor chain, Geol. Soc. Am. Bull., 84, 1135-1154, 1973.

Cox, A., Paleolatitudes determined from paleomagnetic data from vertical cores, in prep.

Creer, K.M., The remanent magnetization of unstable Kemper marls, Phil. Trans. Roy. Soc. London, ser. A., 250, 130-143, 1957.

Creer, K.M., N. Peterson, and J. Petherbridge, Partial self-reversal of remanent magnetization in basalts, Geophys. J., 21, 471-483, 1970.

Creer, K.M., R. Thompson, L. Molyneux, and F.J.H. Mackereth, Geomagnetic secular variation recorded in the stable magnetic remanence of recent sediments, Earth Planet. Sci. Lett., 14, 115-127, 1972.

Dunlop, D.J., Theory of the magnetic viscosity of lunar and terrestrial rocks, Rev. Geophys. Space Phys., 11, 855-901, 1973.

Fitch, T.J., Plate convergence, transcurrent faults and internal deformation adjacent to southeast Asia and the western Pacific, J. Geophys. Res., 77, 4432-4460, 1972.

Francheteau, J., C.G.A. Harrison, J.G. Sclater, and M.L. Richards, Magnetization of Pacific seamounts: a preliminary polar curve for the northeastern Pacific, J. Geophys. Res., 75, 2035-2061, 1970.

Green, K.E. and A. Brecher, Preliminary paleomagnetic results for sediments from site 263, leg 27, in Initial Reports of the Deep-Sea Drilling Project, ed. J.J. Veevers, J.R. Heirtzler, et al., v. 27, U. S. Government Printing Office, Washington, D. C., 405-413, 1974.

Hammond, S.R., L.W. Kroenke, F. Theyer, and D.L. Keeling, Late Cretaceous and Paleogene paleolatitudes of the Ontong Java Plateau, Nature, 255, 46-47, 1975.

Hammond, S.R., F. Theyer, and G.H. Sutton, Paleomagnetic evidence of northward movement of the Pacific plate in deep-sea cores from the central Pacific basin, Earth Planet. Sci. Lett., 22, 22-28, 1974.

Harrison, C.G.A., The paleomagnetic record from deep-sea sediment cores, Earth Sci. Rev., 10, 1-36, 1974.

Harrison, C.G.A., R.D. Jarrard, V. Vacquier, and R.L. Larson, Paleomagnetism of Cretaceous Pacific seamounts, Geophys. J.Roy. Astron. Soc., 42, 859-882, 1975.

Herroun, E.F. and A.F. Hallimond, Laboratory experiments on the magnetization of rocks, Proc. Phys. Soc. London, 55, 214-221, 1943.

Ingle, J.C., D.E. Karig, Initial Reports of the Deep-Sea Drilling Project, v. 31, U. S. Government Printing Office, Washington, D. C., 1975.

Karig, D.E., Basin genesis in the Philippine Sea, in Initial Reports of the Deep-Sea Drilling Project, ed. J.C. Ingle, D.E. Karig, et al., v. 31, U. S. Government Printing Office, Washington D. C., 857-879, 1975.

Katsumata, M. and L.R. Sykes, Seismicity and tectonics of the western Pacific: Izu-Mariana, Caroline and Ryukyu-Taiwan regions, J. Geophys. Res., 74, 5923-5948, 1969.

Larson, R.L. and C.G. Chase, Late Mesozoic evolution of the western Pacific Ocean, Geol. Soc. Am. Bull., 83, 3627-3644, 1972.

Larson, E.E., R.L. Reynolds, M. Ozima, Y. Aoki, H. Kinoshita, S. Zasshu, N. Kawai, T. Nakajima, K. Hirooka, R. Merrill, and S. Levi, Paleomagnetism of Miocene volcanic rocks of Guam and the curvature of the southern Mariana island arc, Geol. Soc. Am. Bull., 86, 346-350, 1975.

Louden, K. E., Magnetic anomalies in the West Philippine
    Basin, in The Geophysics of the Pacific Ocean Basin and
    Its Margin, ed. G. P. Woollard et al., Geophys. Monogr. Ser.,
    19, Am. Geophys. Un., Washington, D.C., in press, 1976.

Lowrie, W., Viscous remanent magnetization in oceanic basalts,
    Nature, 243, 27-29, 1973.

Lowrie, W., Oceanic basalt magnetic properties and the Vine
    and Matthews hypothesis, J. Geophys. Res., 40, 513-
    536, 1974.

Lowrie, W., R. Løvlie, and N.D. Opdyke, Magnetic properties
    of Deep-Sea Drilling Project basalts from the north
    Pacific Ocean, J. Geophys. Res., __, 7646-7660, 1973a.

Lowrie, W., R. Løvlie, and N.D. Opdyke, The magnetic properties
    of Deep-Sea Drilling Project basalts from the Atlantic
    Ocean, Earth Planet. Sci. Lett., 17, 338-349, 1973b.

Minster, J.B., T.H. Jordan, P. Molnar, and E. Haines, Numerical
    modeling of instantaneous plate tectonics, Geophys.
    J. Roy. Astron. Soc., 36, 541-576, 1974.

McElhinney, M.W., Paleomagnetism and Plate Tectonics, Cambridge
    University Press, London, 358 pp., 1973.

McKenzie, D.P. and J.G. Sclater, The evolution of the
    Indian Ocean since the Late Cretaceous, Geophys. J.Roy.
    Astron. Soc., 25, 437-528, 1971.

Neel, L., Theorie du treunage magnetique des substances
    massives dans domaine de Rayleigh, J. Phys. Radium, 11,
    49-61, 1950.

Opdyke, N.D., Paleomagnetism of deep-sea cores, Rev. Geophys. Space Phys., 10, 213-249, 1972.

Peirce, J.W., Assessing the reliability of DSDP paleolatitudes, J. Geophys. Res., in press, 1976.

Peirce, J.W., C.R. Denham, and B.P. Luyendyk, Paleomagnetic results of basalt samples from DSDP leg 26, in Initial Reports of the Deep-Sea Drilling Project, ed. T.A. Davies, B.P. Luyendyk, et al., v. 26, U. S. Government Printing Office, Washington, D. C., 1975.

Phillips, J.D. and D. Forsyth, Plate tectonics, paleomagnetism, and the opening of the Atlantic, Geol. Soc. Am. Bull., 83, 1579-1600, 1972.

Schouten, H. and S.C. Cande, Paleomagnetic poles from sea-floor spreading anomalies, Geophys. J. Roy. Astron. Soc., 44, 567-575, 1976.

Schouten, H. and K. McCamy, Filtering marine magnetic anomalies, J. Geophys. Res., 77, 7089-7099, 1972.

Sclater, J.G., R.N. Anderson, and M.L. Bell, Elevation of ridges and evolution of the central eastern Pacific, J. Geophys. Res., 76, 7888-7915, 1971.

Sclater, J.G. and A. Cox, Paleolatitudes from JOIDES deep sea sediment cores, Nature, 226, 934-935, 1970.

Sclater, J.G., D. Karig, L.A. Lawver, and K. Louden, Heat flow, depth, and crustal thickness of the marginal basins of the South Philippine Sea, J. Geophys. Res., 81, 309-318, 1976.

Solomon, S.C. and N.H. Sleep, Some simple physical models for absolute plate motions, J. Geophys. Res., 79, 2557-2567, 1974.

Stacey, F.D., The physical theory of rock magnetism, Advan. Phys., 12, 45-133, 1963.

Symons, D.T.A. and M. Stupavsky, A rational paleomagnetic stability index, J. Geophys. Res., 79, 1718-1720, 1974.

Uyeda, S. and Z. Ben-Avraham, Origin and development of the Philippine Sea, Nature Phys. Sci., 240, 176-178, 1972.

Wilson, R.L., Permanent aspects of the earth's non-dipole magnetic field over upper Tertiary times, Geophys. J. Roy. Astron. Soc., 19, 417-437, 1970.

Wilson, R.L. and M.W. McElhinny, Investigations of the large scale paleomagnetic field over the past 25 million years. Eastward shift of the Icelandic spreading ridge, Geophys. J. Roy. Astron. Soc., 39, 570-586, 1974.

Acknowledgements

APPENDIX A

HEAT FLOW, DEPTH AND CRUSTAL THICKNESS OF

THE MARGINAL BASINS OF THE SOUTH

PHILIPPINE SEA

Heat Flow, Depth, and Crustal Thickness of the Marginal Basins of the South Philippine Sea

JOHN G. SCLATER,[1] DAN KARIG,[2] LAURENCE A. LAWVER,[3] AND KEITH LOUDEN[4]

We present 51 heat flow measurements and two geophysical profiles across the West Philippine and Parece Vela basins. We show that both regions have a variable heat flow but that the scatter decreases markedly if we accept as reliable only measurements in areas of uniform sediment drape. Extending this argument to the deep ocean floor shows that the heat flow in these two marginal basins is not necessarily higher than that for deep ocean floor of the same age. On the other hand, the mean depth of both basins is greater and the oceanic crust thinner than the depth and crust of ocean floor of the same age. In the absence of a significant free air gravity anomaly over both basins, we suggest that the thinner crust may account for most of the increase in depth of the two basins. However, more refraction studies are needed to substantiate this difference before this explanation can be unreservedly accepted.

INTRODUCTION

In the marginal basins of the western Pacific (Figure 1) there appears to be a simple relationship between increasing depth, decreasing heat flow, and increasing age [*Karig,* 1971]. This relationship is similar to that shown by the midocean ridges, although the heat flow in the younger marginal basins appears to be higher than that for oceanic crust of the same age [*Sclater,* 1972]. Apart from this difference in heat flow, the general similarity in the dredged rocks and other geological and geophysical parameters has led many to suggest that the intrusion process behind island arcs is similar to that now occurring at the crest of midocean ridges.

The southern half of the Philippine Sea exhibits the classic section of oceanic crust with both active and inactive basins (Figures 2 and 3). Immediately to the west of the volcanic chain of the Mariana arc system lies the Mariana Trough. This active basin has a shallow depth of 2500–3000 m, has outcropping fresh basalt, and is a region in which crustal extension has taken place at least until the recent past [*Karig,* 1971]. A remanent arc, the South Honshu Ridge, separates this active marginal basin from the inactive Parece Vela Basin. This inactive basin has an average depth of nearly 5 km except for a slightly shallower broad volcaniclastic apron flanking the western side of the South Honshu Ridge (Figure 3a). A zone of high-amplitude ridges and troughs lies close to the center of the basin. These features are best developed south of 20°N but appear to continue to the northern end of the basin. Near 17°N they veer southwestward and may continue as far south as 11°N as a central feature. Sparse calcareous nannofossils at the base of two Deep-Sea Drilling Project (DSDP) holes, 53 and 54, in the basin gave a middle Oligocene to early Miocene age for the lowermost sediment section near the center of the basin.

Apart from greater size and depth, the general structure of the Parece Vela Basin is similar to that of the Mariana Basin. On the basis of these similarities and the sediment ages from the DSDP holes, *Karig* [1971] has suggested that the Parece Vela Basin is an extensional feature formed by the intrusion of oceanic crust between the late Oligocene and early Miocene.

He has further suggested that the central ridge and trough feature marks the final position of the spreading center and that extension within this marginal basin is symmetrical.

The Palau-Kyushu Ridge, a supposed east-facing remanent arc associated with spreading in the Parece Vela Basin, separates this basin and the West Philippine Basin. The West Philippine Basin is by far the largest of the basins in the Philippine Sea and is the largest and the deepest (5500–6000 m) marginal basin in the world. A major system of troughs and ridges called the Central Basin Fault runs from northwest to southeast through the center of the basin. Deep-sea drilling in the West Philippine Basin yielded sediments no older than middle Eocene [*Ingle et al.,* 1975]. Careful analysis of the lineated magnetic anomalies in this basin, first observed by *Ben-Avraham et al.* [1972] and related to the magnetic time scale by *Louden* [1976], has shown that they are lineated N110°E. The anomalies are best matched by a symmetrical sequence on either side of the Central Basin Fault starting with anomaly 17 and ending with anomaly 22. On both the time scales of *Heirtzler et al.* [1968] and the modification of *Sclater et al.* [1974a] this sequence yields a middle to late Eocene age for the southwestern portion of the West Philippine Basin. These results are in excellent agreement with the age suggested from the analysis of piston cores in slumps [*Karig,* 1971] and from the provisional ages of the sediments at the base of the DSDP holes in the area [*Ingle et al.,* 1975]. North of the Central Basin Fault the anomalies are lineated, but identification is less certain. At present they are best matched by assuming symmetry about the fault. Unfortunately, the identification is sufficiently ill-defined so that it is possible that the anomalies could be a sequence younger than 17. Whichever interpretation is correct, we are confident that the basin is no older than Paleocene. The major question still unanswered is whether this crust was formed at a simple midocean ridge system [*Uyeda and Ben-Avraham,* 1972] or whether its tectonic environment was that of extension immediately behind an active subduction zone.

In this paper we present two each of bathymetric, seismic reflection, heat flow, and magnetic profiles and one gravity profile across the southern section of the Philippine Sea (Figure 3). We ran these profiles, concentrating on the surface heat flow, to investigate the similarities and differences between the West Philippine and Parece Vela basins and the ocean floor of the same age. We will show with a reanalysis of the relation of surface heat flow values and continuous uniform sediment cover that the high heat flow behind island arcs may not be
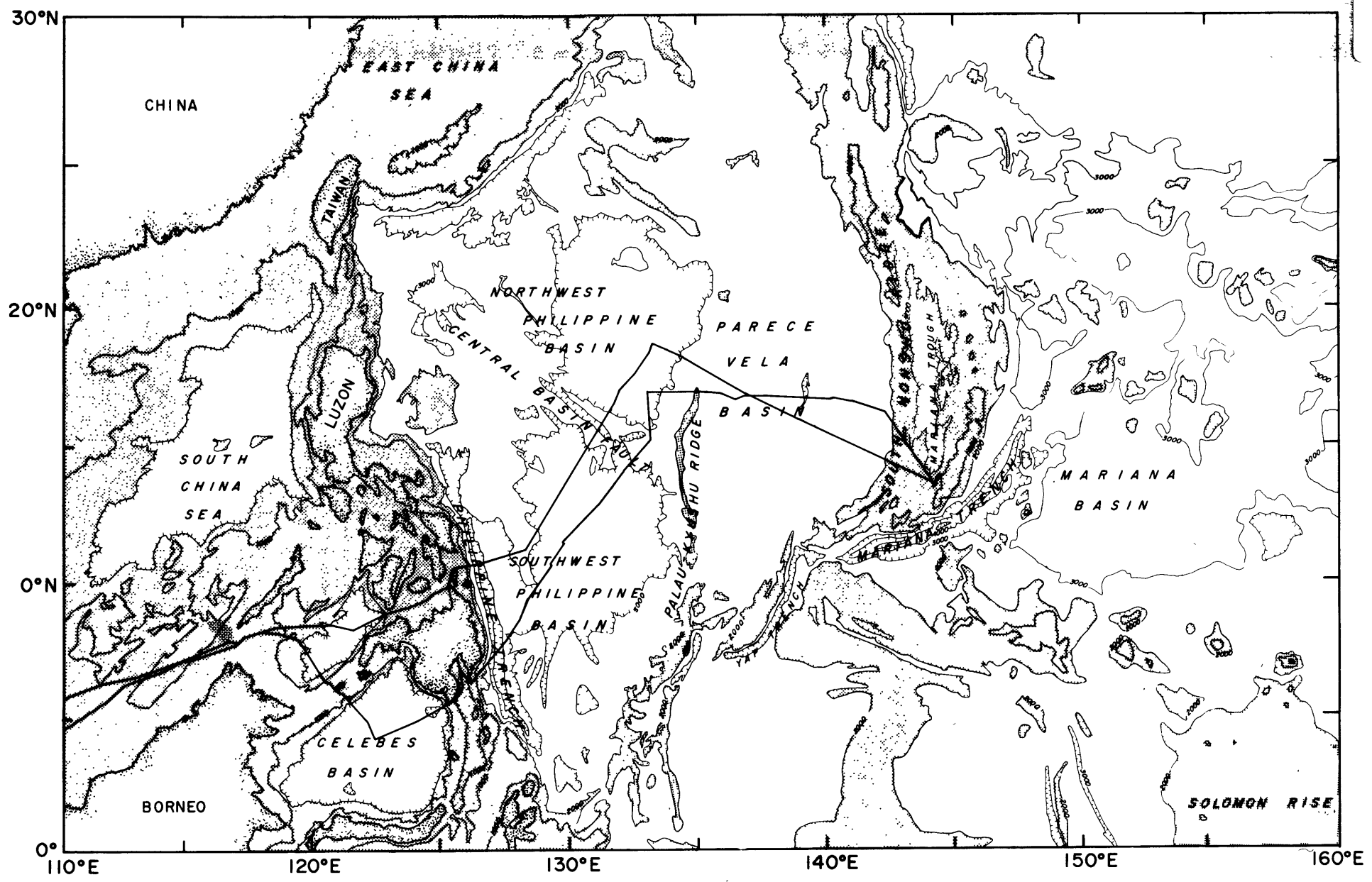
Fig. 1. A sketch of the Philippine Basin showing the principal topographic features and the track of the Antipode and Tasaday lines. The depths above 2000 fm (1 fm = 1.82 m) have been shaded.

significantly higher than that in normal oceanic crust of the same age. However, both marginal basins differ in two important features from oceanic crust of the same age. The basins are deeper and have a thinner oceanic crust. We suggest that these two features may be related.

HEAT FLOW MEASUREMENTS

In June and July 1971 we obtained 39 heat flow measurements in the marginal basins of the Indonesian region and across the Philippine Sea from the R/V *Melville* on leg 13 of expedition Antipode of the Scripps Institution of Oceanography. Twelve further measurements in this area were added during July 1973 from the R/V *Thomas Washington* during leg 7 of Scripps Institution of Oceanography expedition Tasaday. We measured all the temperatures with a 2.5-m-long Bullard probe [*Corry et al.*, 1968]. On the first expedition we determined the thermal conductivities by two methods. In the first method we measured the conductivity of sediment recovered

TABLE 1. Heat Flow Stations in the Western Pacific

Station	Location N	Location E	Corrected Depth, m	Gradient, °C/m	Conductivity,* 10^{-3} cal/°C cm s	Heat Flow, μcal/cm² s	Penetration†	Tilt, deg	Type of Environment
Antipode 13									
176	6°34.9'	113°50.5'	2350	0.92	1.68 (N)	1.55	f	0–15	B
177	6°46.3'	114°15.3'	2863	0.80	1.67 (A)	1.33	f	0–15	A
178	6°58.3'	114°39.7'	2882	0.92	1.66 (N)	1.52	f	0–15	A
179	7°07.7'	115°07.0'	2844	0.83	1.67 (A)	1.39	f	0–15	B
180	7°51.5'	119°19.5'	3641						
181	7°17.6'	119°45.9'	3801	1.08	1.74 (A)	1.90	f	0–15	A
182	6°41.0'	120°09.0'	3641	1.02	1.74 (N)	1.77	f	0–15	B-D
183	4°55.0'	121°53.0'	4790						
184	3°58.2'	122°14.0'	4965	0.90	1.66 (N)	1.49	f	0–15	A
185	4°39.7'	123°48.5'	4942	0.88	1.66 (A)	1.49	f	0–15	A
186	5°53.5'	125°48.5'	3007	0.24	1.66 (A)	0.41	f	0–15	D
188	8°04.0'	127°46.1'	5460	0.55	1.90 (A)	1.04	f	0–15	B-D
189	8°59.5'	128°18.0'	5827	0.78	2.00 (I)	1.56	f	0–15	A
190	9°41.9'	128°45.1'	5746	0.86	1.90 (I)	1.65	f	0–15	A
191	10°30.2'	129°11.6'	5766	0.81	2.00 (I)	1.62	f	0–15	A
192	11°23.2'	129°43.9'	5470	1.03	1.90 (A)	1.96	f	0–15	A-B
193	12°13.0'	130°27.2'	5754	0.88	1.96 (I)	1.73	f	0–15	B
194	12°57.5'	131°16.5'	5752	0.60	1.83 (I)	1.10	f	0–15	B-D
195	13°43.6'	131°55.2'	5900	2.02	1.98 (I)	3.99	f	0–15	C
196	13°59.5'	132°08.9'	5959	0.86	1.90 (A)	1.63	f	0–15	C
197	14°43.8'	132°46.7'	5343	· · ·	1.93 (I)	0.95	75 cm	>30	C
199	15°33.7'	133°14.2'	5782	0.24	2.01 (I)	0.49	f	0–15	D
200	16°26.5'	133°12.8'	5790	0.61	2.09 (I)	1.28	f	0–15	C-D
201	17°03.6'	133°15.3'	5712	0.55	1.95 (I)	1.07	f	0–15	B
202	17°03.0'	134°02.0'	5493	0.10	2.05 (I)	0.20	f	0–15	A
203	17°05.8'	134°33.7'	5398	0.87	1.98 (I)	1.72	f	0–15	A
205	17°00.0'	135°22.1'	5073	0.40	1.82 (I)	0.73	f	0–15	D
206	16°57.1'	135°54.0'	5084	0.41	1.92 (I)	0.78	f	0–15	C
207	16°49.0'	136°35.5'	4716	0.28	1.91 (I)	0.54	f	0–15	C
208	16°55.0'	136°57.5'	4797?	0.24	1.91 (I)	0.45	f	0–15	C-D
209	16°53.1'	137°24.8'	5201	0.43 ·	1.79 (I)	0.78	f	0–15	C
210	16°53.0'	137°53.0'	4586	2.68	1.83 (I)	4.91	f	0–15	C
211	16°52.3'	138°15.8'	4171						
214	16°46.6'	140°10.2'	4609	1.50	2.07 (I)	3.11	f	0–15	C
215	16°47.2'	140°44.6'	4816	0.28	1.85 (I)	0.53	f	0–15	A
216	16°39.7'	141°24.4'	4653	1.03	1.88 (I)	1.94	f	0–15	A
217	16°31.3'	141°49.0'	4506	1.14	1.90 (I)	2.16	f	0–15	A
218	16°22.9'	142°09.6'	4170	1.10	1.89 (I)	2.08	f	0–15	A
220	16°20.2'	142°33.8'	3672	0.23	1.98 (I)	0.46	f	0–15	B-D
Tasaday 7	·								
01	8°17.5'	120°50.2'	3932	1.03	1.90 (A)	1.96	f	0–15	?
02	8°25.8'	121°43.1'	4857	0.31	1.90 (A)	0.59	f	0–15	D
03	13°31.8'	129°58.2'	5673	0.94	1.90 (A)	1.79	f	0–15	A
04	15°28.6'	131°12.1'	5450	1.00	1.90 (A)	1.90	f	0–15	C
05	16°43.6'	132°06.9'	5761	0.49	1.90 (A)	0.93	f	0–15	C
06	17°23.9'	132°31.0'	5958	0.38	1.90 (A)	0.72	f	0–15	D
07	18°42.8'	133°24.8'	6132	1.28	1.90 (A)	2.43	f	0–15	A
08	17°34.7'	135°49.4'	4859	0.61	1.90 (A)	1.16	f	0–15	C
09	17°18.2'	136°22.2'	5053	0.19	1.90 (A)	0.36	f	0–15	D
10	17°00.6'	137°03.0'	5072	0.37	1.90 (A)	0.70	190 cm	>30	C-D
11	16°30.8'	138°03.9'	4883	0.29	1.90 (A)	0.55	f	0–15	C-D
12	16°08.6'	138°56.1'	5120	0.47	1.90 (A)	0.89	f	0–15	C-D
13	15°52.4'	139°34.3'	5206						C

Absence of data at station 180 was caused by the instrument catching fire and at stations 183 and 211 by the instruments falling over. At station 13 no data were recorded.

* Here N indicates needle probe conductivity measurement, I indicates in situ conductivity measurement, and A indicates assumed conductivity.
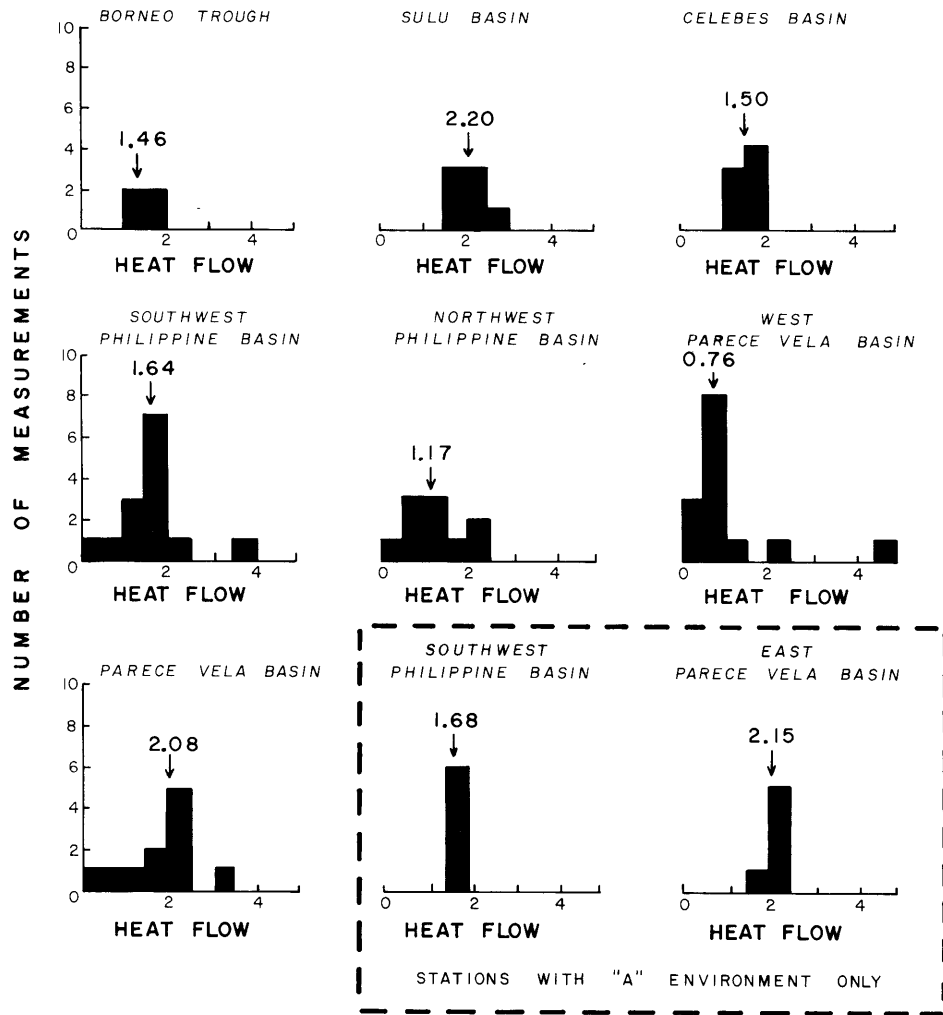
† Here f indicates full penetration.

-170-

Fig. 4. Histogram of heat flow values in the tectonic provinces of the south Philippine Sea and marginal basins of the Indonesian area. The median values are presented above each histogram.

by deep-sea cores, using the needle probe technique described by *von Herzen and Maxwell* [1959]. In the second we determined the in situ conductivity while the Bullard probe was on the bottom during the temperature gradient measurement, utilizing the technique of *Corry et al.* [1968]. For the Tasaday stations in the Philippine Sea we assumed a value of 1.90×10^{-3} cal/°C cm s, the mean value of the conductivities measured in the south Philippine Sea. For all the stations the heat flow was taken as the product of the temperature gradient and the conductivity.

TABLE 2. Heat Flow Statistics

| Area | Number of Measurements | Heat Flow, μcal/cm² s | | |
		Median	Mean	Standard Deviation
Raw Data				
Borneo Trough	4	1.46	1.45	0.12
Sulu Basin	7	2.20	2.13	0.30
Celebes Basin	7	1.50	1.51	0.23
Southwest Philippine Basin	14	1.64	1.59	0.86
Northeast Philippine Basin	10	1.17	1.24	0.69
Western Parece Vela Basin	14	0.76	1.10	1.19
Eastern Parece Vela Basin	11	2.08	1.80	0.81
All West Philippine Basin	24	1.48	1.44	0.80
All Parece Vela Basin	25	1.00	1.40	1.08
Reliable Data				
Southwest Philippine Basin	6	1.68	1.72	0.16
Eastern Parece Vela Basin	6	2.15	2.15	0.16

Reliable data are defined as measurements taken in an area of uniform sediment drape.
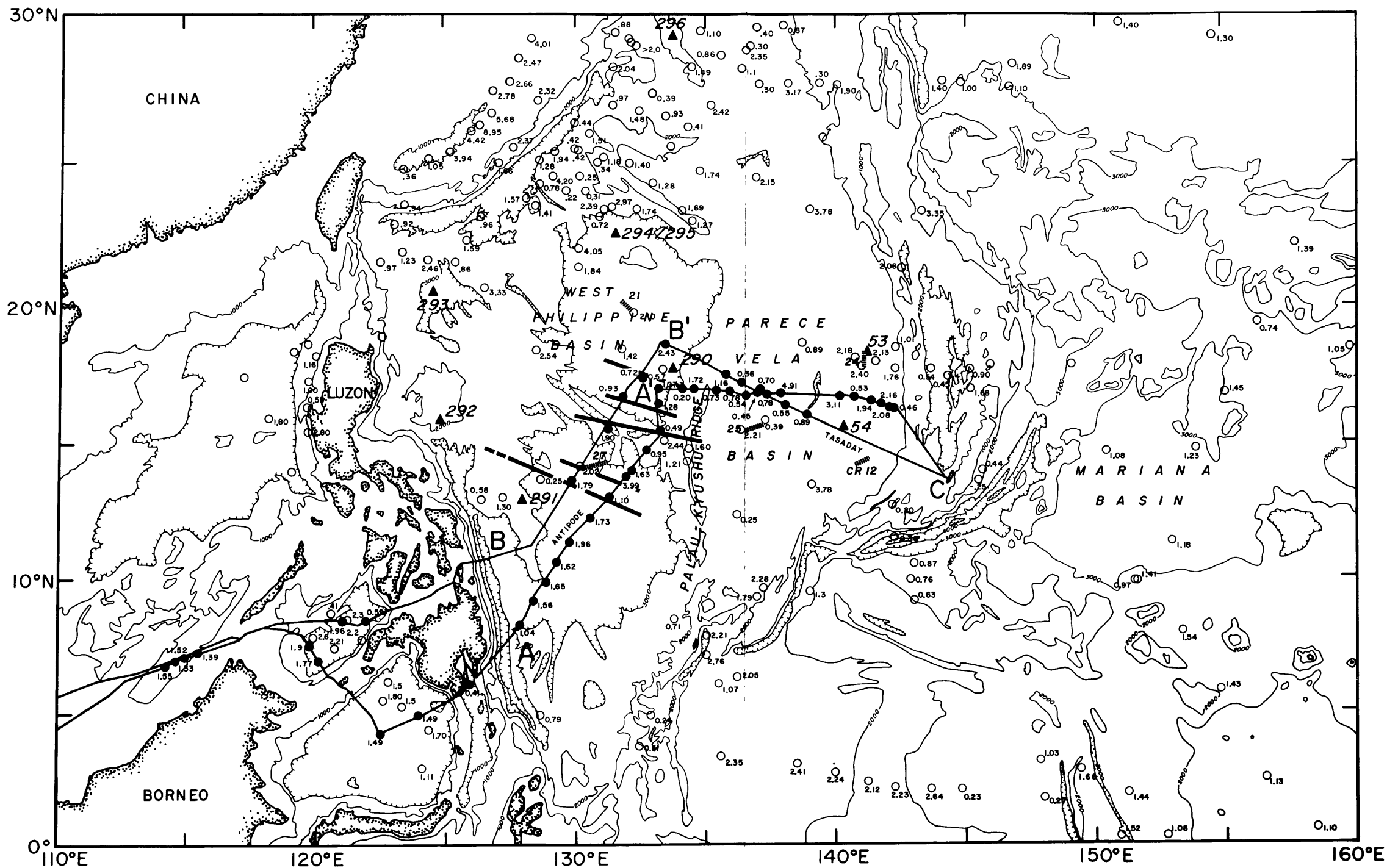
Fig. 2. Topographic chart of the Philippine Sea and marginal basins close to Indonesia. Heat flow stations, the track of Antipode 13 and Tasaday 7, and identified magnetic anomalies (after *Louden* [1976]) have been superimposed upon the chart. The solid circles are heat flow stations presented in this paper, and the solid triangles are Joides sites. Note the refraction stations.
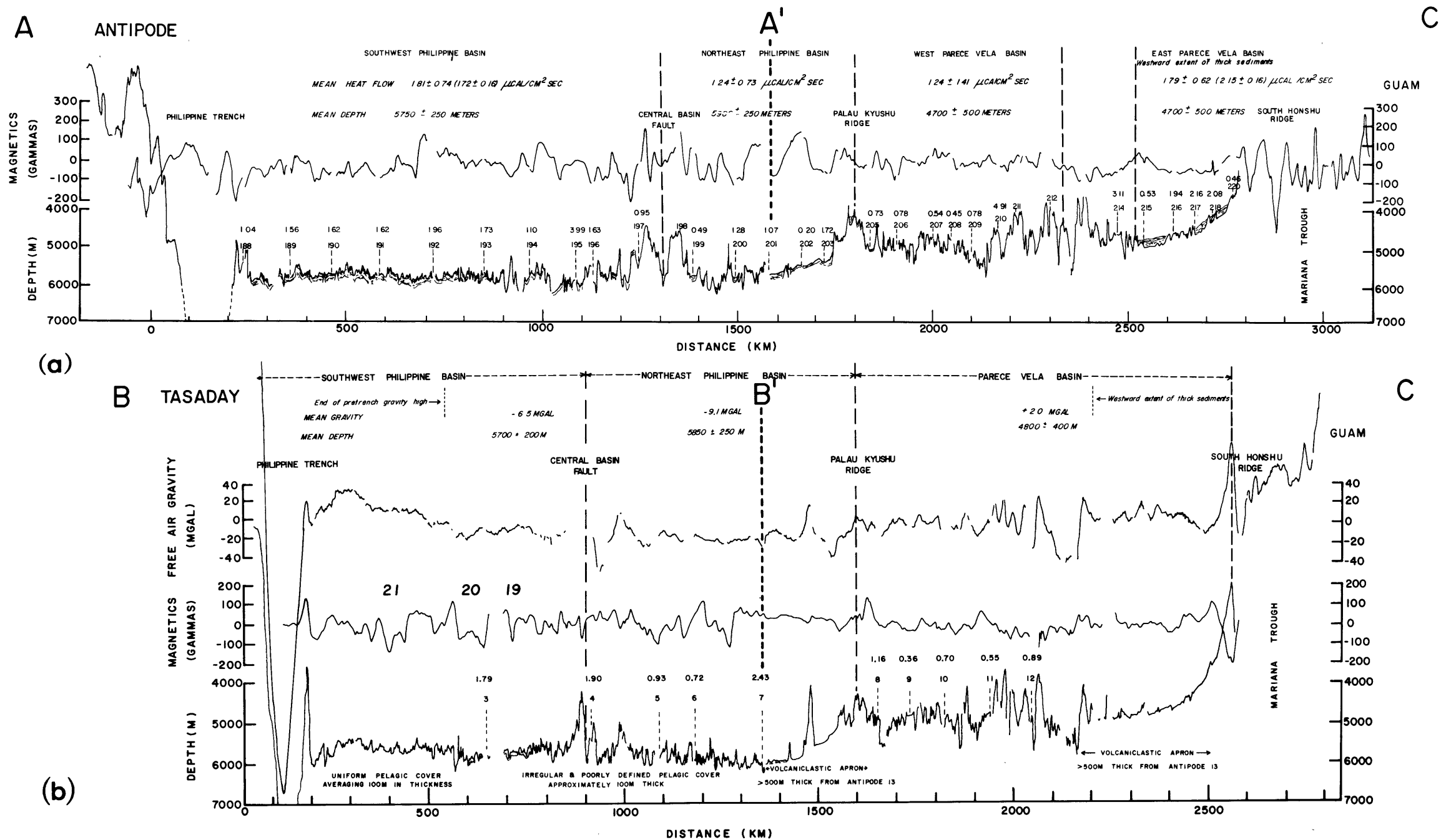
A ANTIPODE

SOUTHWEST PHILIPPINE BASIN

MEAN HEAT FLOW 181 ± 0 74 (172 ± 0 16) μCAL/CM² SEC

MEAN DEPTH 5750 ± 250 METERS

PHILIPPINE TRENCH

CENTRAL BASIN FAULT

NORTHEAST PHILIPPINE BASIN

124 ± 0 73 μCAL/CM² SEC

550 ± 250 METERS

PALAU KYUSHU RIDGE

WEST PARECE VELA BASIN

124 ± 141 μCAL/CM² SEC

4700 ± 500 METERS

EAST PARECE VELA BASIN
Westward extent of thick sediments

179 ± 0 62 (215 ± 0 16) μCAL /CM² SEC

4700 ± 500 METERS

SOUTH HONSHU RIDGE

GUAM

MAGNETICS (GAMMAS)

DEPTH (M)

MARIANA TROUGH

DISTANCE (KM)

C

(a)

B TASADAY

SOUTHWEST PHILIPPINE BASIN ── NORTHEAST PHILIPPINE BASIN ── PARECE VELA BASIN

End of pretrench gravity high

MEAN GRAVITY

MEAN DEPTH

- 6 5 MGAL

5700 ± 200 M

- 9.1 MGAL

5850 ± 250 M

+ 20 MGAL

4800 ± 400 M

Westward extent of thick sediments

PHILIPPINE TRENCH

CENTRAL BASIN FAULT

PALAU KYUSHU RIDGE

SOUTH HONSHU RIDGE

GUAM

FREE AIR GRAVITY (MGAL)

MAGNETICS (GAMMAS)

DEPTH (M)

MARIANA TROUGH

UNIFORM PELAGIC COVER AVERAGING 100M IN THICKNESS

IRREGULAR & POORLY DEFINED PELAGIC COVER APPROXIMATELY 100M THICK

←VOLCANICLASTIC APRON→
>500M THICK FROM ANTIPODE 13

←VOLCANICLASTIC APRON→
>500M THICK FROM ANTIPODE 13

DISTANCE (KM)

C

(b)

Fig. 3. (a) Bathymetric and line drawing of the sediments and magnetic anomalies along the Antipode 13 profile between the Philippine trench and the South Honshu Ridge. Heat flow measurements are shown along the track. Also presented are the mean heat flow and depth range for each of the separate tectonic provinces traversed by the profile. Because of instrument failure, only a magnetic profile was obtained across the Mariana Basin. (b) Same as Figure 3a, with free air gravity anomaly added for Tasaday 7 profile. (There is some evidence from cross-checking with an unpublished compilation of gravity data in the Philippine area (T. Watts, personal communication, 1975) that the gravity data west of the Central Basin Fault are 15 mGal low. The rest of the data agree with the unpublished compilation.) Also presented are mean gravity, mean depth, and range in depth for the separate tectonic provinces. Because of instrument failure, only a gravity profile was obtained across the Mariana Basin.

TABLE 3a.   Depth and Age From Joides Deep-Sea Drilling Sites

Basin	Site	Location N	Location E	Depth, m	Sediment, m Thickness	Sediment, m Correction	Topographic Correction, m	Corrected Depth, m	Biostratigraphic Age Period	Biostratigraphic Age Age, m.y.	Magnetic Anomaly Number	Magnetic Anomaly Age, m.y.
Parece Vela	53	18°02.0'	141°11.5'	4629	201	144	200*	~4830	Oligocene to early Miocene	32–18	· · ·	· · ·
	54	15°36.6'	140°18.1'	4990	294	212	· · ·	5102	Oligocene to early Miocene	32–18	· · ·	· · ·
Philippine	290	17°44.9'	133°28.1'	6062	255	185	−150†	~5900	Late Eocene	45–38	<21	<53
	291	12°48.4'	127°49.9'	5217	127	93	+400†	~5600	Middle to late Eocene	50–38	21	53–49
	293	20°21.3'	124°05.6'	5599	563	405	?	~6004	?	?		
	294	22°34.7'	131°23.1'	5784	118	85	· · ·	5869	Eocene?	54–45		

Parece Vela Basin-sites are taken from *Fischer et al.* [1971], Philippine Basin sites from *Ingle et al.* [1975], and biostratigraphic ages from *Berggren and Van Couvering* [1974].

* Correction from site 53 bathymetric chart [*Fischer et al.*, 1971].

† Correction from *Chase et al.* [1970].

The heat flow measurements were taken in a wide variety of places ranging from the enclosed Borneo, Sulu, and Celebes basins to the open and deep West Philippine Basin (Figure 2 and Table 1). On initial inspection the measurements, except for those of the enclosed basins, are not consistent (Figure 4 and Table 2). Even when the results are consistent, we do not know how to interpret them. For instance, the Borneo Basin has a uniform flow of 1.45 μcal/cm² s. The Sulu Trough has a higher mean heat flow, 2.13 μcal/cm² s, than the Celebes Basin, 1.51 μcal/cm² s (Table 2), but the reason for this difference is not known.

The variability in heat flow values starts in the West Philippine Basin and continues through the Parece Vela Basin. In both basins (Figures 3a and 3b) there is a reasonable correlation between lack of variability and a uniform sediment cover. The West Philippine Basin south of the Central Basin Fault has a uniform sediment drape, and the heat flow has little scatter. Within the fault and to the north, the topography is rough, the sediment drape less obvious, and the heat flow more variable. A spectacular example of such variability is found in the Parece Vela Basin. This basin is cut in two by a north-south central region of peaks and troughs which is the presumed termination point of the active spreading center. Both sides of the basin are thought to be of the same age. Deep-sea drilling sites in the eastern basin gave an Oligocene to early Miocene age (Table 3). The only striking difference is that the eastern basin is covered by a uniform drape of sediments. The heat flow measurements in this well-sedimented area are high and fairly uniform (1.80 ± 0.81 μcal/cm² s). On the other hand, the heat flow measurements in the western basin are generally low with a few very scattered high values (1.10 ± 1.19 μcal/cm² s) which usually occur on top of topographic highs (stations 210 and 214 in Figure 3a).

This wide difference in heat flow variability in two supposedly similar tectonic basins is very disturbing. *Lister* [1972] and *Williams et al.* [1974] have suggested that because of cooling cracks and faulting the oceanic crust is permeable to fluid flow. *Sclater et al.* [1974b] have further suggested that if this effective permeability is never completely destroyed, then in any region of rough topography with outcropping basement highs, hydrothermal circulation will occur. These circulation patterns will cause much of the heat loss to the sea water to occur by mass transport through the permeable basement. Also, the patterns that they set up will tend to lower the conductive heat flow in the sediment ponds between the outcropping basement highs. As a consequence, conductive measurements in such regions, except in isolated cases on top of basement highs, will yield low values.

We believe that this model gives a good qualitative explanation of the heat flow across the Parece Vela Basin. In the western basin, where there is little sediment cover and a highly variable topography, most of the values lie below 1.00 μcal/cm² s. In fact, the median is 0.76 μcal/cm² s. However, in the eastern Parece Vela Basin just west of the South Honshu Ridge there is a thick sediment drape extending 200 km from the ridge (Figure 3). In this area, except for the two stations at the edge, the heat flow values show much less scatter (Figure 3a) and have a median of 2.08 μcal/cm² s.

On the basis of our qualitative explanation of the low values we reexamined the environment around each of the stations on the Tasaday, Antipode, and Scan [*Sclater et al.*, 1972] cruises in the area. We divided the environments into four groups: A, a uniform sediment drape with no nearby sediment outcrops; B, a uniform sediment drape with isolated nearby outcrops; C, very thin or no sediment drape; and D, a sediment pond in rough topography next to an outcropping basement high.

TABLE 3b.   Depth and Age From Magnetic Anomalies and Topographic Profiles in the Philippine Basin

Area	Number of Measurements, m	Mean Depth, m	Estimated Range, m	Age Range, m.y.
Anomaly 17, Central Basin Fault	6	5050	±200	43–39
Anomaly 21, southwest Philippine Basin	5	5750	±300	53–49
Anomaly 21, northeast Philippine Basin	5	5950	±200	53–49

Topographic profiles are taken from the present paper and *Louden* [1976], and magnetic anomaly identifications from *Louden* [1976].
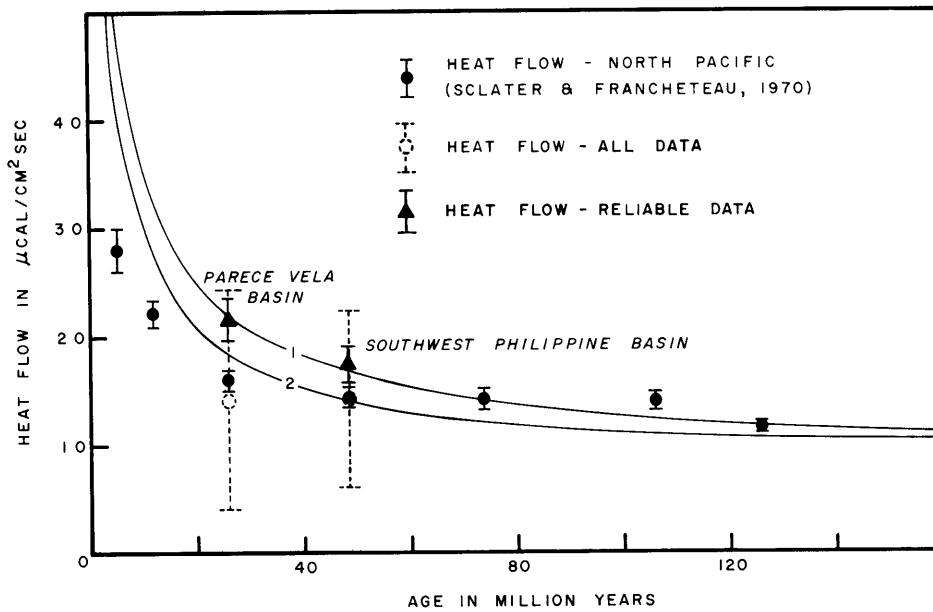
Fig. 5. The mean and standard deviation for all data and for selected reliable data from the southwest Philippine and Parece Vela basins superimposed upon a plot of mean heat flow and standard error for tectonic provinces in the North Pacific against age. Curves 1 and 2 represent the theoretical heat flow for 100-km- and 75-km-thick lithosphere plates, respectively (after *Sclater and Francheteau* [1970]).

We found six stations in the eastern Parece Vela Basin with an A environment. The median was 2.15 with a standard deviation of ± 0.16 μcal/cm^2 s (Figure 4). The fact that the scatter has been considerably reduced by using only A environment stations is significant. It indicates that only where the sediment cover (which is presumed to be impermeable) is thick enough and sufficiently wide to stop any regional loss of heat
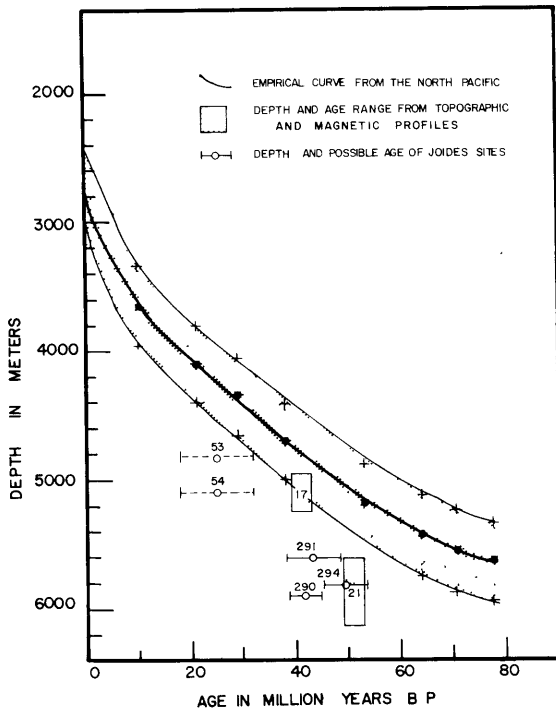

Fig. 6. Depth versus age data for the northeastern Pacific compared with similar data from the Philippine Sea. The stippled area represents a range of ± 300 m about the empirical curve for the northeastern Pacific. This is the expected range for an area with no free air gravity anomaly [*Parsons and Sclater*, 1975].

by mass transport will reliable measurements of low scatter be obtained. We believe that the true heat flow from the eastern Parece Vela Basin is 2.15 $\pm$ 0.16 μcal/cm^2 s. This is high and significantly different from that in the western basin. We carried out a similar exercise for the southwestern Philippine Basin. Again, when only the A stations are considered, the scatter is low, and we obtained a value of 1.72 $\pm$ 0.16 μcal/cm^2 s (Figure 4).

This reinterpretation of data demonstrates an important and well-known fact; namely, much of the variability of oceanic heat flow measurement is a function of environment. However, if regions can be found with a uniform sediment drape of thickness greater than 100 m and an extent that is wider than that of probable hydrothermal convection cells (5–10 km), then heat flow measurements of surprisingly low scatter should be observed. If, in these areas, the effects of slumping and bottom water temperature variations can be shown to be small, then these heat flow values may be a true measure of the flow of depth beneath the oceanic crust.

COMPARISON OF HEAT FLOW
AND DEPTH MEASUREMENTS

We compared the reliable heat flow average over the southern section of the West Philippine Basin and the eastern Parece Vela Basin with that over areas of the Pacific of the same age (Figure 5). Though both areas have higher heat flows than the North Pacific, the difference cannot be considered significant. In the North Pacific no account was taken of local environment, and as a consequence, the averages in the midocean ridges are almost certainly biased in the low direction. Recently, *Sclater et al.* [1975] have shown that if only heat flow values from well-sedimented areas are considered, the means when plotted against age are very close to the values predicted by a 100-km-thick lithosphere. Even the heat flow through the Parece Vela Basin is not significantly greater than the values observed over Oligocene crust in the North Pacific when the large number of unreliable low values used in determining the mean for ocean floor of the same age are removed.

TABLE 4a. A Comparison of Velocity and Thickness of the Crustal Layers in the West Philippine and Parece Vela Basins and the North Pacific

Area	Layer	Velocity, km/s	Thickness, km	Assumed Density, g/m³	Data Source
West Philippine Basin	T	5.30 ±	0.92 ±	2.5	*Murauchi et al.* [1968] (stations 21 and 27)
	O	6.70 ±	4.03 ±	2.9	*Henry et al.* [1975] (station Tasaday 5-2)
Parece Vela Basin*	T	4.45	1.39	2.4	*Murauchi et al.* [1968] (stations 24N, 25W and 25E)
	O	6.81	3.00	2.9	*Gaskell et al.* [1959] (CR 12)
Western North Pacific	T	5.02 ± 0.63	2.05 ± 0.50	2.5	*Raitt* [1963]
	O	6.73 ± 0.25	5.08 ± 1.72	2.9	
North Pacific	T	5.19 ± 0.64	1.49 ± 0.98	2.5	*Shor et al.* [1970]
	O	6.81 ± 0.16	4.62 ± 1.30	2.9	
Hypothetical crust, 45 m.y. B.P.	T	5.1	1.66	2.5	*Le Pichon et al.* [1973]
	O	6.7	5.33	2.9	

T and O are the transition and oceanic layers, respectively, after *Shor et al.* [1970].
* These data are not reliable; 24S was omitted because it had an unusually thick oceanic layer.

To investigate the tectonic similarities of the basins in the Philippine Sea further, we plotted their depth as a function of age and compared the basins with the North Pacific (Figure 6). In this case, both the Parece Vela and the West Philippine basins north and south of the Central Basin Fault have depths that are significantly greater than the depth predicted by the empirical curve for the North Pacific. A possible explanation of the differences for the Parece Vela Basin is that the lithospheric plate is thinner landward of the trench because of shear stresses along the bottom of the plate [*McKenzie*, 1969]. In this case the thinner plate cools more quickly, and by 30 m.y. B.P. it has reached equilibrium. The thinner lithosphere results in a high heat flow and a depth close to 4600 m [*Sclater*, 1972]. Though this mechanism can be invoked to account for the heat flow and elevation in the Parece Vela Basin, it cannot also work for the West Philippine Basin. In this case the depths are so deep that the residual elevation anomaly (actual depth minus predicted depth for crust of the same age) cannot be caused by thinning the plate. Any decrease in thickness of the lithosphere in equilibrium crust will increase the elevation, not decrease it [*Sclater*, 1972]. Thus some other explanation must be found for the deeper than normal depths in these two basins.

Karig [1971] pointed out that there was some evidence that the oceanic crust in the marginal basins of the Philippine Sea was thinner than that under the deep oceans and that this difference could account for the greater than normal depths [*Karig*, 1974]. We also observe that the mean free air gravity anomaly over both basins is less than ±10 mGal (Figure 3b). Thus it appears that the basins are compensated and that the thinner crust could account for the deeper depths. To investigate this effect, we have compiled the reliable seismic data from *Murauchi et al.* [1968, *Henry et al.* [1975], and *Gaskell et al.* [1959] for the West Philippine Basin and the Parece Vela Basin. We separated the oceanic crust into three layers, sediment, transition, and oceanic, after the definition presented in Figure 1 of *Shor et al.* [1970], and we compared these with the compilations of *Raitt* [1963] and *Shor et al.* [1970] and with the theoretical northwestern Pacific crustal section of *Le Pichon et al.* [1973] (Table 4a). We included the three different compilations which represent the average for old ocean floor, the average for a fairly young ocean floor, and an empirical curve to give an estimate of the likely range of thickness of the two layers in normal oceanic crust. Both the West Philippine and the Parece Vela basins have a crustal thickness which is much less than that of any of the three

estimates for normal oceanic crust. We have calculated (Table 4b) that in the West Philippine Basin this decrease in crustal thickness will produce a residual depth anomaly of between 300 and 600 m. In the Parece Vela Basin the anomaly will be slightly less, 280-570 m. Clearly, much of the extra depth in these two basins can be accounted for by a thinner crust.

Before this explanation of the excess depths in the marginal basins can be unreservedly accepted, it is necessary to point out that there are problems with this mechanism. First, the seismic data coverage in both basins is poor, and more reversed lines are needed to substantiate the evidence of a thinner crust. As a consequence, the data have a high scatter, and the differences between the means for the basins and those for oceanic crust of the same age are only marginally significant. Second, there is no evidence from dredged rocks to indicate that the oceanic crustal layers may have a different composition under the marginal basins. Finally, the deep ocean floor in the North Pacific does not have such a large variation in crustal thickness [*Shor et al.*, 1970]. Thus some new special mechanism must be advanced to explain how and why this small section of the ocean floor should have a thinner crust than that created at an oceanic spreading center.

Conclusions

We have shown that both the Parece Vela and the West Philippine basins have mean depths that are deeper and an oceanic crust that is thinner than ocean floor of the same age. Both have higher than normal heat flow, but this heat flow is not necessarily greater than that of ocean floor of the same age. Both basins appear to have been formed by crustal extension originating at the center of the basin. However, in the case of the Parece Vela Basin this extension was east-west, while in the West Philippine Basin it was north-south. The West Philip-

TABLE 4b. Expected Increase In Depth Resulting From Thinner Crustal Layers

	Depth Increase, m
West Philippine Basin	
with respect to western North Pacific	~110
with respect to North Pacific	~320
with respect to hypothetical crust, 45 m.y. B.P.	~500
Parece Vela Basin	
with respect to western North Pacific	~570
with respect to North Pacific	~280
with respect to hypothetical crust, 30 m.y. B.P.	~360

pine Basin has clearly identifiable magnetic anomalies showing a spreading rate during extension of 6-cm/yr half rate. Only one other marginal basin, the Scotia spreading center [*Barker*, 1972], shows more easily identified magnetic lineations, and it has a half rate of 3 cm/yr. With present information it is clear that the West Philippine Basin is different from the other marginal basins in the western Pacific. However, it also has two significant differences from deep ocean floor of the same age. Hence it is not possible at the present moment to determine the environment in which this basin was formed.

In this view it is important to realize that explanations other than crustal variations exist to explain residual depth anomalies. It is possible that in such an area behind one downgoing slab and near another, complex dynamic forces could be acting to decrease the observed depth. A similar mechanism invoking dynamic forces in the upper mantle has already been advanced by *Sclater et al.* [1975] to explain the observed correlation between free air gravity anomalies and residual elevation anomalies in the North Atlantic. One of the disturbing features of accepting the thinner oceanic crust to explain the deeper depths in the marginal basins is that it adds another hypothesis to be considered when the worldwide correlation of residual depth and free air gravity anomalies is interpreted.

REFERENCES

Barker, P. F., A spreading center in the East Scotia Sea, *Earth Planet. Sci. Lett., 15*, 123–132, 1972.

Ben-Avraham, Z., J. Segawa, and C. Bowin, An extinct spreading center in the Philippine Sea, *Nature, 240*, 453–455, 1972.

Berggren, W. A., and J. A. Van Couvering, The late Neogene: Biostratigraphy, geochronology and palaeoclimatology of the last 15 million years in marine and continental sequences, *Palaeogeogr. Palaeoclimatol. Palaeoecol., 16*(1, 2) 1–216, 1974.

Chase, T. E., H. W. Menard, and J. Mammerickx, Bathymetry of the northern Pacific, charts 1–10, Inst. Mar. Resour., La Jolla, Calif., 1970.

Corry, C., C. Dubois, and V. Vacquier, Instrument for measuring terrestrial heat flow through the ocean floor, *J. Mar. Res., 26*, 165–177, 1968.

Fischer, A. G., B. C. Heezen, A. P. Lisitzin, A. C. Pimm, R. E. Garrison, R. E. Boyce, S. A. Kling, D. Bukry, V. Krasheninnikov, R. C. Douglas, D. E. Karig, and G. G. Shor, Jr., *Initial Reports of the Deep-Sea Drilling Program,* vol. 6, U.S. Government Printing Office, Washington, D. C., 1971.

Gaskell, T. F., M. N. Hill, and J. C. Swallow, Seismic measurements made by H.M.S. *Challenger* in the Atlantic, Pacific, and Indian oceans and in the Mediterranean Sea, 1950–53, *Phil. Trans. Roy. Soc. London, Ser. A, 251*, 23–85, 1959.

Heirtzler, J. R., G. O. Dickson, E. M. Herron, W. C. Pitman, and X. Le Pichon, Marine magnetic anomalies, geomagnetic field reversals, and motions of the ocean floor and continents, *J. Geophys. Res., 73*, 2119–2136, 1968.

Henry, M., D. E. Karig, and G. G. Shor, Two seismic refraction profiles in the west Philippine Sea, in *Initial Reports of the Deep-Sea Drilling Program,* vol. 31, edited by J. C. Ingle et al., U.S. Government Printing Office, Washington, D. C., 1975.

Ingle, J. C., D. E. Karig, A. H. Bouma, C. H. Ellis, N. Haile, I. Koizumi, H. Y. Ling, I. MacGregor, C. Moore, H. Ujiie, T. Watanabe, S. M. White, and M. Yasui, *Initial Reports of the Deep-Sea Drilling Program,* vol. 31, U.S. Government Printing Office, Washington, D. C., 1975.

Karig, D. E., Origin and development of marginal basins in the western Pacific, *J. Geophys. Res., 76*, 2542, 1971.

Karig, D. E., Evolution of arc systems in the western Pacific, *Annu. Rev. Earth Planet Sci., 2*, 51–75, 1974.

Le Pichon, X., J. Francheteau, and J. Bonin, *Plate Tectonics, Develop. in Geotectonics,* vol. 6, 300 pp., Elsevier, New York, 1973.

Lister, C. R. B., On the thermal balance of a mid-ocean ridge, *Geophys. J. Roy. Astron. Soc., 26*, 515–535, 1972.

Louden, K. E., Magnetic anomalies in the West Philippine Basin, in *The Geophysics of the Pacific Ocean Basin and Its Margin, Geophys. Monogr. Ser.,* vol. 19, AGU, Washington, D. C., in press, 1976.

McKenzie, D. P., Speculations on the consequences and causes of plate motions, *Geophys. J. Roy. Astron. Soc., 18*, 1–32, 1969.

Murauchi, S., N. Den, S. Asano, H. Hotta, T. Yoshii, T. Asanuma, K. Hagiwara, K. Ichikawa, T. Sata, W. J. Ludwig, J. I. Ewing, N. T. Edgar, and R. E. Houtz, Crustal structure of the Philippine Sea, *J. Geophys. Res., 73*, 3143–3171, 1968.

Parsons, B., and J. G. Sclater, An analysis of the variation of ocean floor heat flow and bathymetry with age, submitted to *J. Geophys. Res.,* 1975.

Raitt, R. W., The crustal rocks, in *The Sea,* vol. 3, edited by M. N. Hill, pp. 85–101, John Wiley, New York, 1963.

Sclater, J. G., Heat flow and elevation of the marginal basins of the western Pacific, *J. Geophys. Res., 77*, 5705–5719, 1972.

Sclater, J. G., and J. Francheteau, The implications of terrestrial heat flow observations on current tectonic and geochemical models of the crust and upper mantle of the earth, *Geophys. J. Roy. Astron. Soc., 20*, 509–542, 1970.

Sclater, J. G., U. G. Ritter, and F. S. Dixon, Heat flow in the southwestern Pacific, *J. Geophys. Res., 77*, 5697–5704, 1972.

Sclater, J. G., R. Jarrard, B. McGowran, and S. Gartner, Comparison of the magnetic and biostratigraphic time scales since the late Cretaceous, in *Initial Reports of the Deep-Sea Drilling Program,* vol. 22, edited by C. Von der Borch et al., U.S. Government Printing Office, Washington, D. C., 1974a.

Sclater, J. G., R. P. von Herzen, D. L. Williams, R. N. Anderson, and K. Klitgord, The Galapagos spreading centre: Heat-flow low on the north flank, *Geophys. J. Roy. Astron. Soc., 38*, 609–626, 1974b.

Sclater, J. G., B. Parsons, and L. Lawver, Comparison of long wavelength elevation and free air gravity anomalies in the North Atlantic, *J. Geophys. Res., 80*, 1031–1052, 1975.

Sclater, J. G., J. Crowe, and R. N. Anderson, On the reliability of oceanic heat flow averages, submitted to *J. Geophys. Res.,* 1975.

Shor, G. G., H. W. Menard, and R. W. Raitt, Structure of the Pacific Basin, in *The Sea,* vol. 4, part 2, edited by A. E. Maxwell, pp. 29–173, John Wiley, New York, 1970.

Uyeda, S., and Z. Ben-Avraham, Origin and development of the Philippine Sea, *Nature Phys. Sci., 240*, 176–178, 1972.

von Herzen, R. P., and A. E. Maxwell, The measurement of thermal conductivity of deep-sea sediments by a needle probe method, *J. Geophys. Res., 64*, 1557–1565, 1959.

Williams, D. L., R. P. Von Herzen, J. G. Sclater, and R. N. Anderson, The Galapagos spreading centre: Lithospheric cooling and hydrothermal circulation, *Geophys. J. Roy. Astron. Soc., 38*, 587–608, 1974.

APPENDIX B

PLOTS OF MAGNETIC ANOMALIES ALONG

TRACK IN THE PHILIPPINE SEA

ABSTRACT

We present charts of the residual magnetic field along ship tracks in the Philippine Sea. A separate chart shows major bathymetric features together with a summary of identifiable magnetic anomalies in the West Philippine Basin.

INTRODUCTION

The Philippine Sea represents one of the largest marginal basins in the West Pacific and is one of the best understood examples of basin formation by inner arc spreading (Karig, 1971). However, no comprehensive collection of magnetic anomalies exists for this region. This report is a first attempt at such a compilation and, hopefully, will serve as a data base for future work. Parts of this data have been used by Louden (in press) for his identification of magnetic anomalies in the West Philippine Basin.

DATA SOURCES AND REDUCTION

The data presented in the charts come from seven sources and represent four basic types of data reduction. In all cases the regional field has been removed by identical methods to those of Sclater, et al. (1971).

Type A

1. Lamont-Doherty Geological Observatory cruises: VEMA 19, 21 and 24; CONRAD 11 and 12.

2. Scripps Institution of Oceanography cruises: CIRCE, ANTIPODE, LUSIAD ARGO, and TASADAY.

3. Deep Sea Drilling Project: Leg 31 of the R/V GLOMAR CHALLANGER.

4. Ocean Research Institute of the University of Tokyo: cruises of the R/V UMITAKE MARU (1963-67) and R/V

HAKUHO MARU (1972).

For the above sources, cards or tapes of magnetics and bathymetry vs. time and time vs. position were obtained from the original data library. These were then merged at five minute intervals.

Type B - U. S. Naval Oceanographic Office

1. Project Magnet lines: 301, 302B, 304, 307, 311, 313B, 318, 326, 356, 371, 372A, 374, 385, and 395.

2. Leg 6 of the R/V RUTH ANN.

Analogue records of magnetics vs. time were obtained on microfilm from NAVOCEANO. These were photographically enlarged and then digitized. The digitized output was merged (at five minute intervals for ship tracks or twenty second intervals for airplane lines) with position vs. time data, read either from plots (R/V RUTH ANN) or listings (Project Magnet).

Type C

U. S. Coast and Geodetic Survey: International Indian Ocean Expedition (1964) of the R/V PIONEER.

This data was punched from merged listings of position, bathymetry and magnetics at five minute intervals (Coast and Geodetic Survey, 1965).

Type D

National Ocean and Atmospheric Administration:

Trans-Pacific Survey 7201.

A tape of merged position, bathymetry, magnetics and gravity was obtained from NOAA. Readings were recorded every five minutes.

CHARTS

The above mentioned data was plotted at a scale of 1.8 inch/deg longitude and 333 gammas/inch in figures 1-8. In all cases positive anomalies are plotted above the ship track. On a North-South line they are plotted to the left.

FIGURES 1-8

Magnetic anomalies in the Philippine Sea plotted

at right angles to track. Positive anomalies

are plotted above the ship track except for a

North-South line when they are plotted to the

left.

120°E 125° E 130°E 135°E.
20°N

LSD 1
GC 31
311
TAS 5
V 21-08
V20-08
ANT 4
V 24-05
TAS 5
ANT 4
14
V 28-14
GC-31
ANT 13
C11-07

15°N
301
V 21-08
371
V 28-14
V 21-08
GC-31
301
V19-07
301
318
318
318
10°N
CIRCE 2
371
ANT 13
CIRCE 2
C11-07
ANT 13
5°N
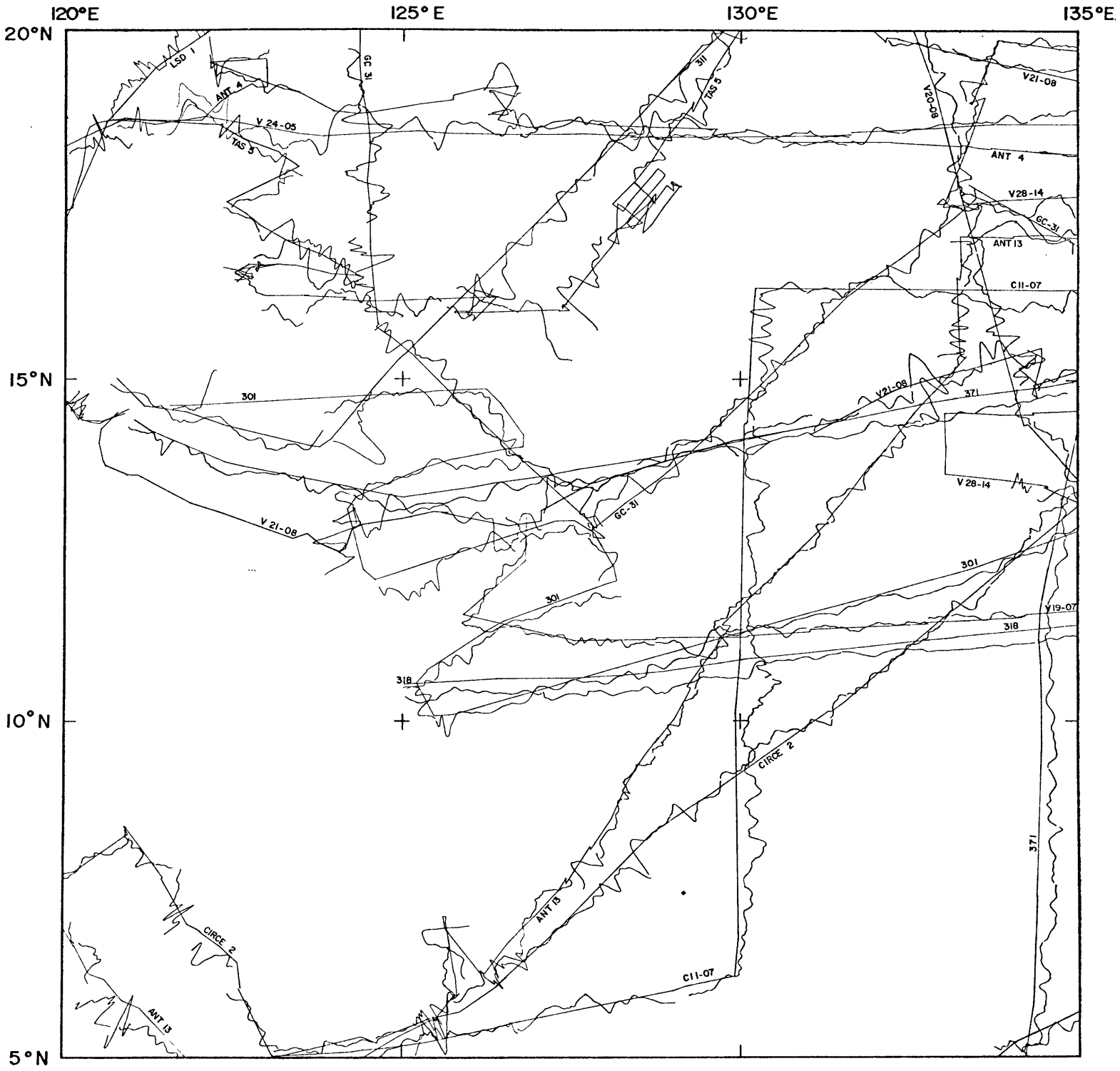
SCLATER & LOUDEN FIG 1A
MIT-0-75-160/PT 1-8-75
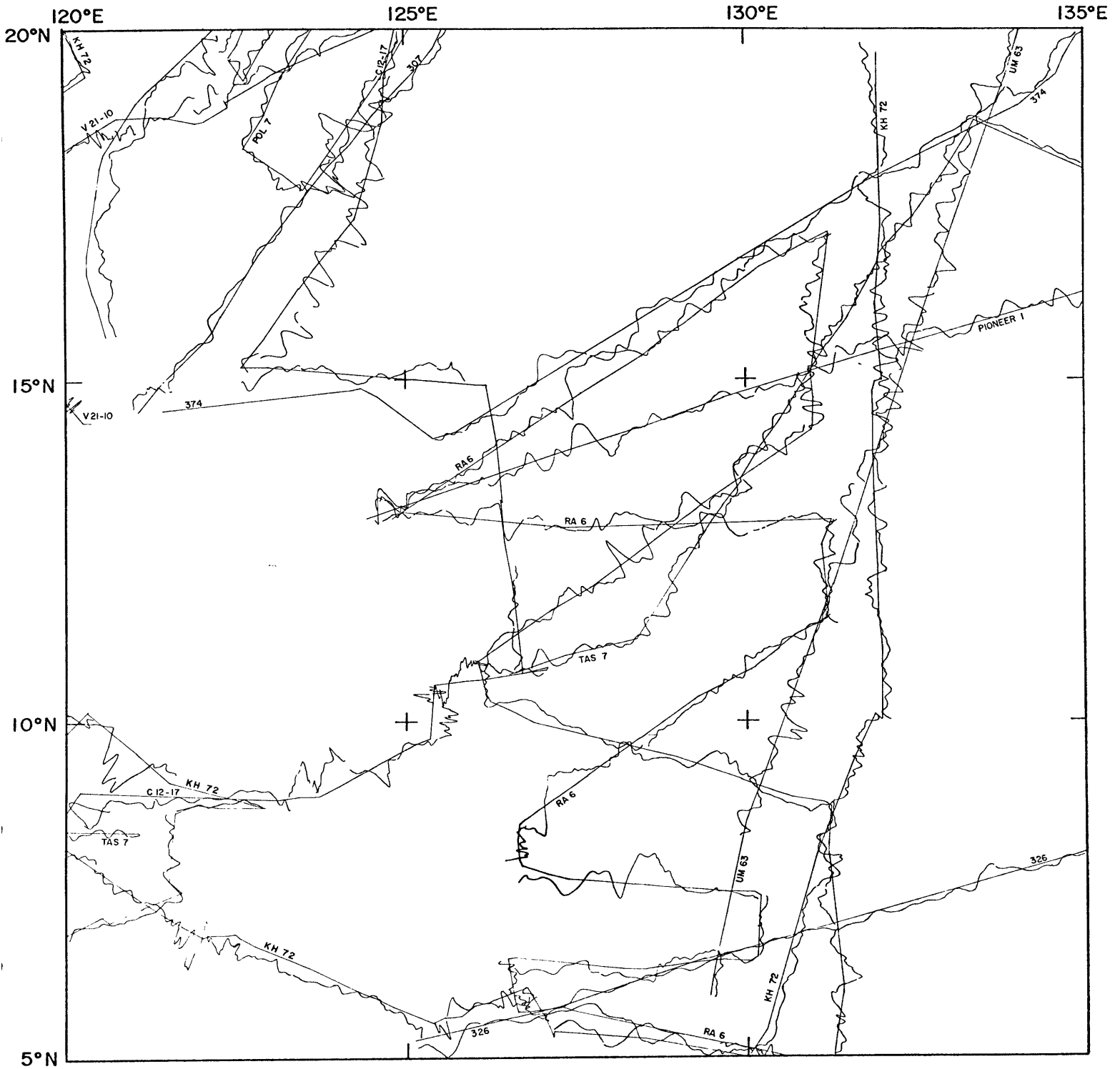
SCLATER & LOUDEN FIG 1B
MIT-O-75-161/PT 1-8-75
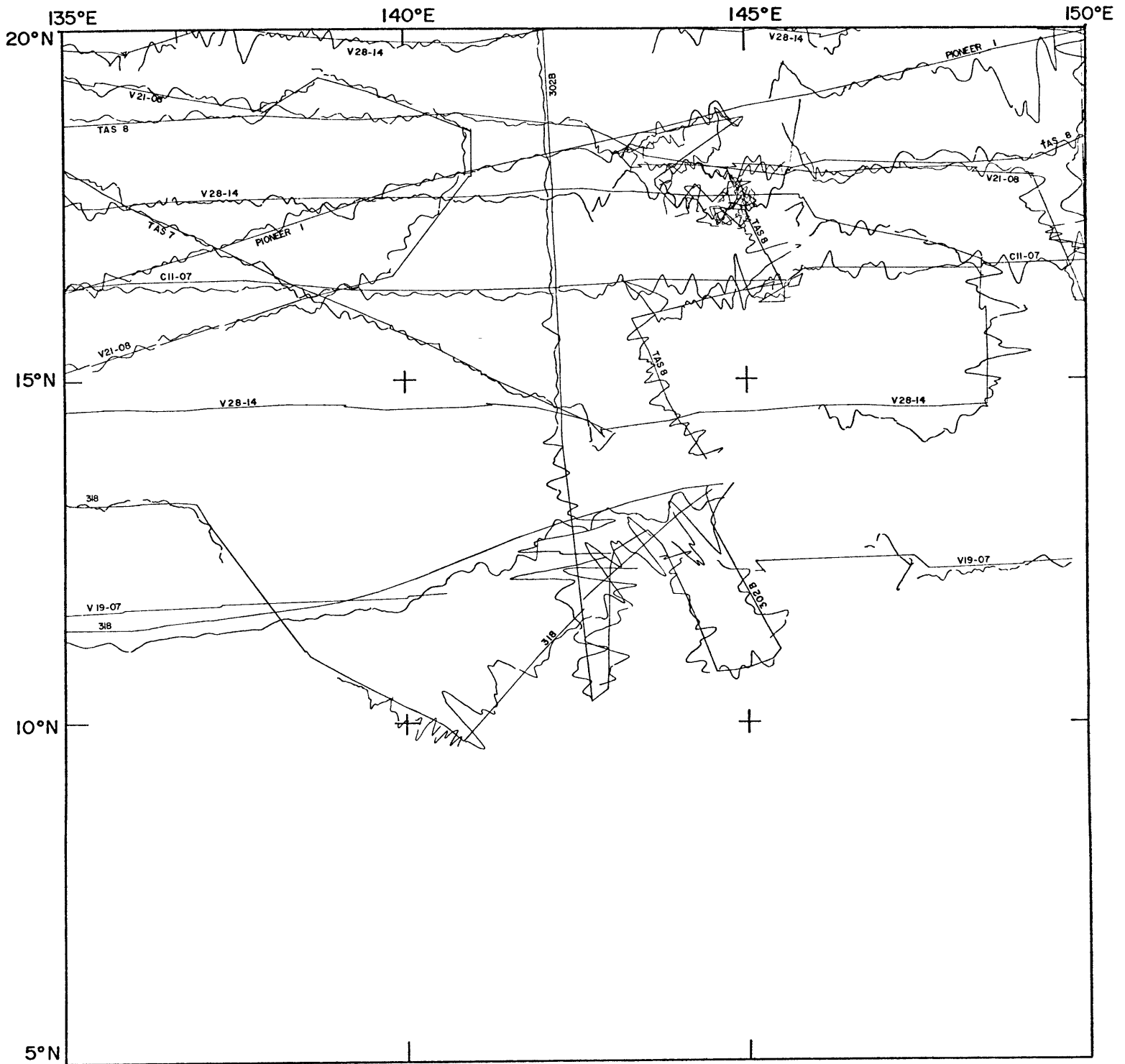
SCLATER & LOUDEN · FIG 2A
MIT-O-75-162/ PT 1-8-75
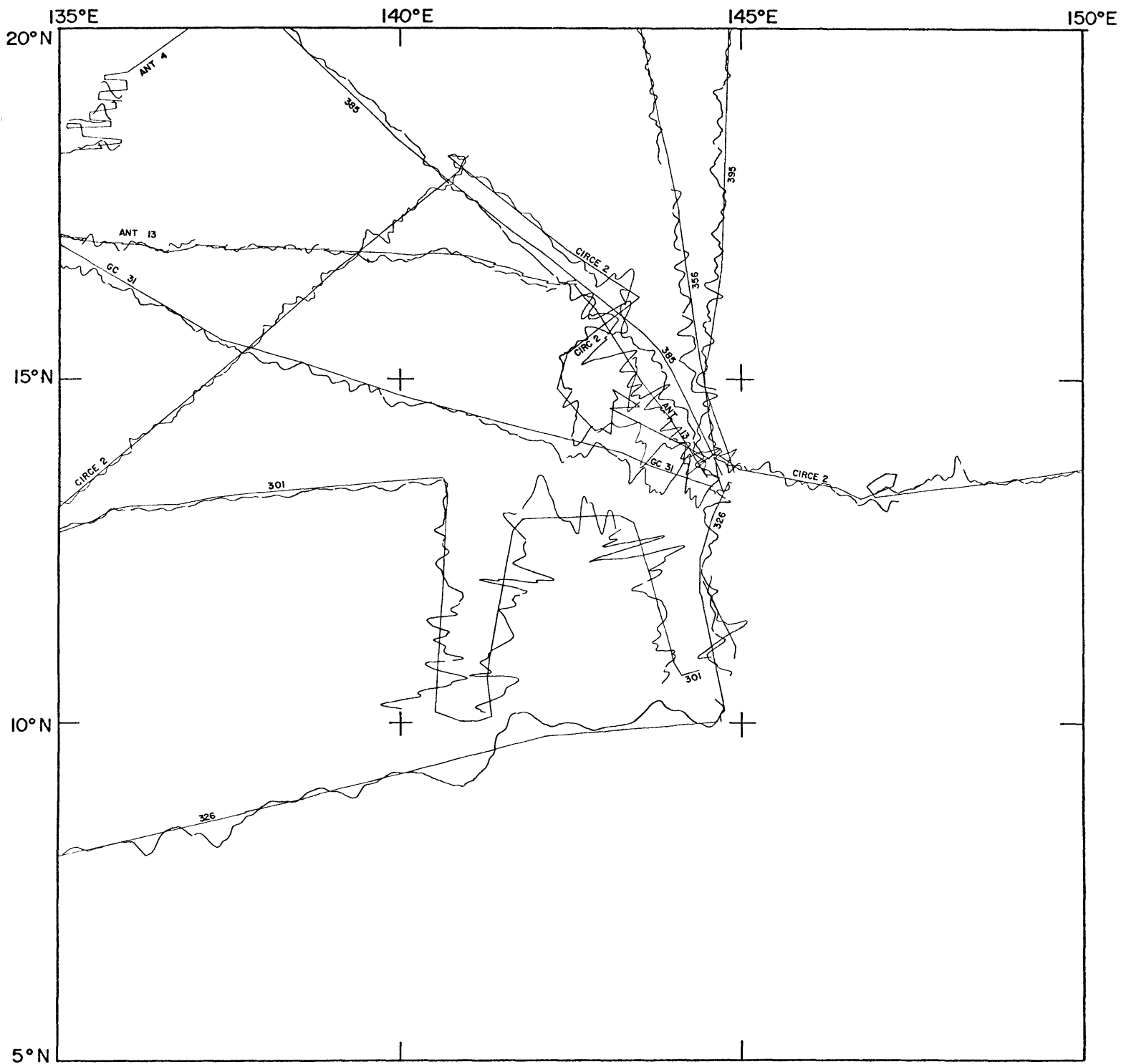
SCLATER & LOUDEN · FIG 2B
MIT-0-75-163/PT 1-8-75
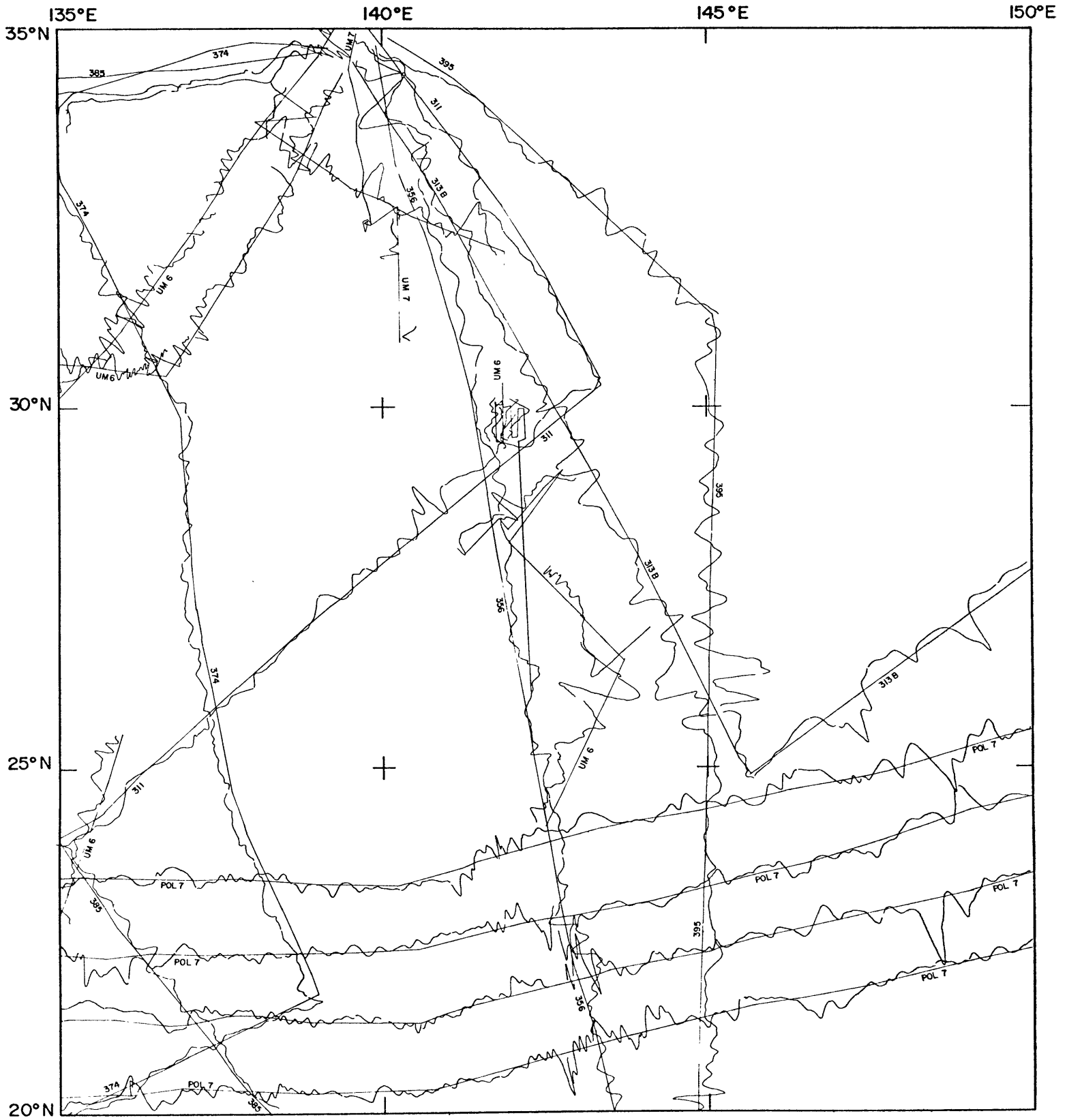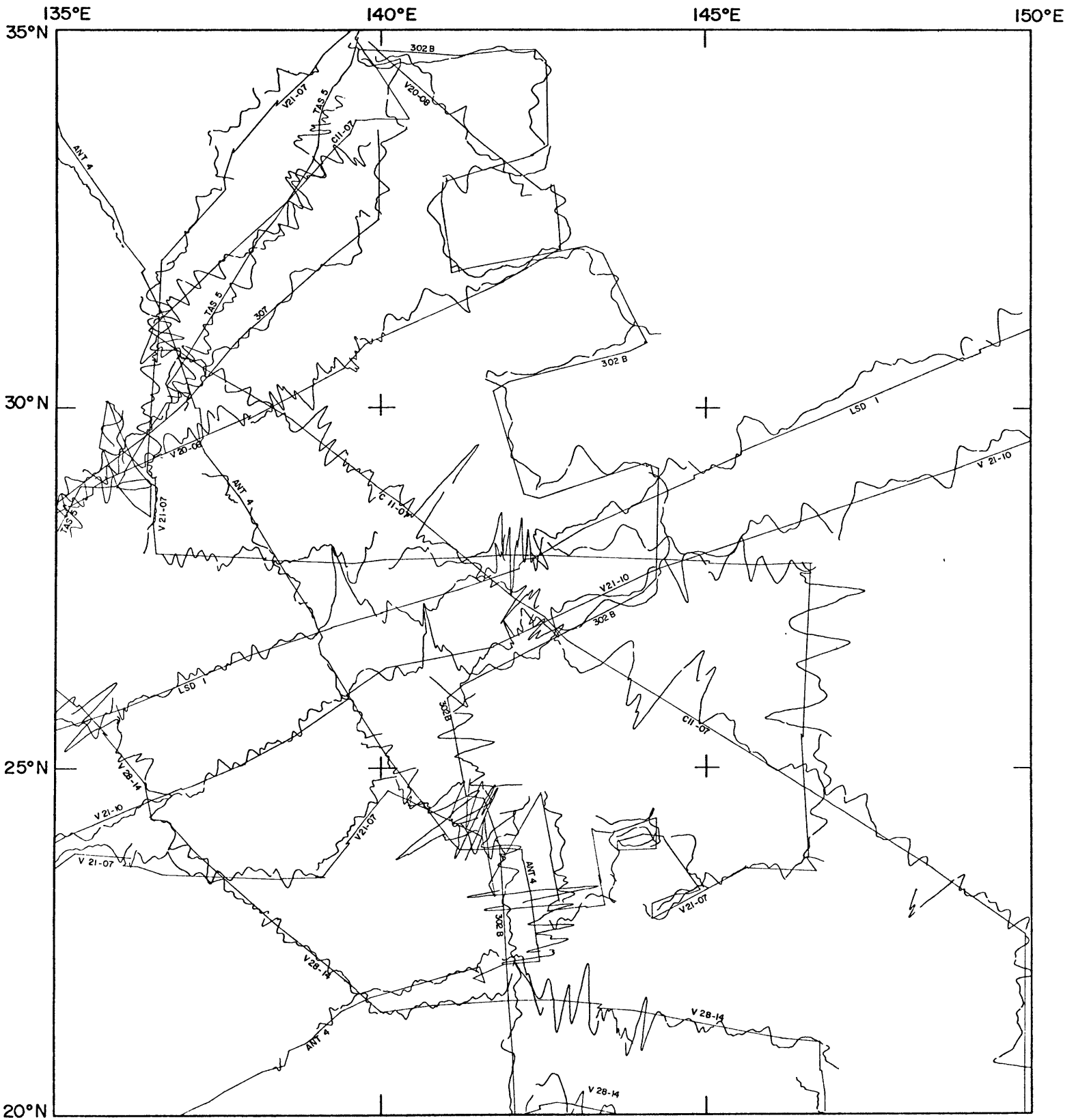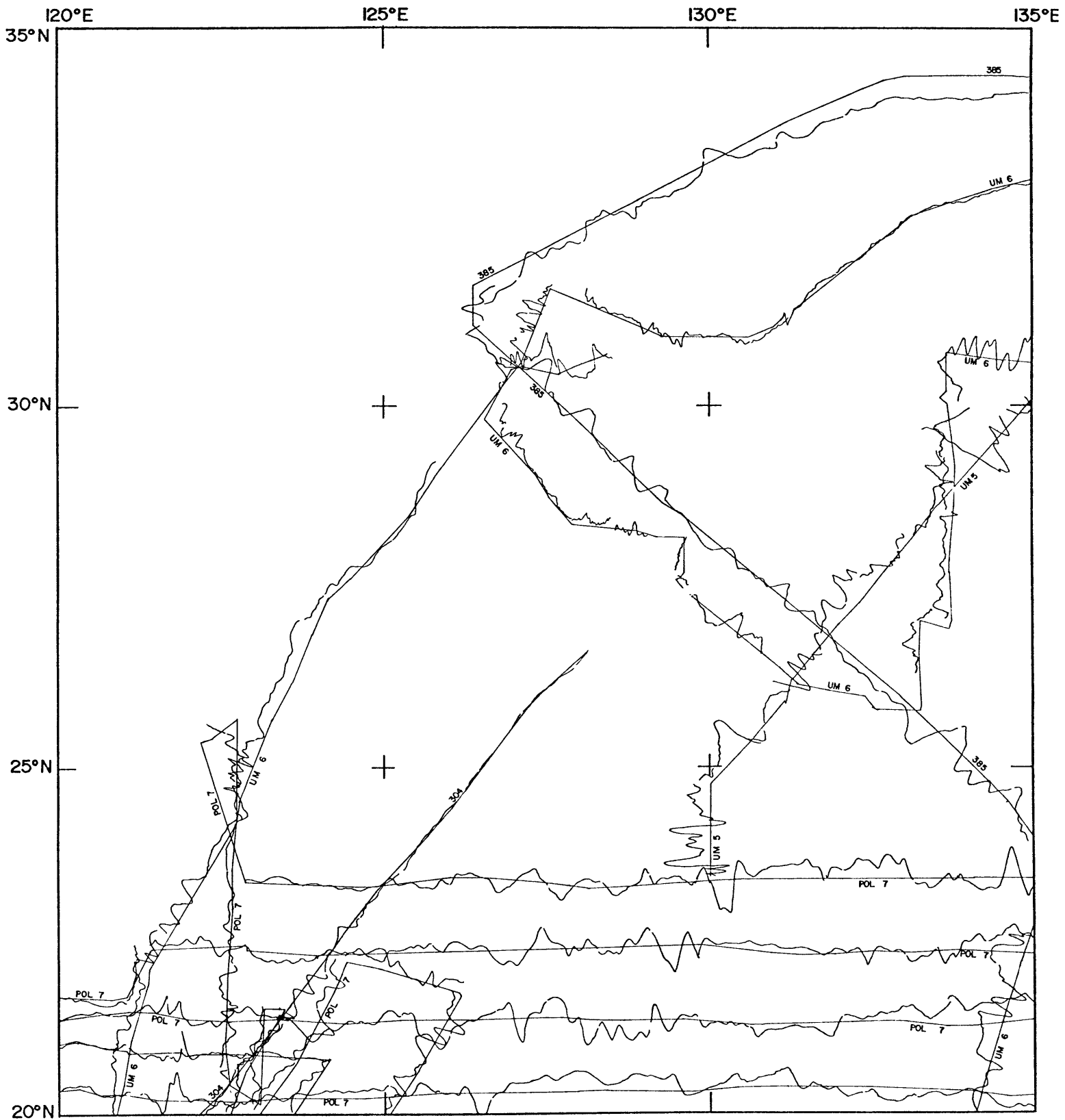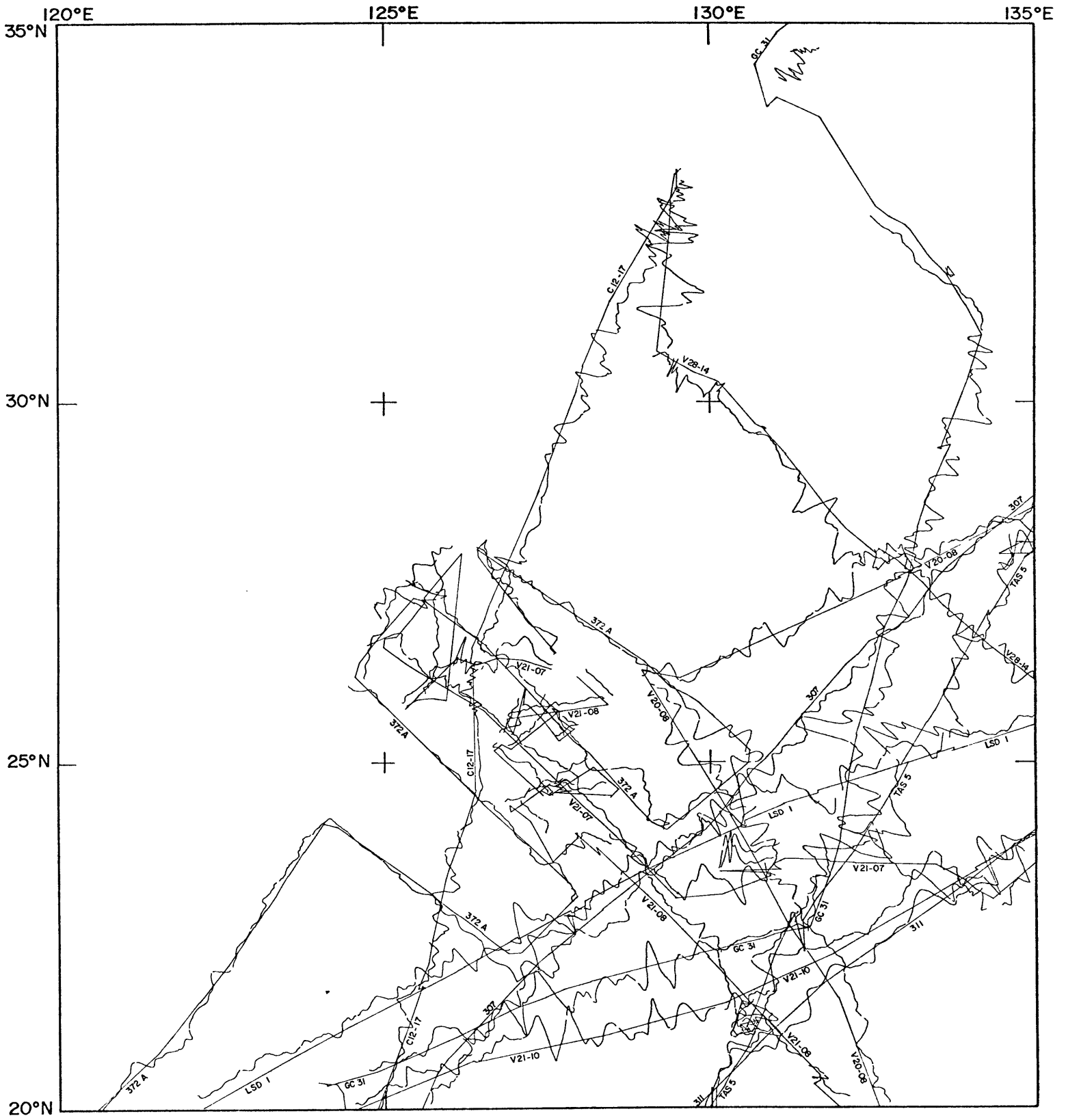
ACKNOWLEDGEMENTS

REFERENCES

Coast and Geodetic Survey, International Indian Ocean
Expedition, ESSA, U. S. Dept. of Commerce, 3, 1965.

Karig, D. E., Origin and development of marginal basins in
the western Pacific, J. Geophys. Res., 76, 2543-
2561, 1971.

Louden, K. E., Magnetic anomalies in the West Philippine
Basin, AGU Woollard Monograph, in press.

Sclater, J. G., U. Ritter, W. Hilton, L. Meinke, and R. L.
Fisher, Charts of residual magnetic field plotted
along track for the Indian Ocean, Tech. report
#SIO 71-7 of the Marine Phys. Lab., S.I.O., 1971.